LASER RAMAN SPECTROSCOPIC STUDIES OF BINARY AND TERNARY BORATE GLASSES

ABSTRACT

THESIS

SUBMITTED FOR THE DEGREE OF

Doctor of Philosophy

IN

PHYSICS

BY

MD. HAFIZUR RAHMAN

DEPARTMENT OF PHYSICS
ALIGARH MUSLIM UNIVERSITY
ALIGARH (INDIA)

1992

Professor of Physics
and Chairman of the Department

DEPARTMENT OF PHYSICS
ALIGARH MUSLIM UNIVERSITY
ALIGARH, U.P. (India)
Tel No. 2?001

September 28, 1992

CERTIFICATE

This is to certify that the thesis entitled **Laser Raman Spectroscopic Studies of binary and ternary borate glasses** being submitted by **Mr. Md. Hafizur Rahman** for the award of the Degree of Doctor of Philosophy in Physics of this university is a record of original research work done by him under my supervision.

(PROF. B.H. KHAN)
RESEARCH SUPERVISOR

ABSTRACT

The boric oxide (B_2O_3) is a well known glass network former oxide. The laser Raman spectroscopic investigations reported in this thesis have been carried out on both binary and ternary borate systems. The binary systems studied here are $xMO.(1-x)B_2O_3$, where M=Ca, Sr, Ba & Cd and the ternary systems are obtained by doping alkaline earth chlorides, rare earth and transition metal oxides into the above binary systems. The low frequency Raman scattering in these borate glasses has been interpreted on the basis of the Martin-Brenig model. As a complementry to these Raman investigations, infrared spectral studies of the same glass systems have also been performed.

The samples studied in this investigation form transparent glasses under specified conditions. The first chapter of this thesis contains introduction and theoretical background while the second chapter deals with the experimental methods employed in the present investigation. Boric oxide glass spectra have been studied in chapter III. The fourth chapter presents the experimental observations and their interpretations about the alkaline earth borate binary $xMO.(1-x)B_2O_3$ and ternary $(MCl_2)_y.[xMO.(1-y-x)B_2O_3]_{1-y}$ glass systems for $Ø.2Ø \leq x \leq Ø.5Ø$ and $Ø,1Ø \leq y \leq Ø.4Ø$, where M=Ca,Sr,Ba & Cd. The cerium di oxide doped calcium borate glasses in the system $(CeO_2)_y.[xCaO.(1-y-x)B_2O_3]_{1-y}$ for x=Ø.2Ø & Ø.35 and y=Ø, Ø.Ø5 & Ø.1Ø, have been

discussed in chapter V, while the investigations about the vanadium oxide doped calcium borate glasses in the system $(V_2O_5)_y.[xCaO.(1-y-x)B_2O_3]_{1-y}$ for y=Ø, Ø.Ø5, Ø.1Ø & Ø.15 and x=Ø.2Ø & Ø.35, have been undertaken in the last (sixth) chapter.

Raman spectra of all the samples have been recorded using Jobin-Yvon laser Raman spectrometer on Ramanor U 1ØØØ & HG2S models. Argon ion laser line of 5145 A° has been used as the exciting radiation. For recording the IR spectra of the glass samples, Perkin-Elmer model 681 infrared spectrophotometer has been used.

The structure of vitreous (v) B_2O_3 has been under investigation for a long time . There is increasing evidence, experimental as well as theoretical, that the structure consists of a network of planar BO_3 triangles, many of them grouped together in threes, to form planar hexagonal "boroxol" (B_3O_6) rings. The Raman spectrum of pure v-B_2O_3 is characterized by a strong and narrow (full width at half maximum is about 15 cm^{-1}) peak near 8Ø6 cm^{-1} which is now unambiguously assigned to the boroxol ring oxygen atom breathing vibrations with little motion of the boron atom involved. The IR spectra of v-B_2O_3 also shows this band around 74Ø-835 cm^{-1} . The low frequency Raman spectrum of v-B_2O_3 is characterized by an unpolarized broad feature at 26 cm^{-1} (known as boson peak). This is a common feature in borate glasses and arises due to an increase in the Bose-Einstein

thermal population number $n(\omega)=1/[\exp(h\omega/kT)-1]$, ω being the Raman shift and the short structural correlation range in the glass structure. The Martin-Brenig model has been applied to interprete the low frequency Raman spectrum. This model attributes the low frequency boson peak to structural disorder which affects the Raman coupling coefficient C_b appearing in the Stokes Raman intensity expression,

$$I_{obs} = C_b[n(\omega,T) + 1]\, g_b/\omega \qquad (1)$$

where g_b is the vibrational density of states for the band b. The frequency (ω) dependence of C_b adapted to the right angle scattering geometry in the VH configuration is given by

$$C_b = A\omega^2\, [3(v_l/v_t)^5 \exp\{-(2\pi c\omega)^2\sigma^2/v_t^2\}+2 \exp\{-(2\pi c\omega)^2\sigma^2/v_l^2\}] \qquad (2)$$

where A is a constant, v_l and v_t are the longitudinal and transverse acoustic velocities, 2σ is the structural correlation range (SCR) in glass structure. The SCR (2σ) value in v-B_2O_3 structure has been estimated from equation (2) to be 7.26 A°. The values of C_b as calculated from equation (2) have been compared with the experimental C_b values obtained from equation (1) as,

$$C_b = I_{obs}.\omega\ /g_b[n(\omega,T)+1]$$

in the Debye approximation where the density of states $g_b=\omega^2$.

Though the structure of v-B_2O_3 mainly comprises of a

network (matrix) of boroxol (B_3O_6) rings, it essentially consists of BO_3 triangles. The introduction of MO (M=Ca, Sr, Ba & Cd) to the v-B_2O_3 matrix causes a change in the boron atom coordination number from 3 to 4 according to the following scheme:

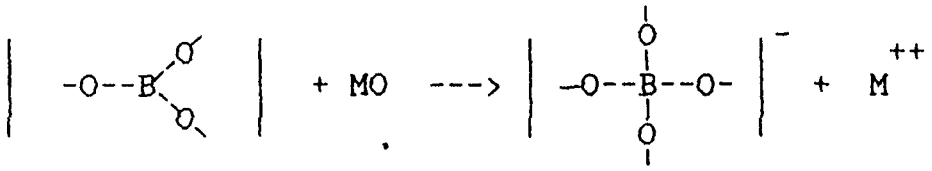

This mechanism liberates cations (M^{++}) to increase the ionic conductivity of the glass. The experimental evidence of such a process is the appearance of a Raman band around (78Ø-755 cm^{-1}) in borate glasses with a corresponding decrease in intensity of the band at 8Ø6 cm^{-1}.

Raman and IR spectra of alkaline earth borate glasses in the system $xMO.(1-x)B_2O_3$ with M=Ca,Sr,Ba and Cd for concentration range Ø.2Ø ≤ x ≤ Ø.5Ø, show experimental evidence of glass network modifying nature of MO (M=Ca,Sr,Ba & Cd) in borate matrix. The gradual increase of concentration of MO in v-B_2O_3 causes not only a change in boron coordination but also results in the formation of complex structural groups comprising of BO_4 and BO_3 units. The type and distribution of these structural groups change with gradual increase of concentration of MO. For lower concentration of MO, x<Ø.35, triborate, pentaborate and tetraborate cyclic groups containing BO_3 and BO_4 units are predominantly formed where as, at higher

concentration, x>Ø.35, di-triborate, diborate cyclic groups are predominant along with some fractions of meta-, pyro-, orthoborates and weakly coupled BO_4 units, mostly associated with non-bridging oxygens (NBOs). At x=Ø.35 (for Ca & Ba), Raman spectra shows that the glass network becomes saturated in the conversion of boron coordination from triangular to tetrahedral.

Cations liberated take their places in the interstitial vacancies of the network near the NBOs or BO_3 triangles. At higher concentrations, the decrease in intensity of the band centered around 76Ø cm^{-1} with the corresponding increase in intensity of other bands, clearly indicates that the complex cyclic groups, i.e., di-triborate or diborates, undergo destruction to form linear groups, e.g., pyro-, ortho-, metaborates etc. with NBOs and the larger size of cations tend to break up the network in accomodating themselves in the interstices of the glass matrix. The glass structure becomes more randomized. The developement of the bands in the region 275-425 cm^{-1} related to the cation motions in the non-bridging oxygen sites, confirms the above argument at higher MO content in these borate glasses (The non-bridged oxygens get influenced by the cations interstitially accomodated).

In calcium borate glasses, at higher concentrations (x=Ø.5Ø), chain type metaborates are found to be formed at the cost of di-triborates. The shifting of the Raman band at 652

cm^{-1} towards higher wave number at ~ 687 cm^{-1} shows the conversion of ring type metaborate to chain type metaborate. In barium borate glasses, the broad feature around 1447 cm^{-1} becomes sharper (at x=Ø.5Ø) and shifts to 1433 cm^{-1} (also observed in IR spectra). This shows the formation of greater number of $B_2O_5^{4-}$ and BO_3^{3-} groups involving $B\text{-}O^-$ units in the glass. The large cation size of Ba^{++} ions enhances the number of NBOs which is supported by the developement of the band at 424 cm^{-1} associated with the motions of Ba^{++} ions. Barium ions are expected to occupy sites near the non-bridged oxygens.

In strontium borate glasses, the network modification becomes saturated in its coherence degree at the concentration of x=Ø.25, which is different in nature from other alkaline earth modifiers. The invariance of the position of 772 cm^{-1} band along with its intensity decrease for increasing concentration x of SrO upto x=Ø.3Ø, shows some characteristic which is unique for this system. However, from the general appearance of the spectra of these alkaline earth borate glasses, the similar characteristic features are obvious. The low frequency wing of Raman spectra of the borate glasses is characterized by the boson peak whose position varies in the range 25-1ØØ cm^{-1} in these borate glasses. In strontium borate glasses, the structural correlation ranges (SCR) are calculated tentatively using Martin-Brenig model (cited earlier).

The introduction of MCl_2 (M=Sr & Ba) into the binary borate matrix does not modify substantially the vibrational dynamics of the binary glass $xMO.(1-x)B_2O_3$ (M=Sr & Ba) in the region above 3ØØ cm^{-1}. However, the addition of MCl_2 to the binary glass causes a noticeable modification in the low frequency region of Raman spectra. The low frequency Raman scattering intensity increases considerably with rise of concentration (y) of MCl_2 and the boson peak shifts towards higher wave number; of course, no new bands arise in the region 12-16ØØ cm^{-1}. The addition of MCl_2 helps either in the formation of BO_4 groups or it takes part in the formation of tetrahedral units, like BO_3Cl. However, the above changes correspond to the more randomization of the glass network and Ba^{++} (or Sr^{++}) and Cl^- ions in the ternary glass leads to an expansion of the network structure.

The cadmium borate binary sample does not form a glass at concentration of less than x=Ø.2Ø. The Raman spectrum of cadmium borate glass of composition $Ø.35CdO.Ø.65B_2O_3$ shows a splitting of the band at 8Ø6 cm^{-1} for $v\text{-}B_2O_3$, such that the band at 775 cm^{-1} due to the formation of cyclic borate groups containing BO_4 and BO_3 units, just begins to appear at this composition. This situation is different in nature from the alkaline earth borate glasses where the band at 8Ø6 cm^{-1} disappears at this composition. This idicates that the structure

of cadmium borate glass is different from that of alkaline earth borates.

In cerium di oxide doped calcium borate glasses, the appearance of the Raman band near 649 cm^{-1} for different concentration (y) of CeO_2 has been asssigned to the motion of metaborate groups. A similar band at 665 cm^{-1} for the binary calcium borate glass also appears in IR spectrum which shifts to 71Ø cm^{-1} along with the substantial increase in its intensity as a result of addition of CeO_2 to the binary calcium borate system $xCaO.(1-x)B_2O_3$. This shift of the band from 665 cm^{-1} to 71Ø cm^{-1} indicates that the metaborate chain is formed. Also the disappearance of the bands at 778 and 8ØØ cm^{-1} due to cyclic borate rings formed in the binary calcium borate glass, shows the absence of cyclic borate rings in CeO_2 doped calcium borate glass. Thus it is concluded that chain type metaborate groups are most probable in CeO_2 doped calcium borate glasses and also it is obvious that CeO_2 acts as modifier in these borate glasses in the composition range $Ø.2Ø \leq x \leq Ø.35$ and $Ø \leq y \leq Ø.1Ø$.

Finally, the invstigations on oxide glasses containing two or more different glass network formers have been performed with specific interest in the case of vanadium borate glass systems where V_2O_5 and B_2O_3 are both glass former oxides. The Raman spectra of vanaium oxide doped calcium borate glasses in the system $(V_2O_5)_y.[xCaO.(1-y-x)B_2O_3]_{1-y}$ for x=Ø.2Ø & Ø.35 and

y=Ø, Ø.Ø5, Ø.1Ø & Ø.15, show that the bands at 8ØØ and 778 cm^{-1} due to cyclic borate groups containing BO_3 and BO_4 units respectively, appear as a result of addition of V_2O_5 (y), along with the corresponding abrupt growth of a broad and intense band around 942 cm^{-1}. Also, with rise of concentration (y) of V_2O_5, these bands at 8ØØ and 778 cm^{-1} disappear and the band at 942 cm^{-1} becomes predominant in the spectra. Calcium (Ca^{++}) ions enter interstitially into the vanadate chains by interacting directly with V=O bonds. The CaO causes the appearance of series of complexes consisting of VO_4 polyhedra. With rising concentration (y) of V_2O_5, the intensity of the band around 942 cm^{-1} again decreases with the appearance of new bands around 75Ø cm^{-1} (due to the formation of the complex B-O-V-O-B) and 85Ø cm^{-1} (associated with pyroborate groups) in the spectra and all other bands tend to disappear. These observations indicate that the two glass formers B_2O_3 and V_2O_5 form a quasi-complex in the concentration range $Ø.Ø5 \leq y \leq Ø.15$ and V_2O_5 acts as modifier up to the concentration y=Ø.Ø5 in the calcium borate glass of composition $Ø.2ØCaO.Ø.8ØB_2O_3$. However, on comparing the Raman and IR spectra of these glasses in the system $(V_2O_5)_y.[xCaO.(1-y-x)B_2O_3]_{1-y}$ and also with the spectra of each corresponding separate systems, it appears that the Raman spectra of these glasses containing two glass forming oxides are not simple addition of the spectra of each system.

LASER RAMAN SPECTROSCOPIC STUDIES OF BINARY AND TERNARY BORATE GLASSES

THESIS

SUBMITTED FOR THE DEGREE OF

Doctor of Philosophy

IN

PHYSICS

BY

MD. HAFIZUR RAHMAN

DEPARTMENT OF PHYSICS
ALIGARH MUSLIM UNIVERSITY
ALIGARH (INDIA)

1992

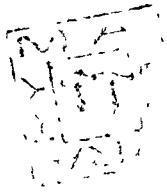

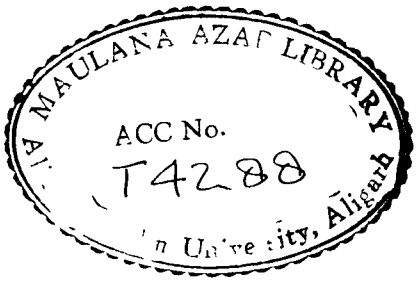

T4288

27 JUN 1994

DEDICATED
TO MY
PARENTS

Professor of Physics
and Chairman of the Department

DEPARTMENT OF PHYSICS
ALIGARH MUSLIM UNIVERSITY
ALIGARH, U.P. (India)
Tel. No. 29001

September 28, 1992

CERTIFICATE

This is to certify that the thesis entitled **Laser Raman Spectroscopic Studies of binary and ternary borate glasses** being submitted by **Mr. Md. Hafizur Rahman** for the award of the Degree of Doctor of Philosophy in Physics of this university is a record of original research work done by him under my supervision.

(PROF. B.N.KHANNA)
RESEARCH SUPERVISOR

PUBLICATIONS

IN JOURNAL:

[1] Raman spectral investigation of alkaline earth borate glasses in the system $xMO.(1-x)B_2O_3$ where M=Ca,Sr,Ba & Cd.
M.H. Rahman, Y. Kumar and B.N. Khanna,
Indian J. Pure & Applied Physics, 30 (1992) 327.

[2] Raman spectra of $v-B_2O_3$, soda borate and calcium borate glasses.
M.H. Rahman, B.P.Dwivedi, Y. Kumar and B.N. Khanna,
Indian J. of Physics, 1991 [accepted]

[3] Raman scattering study of lithium borate glasses.
B.P. Dwivedi, M.H. Rahman, Y. Kumar and B.N. Khanna,
Journal of Phys. and Chem. of Solids (GB), 1992 [accepted]

[4] Inelastic light scattering in strontium borate glasses in the system $xSrO.(1-x)B_2O_3$ and $(SrCl_2)_y.[xSrO.(1-y-x)B_2O_3]_{1-y}$.
M.H. Rahman, B.P.Dwivedi, Y. Kumar and B.N. Khanna,
Pramana J. of Physics, 1992 [accepted]

[5] Low frequency Raman spectra of barium borate glasses in the system $(BaCl_2)_y.[(BaO)_x.(B_2O_3)_{1-y-x}]_{1-y}$ for various x and y.
M.H. Rahman, B.P.Dwivedi, Y. Kumar and B.N. Khanna,
Spectrochimica Acta A (UK), 1992 [accepted]

IN SEMINAR AND CONFERENCES:

[1] Raman and I.R investigation of silver borate glasses in the system $xAg_2O.(1-x)B_2O_3$.
XIII International Conference on Raman Spectroscopy, Sept., 1992 Germany [accepted]

[2] Laser Raman investigation of lithium borate glasses in the system $xLi_2O.(1-x)B_2O_3$.

National Seminar on Vibrational Spectroscopy (Meerut University). 9-10 May 1992, Abstract no.- 28, p-22

[3] Inelastic light scattering in glasses in the system $y(SrCl_2).(1-y)[xSrO.(1-x)B_2O_3]$

National Seminar on Vibrational Spectroscopy (Meerut University), 9-10 May 1992, Abstract no.- 30, p-23

[4] Vibrational dynamics of lithium borate glasses.

XXI. European Congress on Molecular Spectroscopy, Aug 23-28 1992 Vienna, Austria [accepted]

[5] Infrared studies of the structure of silver borate glasses.

in Solid State Ionics of Materials and Applications, eds B.V.R. Chawdari, S. Chandra & Shri Singh (Publisher, World Scientific, 1992) p-521.

[6] Vibrational dynamics of calcium borate glasses containing cerium di oxide.

in Solid State Ionics of Materials and Applications, eds. B.V.R. Chawdari, S. Chandra & Shri Singh (Publisher, World Scientific, 1992) p-515.

WINTER SCHOOL:

[1] Indo-French winter school on Laser spectroscopy and applications, I.I.T., Delhi, 22-23 Jan. 1992

ACKNOWLEDGEMENTS

I have no words to express my deep sense of gratitude and indebtedness to my supervisor **Prof. B.M. Khanna**, Chairman, Department of Physics, Aligarh Muslim University, Aligarh, India, for his constant guidance, invaluable suggestions, encouragement and over all keen interest through out the course of research work and also for extending all the facilities that were required from the Department for the completion of this work.

I heartily acknowledge the cooperation and financial assistance provided by the Coordinator, DSA/COSIST (UGC), Department of Physics, A.M.U., Aligarh. In this connection I would like to give sincere thanks to Prof.M.Z. Rahman and Prof. Israr Ahmed for their cooperation.

I am very much thankful to **Prof. Thyagrajan**, Head, R.S.I.C., I.I.T., Bombay, where a major part of the experimental work had been accomplished.

This is a great opportunity to express sincere sense of gratitude with many thanks to Dr. Y. Kumar, Reader in Physics and Mr. B.P. Dwivedi, Research Scholar, who were always in touch to cooperate with me.

I would like to remember the encouragement by gesture etc. of all the teachers and research scholars of the department,

especially Dr. P.K. Verma, Dr. K.A. Mohammed, Dr. Shabbir Ahmed and research scholars of the Spectroscopy laboratory. I also acknowledge the cooperation and help of Mr. Rahimuddin, technical assistant and Mr. Chandra Sen of the laboratory.

May I recollect the encouragement of my Bangladeshi colleagues, Mrs. Nazma Akhtar Banu, Mr. Mohd. Abul Hossain, Mr. Sirajuddin Ahmed and Mr. Nimai Chan Biswas.

Finally I would like to thank the Govt. of India for providing the cultural scholarship and to the Govt. of Bangladesh for granting me deputation to be on higher studies.

At length, I find no words to express my regards to my parents for their boundless affection, encouragement and support through out the research work and deeply feel the patience of my wife and daughter, Noor-e-Hafza during their stay at Aligarh.

DATE: Sept. 26, 1992

MD. HAFIZUR RAHMAN

CONTENTS

CHAPTER I

INTRODUCTION

CHAPTER II

EXPERIMENTAL METHODS

CHAPTER III

SPECTRAL INVESTIGATION OF BORIC OXIDE GLASS

CHAPTER IV

VIBRATIONAL STUDIES OF ALKALINE EARTH BORATE GLASSES

CHAPTER V

RAMAN AND IR STUDIES OF CeO_2-DOPED CALCIUM BORATE GLASSES

CHAPTER VI

SPECTRAL STUDIES OF V_2O_5-DOPED CALCIUM BORATE GLASSES

CHAPTER I

INTRODUCTION

1.1 General

Spectroscopic studies of the structure of polyatomic molecules are generally complex in nature because of the fact that they involve simultaneous determination of several molecular parameters, i.e electronic charge distribution, harmonic and anharmonic vibrational constants arising from different types of force fields binding the atoms and the rotational constants obtained from the fine structure of a typical vibrational band.

At present the field of glass is extremely exciting and promising for many reasons. There are new glasses, products and processes. Many new experimental and mathematical techniques and ideas have appeared in the last few years. However, the glassy disordered state of matter is a non-equilibrium system which lacks long range order of atomic arrangements. For such a system, a space correlation function is needed to describe the relative positions of the atoms in the structure. Such a correlation function, though mathematically exact, can only be measured with a limited resolution. As a result, its interpretation is ambiguous: since it is a one dimensional representation of a three dimensional structure.

Vibrational spectroscopy is one of the most powerful

techniques for studying the structure of glasses. It is particularly useful for probing vibrational motions of non-bridging atoms/ions or weakly coupled bridging atoms. The vibrational spectra may also be compared with calculations based on models to yield more direct short range or to some extent, intermediate range structural data.

Among the various experimental methods pertaining to the vibrational studies (i.e., infrared absorption or reflection, Raman scattering, inelastic neutron scattering and Brillouin scattering etc), the present thesis will be mainly concerned with Raman and infrared measurements. In these investigations, either directly or through comparison between spectral data and model calculations, structural information can be extracted. For crystalline solids, the factor group[1] and the site group approaches[2] are usually employed to understand the nature of the spectra in different orientations of the crystal and make appropriate assignments to the bands obtained there in. But in the case of non-crystalline materials, the approximate analogs of the previous methods - the "lattice" (delocalized)[3,4] and the "fundamental structural unit" models[5,6], respectively do not give any useful information about the amorphous materials due to their severe limitations.

In the large cluster model calculations of Bell and Dean[7] applied to v-SiO_2, v-GeO_2 and v-BeF_2[8], a good agreement was obtained with experimental results from X-ray and neutron

diffraction studies. But the model faces a severe handicap when applied to the IR and Raman measurements. However, the outcome of these studies revealed that neither a purely molecular approach nor that based on the use of crystal lattice dynamics may be able to give reliable information about the vibrational modes. Some extended models[8] need to be used.

Vibrational spectra can be calculated from computer generated models using, for example, molecular dynamics simulation techniques. Reasonable agreement has been obtained in some cases[9]. Although such numerical methods provide a satisfactory solution to the vibrational problem in glass networks, little physical insight is furnished simultaneously. A molecular model developed by Lucovsky and Martin[10], for the case where the anionic bridging angles are close to $\Pi/2$ and coupling between structural units is weak, has been used successfully to explain the optic modes of chalcogenide glasses of the types As_2X_3 (X=S,Se,Tl).

More recently, Sen and Thorpe[11] developed a random network model for AX_4 tetrahedra with nearest neighbor central force for the determination of vibrational density of states of the glasses, such as SiO_2, in the high frequency region. This model predicted that, as the A-X-A angle increases from $\Pi/2$ to Π, the character of the vibrational modes changes from purely molecular to band-like behaviour. Very simple expressions were obtained for the positions of the main peaks in the vibrational density of states as functions of the bridging angle and force constant. However

calculations for v-B_2O_3 were unable to explain the observed Raman peaks[12]. The phonon spectrum can also be obtained by using the analytical method of "cluster-Bethe-lattice"[13,14] model wherein a number of different versions of this lattice can be used to terminate a glass network. Good agreement with experiment was obtained for several non-crystalline materials, such as a-Si and others[13].

It may. however, be mentioned that no single theory is universally applicable to predict the vibrational spectra of non-crystalline solids. One has to resort to the specific types of models more suited to a typical amorphous network in order to explain the experimentally observed spectra.

The advent of laser era, which is able to provide a highly coherent, intense, monochromatic and polarized beam of light, led to a renaissance in the field of Raman spectroscopy. Moreover, the recent advances in the field of computers and microprocessor based systems have led to a rapid growth of the Fourier transform infrared spectroscopy resulting in greater throughput and better resolution in the infrared region. While a large number of investigations in the past had been carried out on a larger variety of glass systems[15,16] in the mid infrared region, it is only recently that spectral studies in the low frequency region using Raman and IR techniques are made possible due to the technological advances. Studies on some of the low frequency vibrational modes are motivated by their close relationship

associated with thermal,acoustic and dielectric properties. The temperature range of investigations have also been extended from low to the high temperature domains.

The boric oxide (B_2O_3) is a well known network former oxide glass. The investigations reported in this thesis have been carried out on both binary and ternary borate systems. The binary systems studied here are $xMO.(1-x)B_2O_3$, where M = Ca,Sr,Ba and Cd and the ternary systems are obtained by doping alkaline earth chlorides, rare earth and transition metal oxides into the above binary systems. The low frequency Raman scattering in these borate glasses has been interpreted on the basis of Martin-Brenig model[17]. As a complementary to this Raman investigation, IR spectral studies of the same have also been performed.

1.2 Scope of borate glasses

Vitreous (v) B_2O_3 is a transparent hygroscopic glass whose refractive index in the visible region is ~ 1.48 which is nearly the same as that of v-SiO_2 (μ=1.46). It has important technological applications as an additive in SiO_2 based bulk glasses. Also doped borate glasses (such as, alkali-, alkaline earth-, transition metal-, or rare earth ion doped glasses) have some characteristics of considerable importance for applications in optical data transmission, signal detection, sensing and other laser technologies.

The number of borate glasses identified is continuously

increasing and their use is now wide spread in diverse fields. Interest in borate glasses has grown due to the realization that these systems could be used as fast-ion conductors[18,19]. In glassy electronic conductors, the control of the type of charge carriers has been achieved and the formation of p-n junction between these glasses has been reported[20]. The amorphous ionic conductors have several advantages[21] in comparison with the crystals, such as they show higher conductivities over a wide range of glass forming systems, exhibit isotropic properties having no grain boundaries along with the ease of giving them any shape and dimensions. In fact, the proportion of papers concerning the glassy electrolytes is increasing rapidly at international meetings on solid state ionics[22], highlighting the impportance of this field of research.

Ionic conductors in non-crystalline solids are called in several ways: glassy or vitreous electrolytes, fast ion conducting glasses, superionic conducting glasses, superionic glasses and so on. Li^+, Na^+, K^+, Ag^+, Cu^+ and F^- are the ions reported to migrate rapidly in glasses. Rapidly quenched glasses based on V_2O_5 have intensively been investigated in recent years as the cathode materials in the rechargeable cells of the type

"Li/Li^+-electrolyte / V_2O_5-based glass"

Fig.1.1 shows an example of the cycling behaviour of 145 times in the charged cell of the type[23],

"$Li/1.5M\ LiAsF_6$ - 2MeTHF/95% V_2O_5 . 5% P_2O_5 glass"

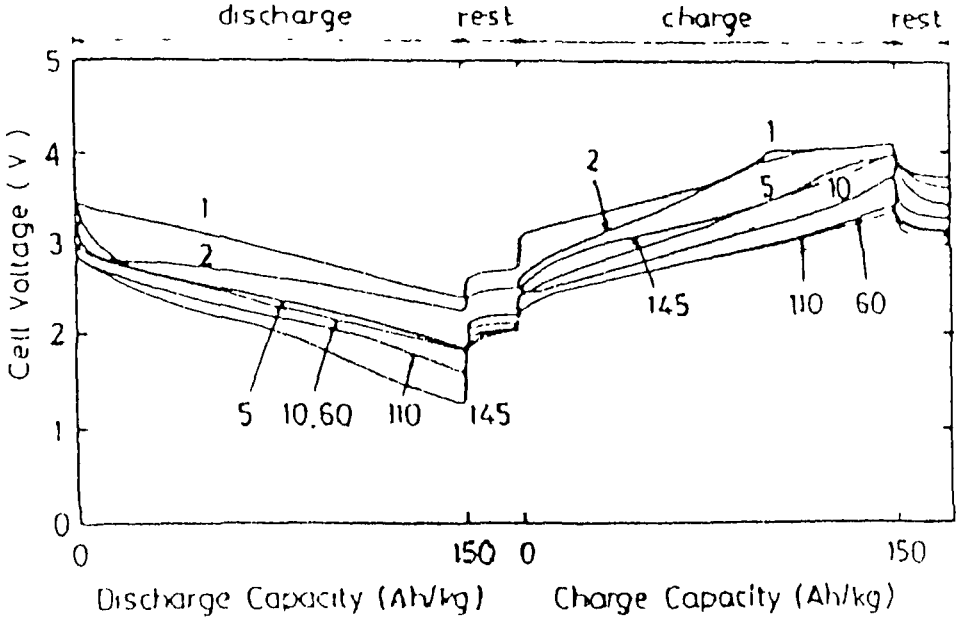

Fig. 1.1 Cyclic behaviour of the cell (based on rapidly quenched glass) at 1 mA/cm^2. Numerals in the figure are cycle numbers (ref.23).

Good reversibility is seen and thus the glass materials are superior as cathode materials in secondary cells as compared to crystalline materials because of their smaller volume change accompanying the intercalation-deintercalation (discharge-recharge cycles.

1.3 Glass transition in amorphous materials

The "amorphous" state of matter is any condensed phase which lacks long range order according to diffraction criterion (x-ray,neutron and electron)[24]. The terms "glassy" and "vitreous" are synonymous and are described to be a restricted class of amorphous materials. A glass is an amorphous[25] solid which exhibits "glass transition" and this "glass transition" is defined as "the phenomenon in which a solid amorphous phase exhibits, with changing temperature, a more or less sudden change in the derivative thermodynamic properties, such as heat capacity and expansion coefficient, from crystal like to liquid like values". A glasss transition is normally menifested by a marked change in viscosity, specific heat and thermal expansion coefficient within a narrow temperature interval. The glass transition temperature is defined as the temperature Tg at which the viscosity of the material becomes very high ($>10^{13}$P). The glassy state is considered to be an extension of the liquid state and is regarded as a disordered solid. The transition from liquid to glassy state may be a thermodynamic phase transition that is influenced

by kinetic effects.

Though there are different models[26] to describe the glass transition phenomenon, the lattice model given by Gibbs and Di-Marzio[27] can be considered here. The theory of this lattice model deals with the glass forming linear polymer chains consisting of backbone units. Rotation of single bonds around each backbone unit is hindered and this gives rise to potential wells in rotational space separated by different barrier heights. The bond spends almost all of its time librating around the minimum of one or another of the potential wells. A configurational state is assigned to describe the state of the whole system and it is assumed that, below Tg, the whole system is frozen into one configurational state that is, in one such minimum. Above Tg, the liquid state explores the possibility of settling into higher configurational states. Each configurational state is associated with a set of vibrational and librational states which are the internal modes of the system. Goldstein[28] used a different kind of molecular mechanism which is based on the assumptions that (i) the heights of the potential minima associated with different configurational states are sufficiently close to each other and at a temperature near Tg, the system remains trapped in one of the minima, (ii) the lattice vibrational properties are characterized by a Debye characteristic frequency, which is a function of temperature, (iii) the lattice frequencies could change at higher temperatures because the potential minima associated with

different configurational states might have different curvatures, and (iv) a change in anharmonicity occurs at high temperature with changing structural states.

1.4 Vibrational spectra of a molecule

The total energy of a free molecule may be associated with its electronic, vibrational and rotational motions, provided the contribution due to the translational motion is negligible. Normally the pure rotational spectrum associated with the transitions between the quantized rotational levels of a molecule appears in the range 1-100 cm^{-1}, whereas its pure vibrational spectrum due to the transitions between the vibrational levels is observed in the range 10^2-10^4 cm^{-1}. The electronic spectrum associated with the transitions between electronic levels is, however, observed in the range 10^4-10^5 cm^{-1} i.e., in the visible and ultraviolet region. In some cases the borders may easily be crossed, where the vibrational spectrum (of a heavy molecule) lies in the far infrared region.

For a particular electronic state, the charge distribution, during the pure vibrational motion of a molecule, undergoes a periodic change and therefore, in general (though not always), the dipole moment changes periodically. Since, in the harmonic oscillator approximation, any vibrational motion of a molecule may be resolved into a sum of normal vibrations with appropriate amplitudes, the normal frequencies are the frequencies that are

emitted or absorbed by the molecule under the influence of the external electro-magnetic radiation. These frequencies usually lie in the near infrared.

Consider the transition between the two vibrational levels v' and v'' of the molecule interacting with the radiation field. Here v' and v'' stand for the sets of the vibrational quantum numbers v_1', v_2', v_3',---and v_1'', v_2'', v_3'',--- of the upper and lower states respectively for a polyatomic molecule. The total eigen function is the product of the electronic, vibrational and rotational eigen-functions:

$$\psi_{total} = \Psi_e \Psi_v \Psi_r \qquad (1.1)$$

For a particular electronic (ground) state, when rotational effects are neglected, the total eigen function may be written as,

$$\psi_{total} = \Psi_e \Psi_v$$

Considering that the electronic wave function is normalized to unity, the vibrational transition probability can be expressed as,

$$[M]^{v'v''} = \int \Psi_{v'} \Psi^*_{v''} M \, d\tau \qquad (1.2)$$

where $\Psi_{v'}$ and $\Psi_{v''}$ are the vibrational eigen functions of the upper and lower states respectively and M is the dipole moment vector with its components M_x, M_y amd M_z. $[M]^{v'v''}$ is called the transition moment of the transition v' <———> v''.

The vibrational selection rules exist only when the molecule under consideration has elements of symmetry. It is clear that the integral of equation(1.2) can be different from zero for a certain transition when at least one of the components of the integrand of

equation (1.2) remain unchanged for any of the symmetry operations permitted by the symmetry of the molecule in its equilibrium position or in other words, when at least one of the quantities

$$\Psi_v,\ \Psi_v^*,,\ M_x\ ,\quad \Psi_v,\ \Psi_v^*,,\ M_y\ ,\quad \Psi_v,\ \Psi_v^*,,\ M_z$$

is totally symmetric. This is the general selection rule for the vibrational transitions in the infrared which is rigorous as long as the interactions with rotation and electronic motions are neglected.

In the case of Raman scattering, the intensity of the scattered light depends on the induced dipole moment P per unit volume, which is represented by the matrix formed from the integrals

$$\int \Psi_n\ P\ \Psi_m\ d\tau \tag{1.3}$$

where the components of P are given by

$$\begin{aligned} P_x &= \alpha_{xx}E_x + \alpha_{xy}E_y + \alpha_{xz}E_z \\ P_y &= \alpha_{yx}E_x + \alpha_{yy}E_y + \alpha_{yz}E_z \\ P_z &= \alpha_{zx}E_x + \alpha_{zy}E_y + \alpha_{zz}E_z \end{aligned} \tag{1.4}$$

where, α_{xx} , α_{xy} ,------ are called the components of the polarizability tensor α.

The time independent part of equation (1.3) is

$$[P^o]^{nm} = \int \Psi_n\ P^o\ \Psi_m\ d\tau \tag{1.5}$$

where, P^o is the amplitude of P. The intensity of a Raman transition n <———>m is proportional to the square of $[P^o]^{nm}$. Substituting P from equation (1.4) we obtain for the components of $[P^o]^{nm}$:

$$[P_x^o]^{nm} = E_x^o \int \alpha_{xx}\Psi_n\Psi_m^* d\tau + E_y^o \int \alpha_{xy}\Psi_n\Psi_m^* d\tau + E_z^o \int \alpha_{xz}\Psi_n\Psi_m^* d\tau$$
$$[P_y^o]^{nm} = E_x^o \int \alpha_{yx}\Psi_n\Psi_m^* d\tau + E_y^o \int \alpha_{yy}\Psi_n\Psi_m^* d\tau + E_z^o \int \alpha_{yz}\Psi_n\Psi_m^* d\tau \quad (1.6)$$
$$[P_z^o]^{nm} = E_x^o \int \alpha_{zx}\Psi_n\Psi_m^* d\tau + E_y^o \int \alpha_{zy}\Psi_n\Psi_m^* d\tau + E_z^o \int \alpha_{zz}\Psi_n\Psi_m^* d\tau$$

where E_x , E_y and E_z are the components of the amplitude of the incident light wave and the integrals

$$[\alpha_{xx}]^{nm} = \int \alpha_{xx}\,\Psi_n\,\Psi_m^*\, d\tau, \text{ etc.} \quad (1.7)$$

are the matrix elements of the six components of the polarizability tensor. The diagonal matrix elements (n=m) of α or P^o correspond to Rayleigh scattering, while the off-diagonal matrix elements correspond to the Raman scattering i.e., to transitions n <——> m induced by the incident light. According to equation (1.6) a Raman transition n <——> m is allowed if at least one of the six quantities

$$[\alpha_{xx}]^{nm} , [\alpha_{yx}]^{nm} , \text{----}$$

is different from zero.

For vibrational Raman scattering we have to substitute for Ψ_n and Ψ_m vibrational eigen functions Ψ_v,and $\Psi_{v''}$ of the upper and lower states. Thus a Raman transition between the two vibrational levels v' and v'' is allowed if at least one of the six products

$$\alpha_{xx}\Psi_{v'},\Psi_{v''} , \alpha_{xy}\Psi_{v'},\Psi_{v''} ,\text{-----} \quad (1.8)$$

is totally symmetrical, that is, remains unchanged for all symmetry operations permitted by the symmetry of the molecule in its equilibrium configuration.

The general (and rigorous) Raman selection rule may be

stated as:

"A Raman transition between two vibrational levels v' and v'' is allowed if the product Ψ_v, $\Psi_{v''}$ has the same species as at least one of the six components α_{xx} ,α_{xy} ,-- of the polarizability tensor".

1.5 Vibrational spectra of amorphous glass

Zwanzig[29] showed that, in a disordered system of amorphous materials, a phonon like excitation (as in crystalline substances) can be defined using forces and momenta as the system coordinates and that such a concept is useful when structural relaxation times are relatively long, just as in moderately viscous liquids and glasses. The existence of the vibrational quantum states for the glassy solids is required by their crystal like behaviour of heat capacity at low temperatures. In a disorderd solid, the molecules move in an effective potential. This potential can be approximated by a harmonic potential where the intermolecular restoring forces are linear in the displacement from the equilibrium. As long as this approximation remains valid, the molecule participates in the harmonic vibrations and one can describe these (coupled) motions in terms of normal modes of oscillations. The change in the polarizability is due to the stretching, bending etc. of the chemical bond. If the displacements of the molecules are small, the linear approximation of the polarizability is adequate (Fig.1.2a) where r is the

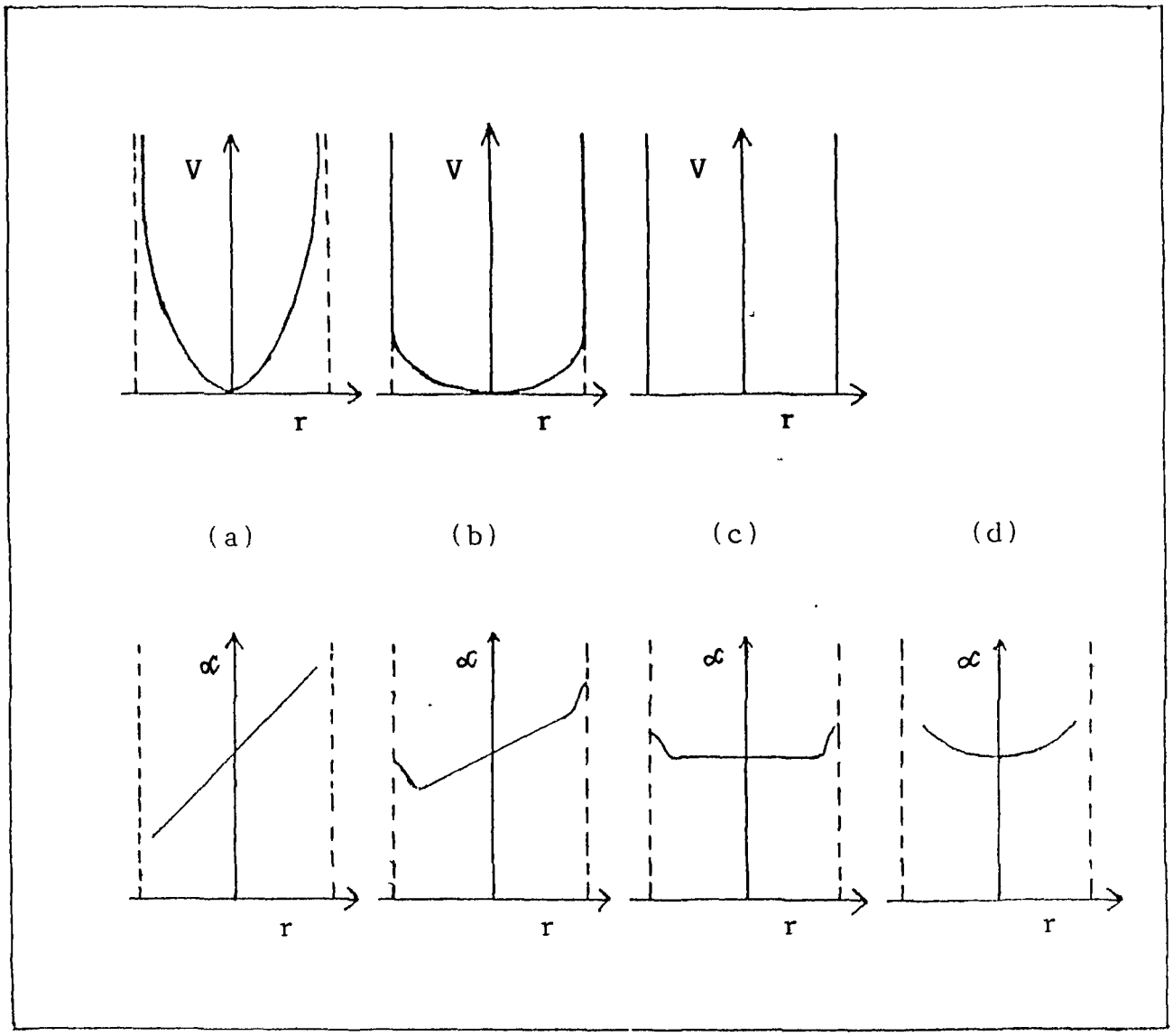

Fig.1.2 Models for the intermolecular potential V and polarizability α versus molecular coordinate r.

intermolecular coordinate, V is the effective potential and α is the polarizability. The r dependence of α is valid if the molecular state does not possess a center of inversion symmetry. Such a microscopic system leads to the disorder-allowed vibrational scattering in amorphous materials[30]. If the molecule is in a site with inversion symmetry then the polarizability must be an even function of displacements (Fig.1.2d) and no first order scattering can be seen. If the variation in polarizability produced by displacements of the molecule is large enough, then there will be second order contributions to the scattering spectrum at sum and difference of frequencies.

At higher temperatures, upper vibrational states are occupied and there is change in the energy and spacing due to anharmonicity of the potential. At a temperature where the material melts, the inter-molecular potential itself changes. A number of bonds are broken and some molecular groups are more weakly bound to their neighbors. For these molecules/groups, the effective potential is a weaker parabola about the equilibrium position. It is still harmonic for small displacements and gives rise to new energy spacings. This should appear in the Raman scattering spectra as a shift to lower frequencies. The effect of anharmonicity on the upper levels would appear as a shift in scattering spectra to higher frequencies. For the large displacements, where the core electrons of the molecule and its neighbors give strong repulsion, the potential becomes severely

anharmonic (Fig.1.2b). At the extremes of the displacements where the molecule "overlaps" with its neighbors, one expects an additional and abrupt contribution to the polarizability representing the strong electronic cloud distortions (Fig.1.2b). This rapid change in the polarizability at the end points of the displacement is collision like and contributes to the scattering in the form of collision spectra[31] in addition to the vibrational mode scattering.

If the temperature is further increased (or viscosity lowered), the number of molecules chemically bonded to any of their neighbors decreases until there is essentially no harmonic potential and the polarizability is independent of position except at the end points (Fig.1.2c). Then the quasi-free motions of the molecules cannot be seen in the scattering spectra since only the collisions change the polarizability.

1.5.1 Nature of the spectra of glasses

It has been observed that though some similarities with the spectra of the crystal of the same substance often occur, broad and continuous bands dominate the spectra of the glasses. The lack of periodic symmetry, characteristic of all glasses, results in a broadening of the dispersion curves, frequency (ω) versus wave vector (q), with increasing q corresponding to decreasing phonon life times. Raman scattering of glasses is stronger compared to usual second order Raman scattering in crystal and, for a given

substance is comparable in integrated intensity to the narrow discrete bands which characterize first order scattering in crystals. Disorder in glasses produces a breakdown in the Raman selection rule so that all the vibrational modes are allowed to contribute to the scattering spectra (see section 1.6).

1.5.2 Infrared spectra in glasses

Infrared absorption spectra of glasses can give useful information (both qualitative and quantitative) about the atomic configurations in the glass even though the absorption peaks are broader than is normally the case for crystals. In the past, infrared spectroscopy has been used successfully to investigate the borates, silicates and phosphates glasses[32-36].Quantitatively, the vibrational spectra of several glass systems including borates[37], silicates[38] and phosphates[39] were analysed, based on either the "localized model" or the "lattice model" as summarized in a paper by Borrelli and Su[40]. Simon[41] had pointed out that true vibrational frequencies could be obtained from the reflectance spectra, since reflectivity depends on both refractive index (n) and absorption index, K. In general, absorption measurements alone do not yield the true frequencies; additional data, such as reflectance measurements are neccessary. This can be seen in the formula,

$$I_x/I_\emptyset = n^2 (1+K^2)^{-1} \exp(-\alpha x) \qquad (1.9)$$

in which I_x and $I_\emptyset$ are the transmitted and incident intensities

respectively, α is the absorption coefficient given by,

$$\alpha = 4\pi K/\lambda \qquad (1.10)$$

and the sample thickness, $x << \lambda$, so that no multiple reflections and interferences can take place.

The two fundamental optical constants, n (real refractive index) and K (the dimensionless absorption index or imaginary part of the complex refractive index) may be obtained through Kramers-Kronig[42] analysis of the IR reflectivity data. Such studies have been performed in v-SiO_2, v-GeO_2 and v-B_2O_3[43].

However, on account of the insensitivity of the reflection technique for weak bands and of tedious procedure for evaluation of peak frequencies from reflectance data , most of the infrared studies on glasses are performed using tranmission technique.

IR absorption spectra may be obtained for thin glass films. But reflectivity data is considered more reliable because reflectance is independent of sample thickness. Even without the knowledge of reflectance, the absorption coefficient can be be estimated from the absorbance (A) measured for two specimens of the same material but having different thickness using the relation[44],

$$\alpha(\lambda) = 2.303.[A_1(\lambda)-A_2(\lambda)] / (x_1-x_2) \qquad (1.11)$$

where, A_1 and A_2 are the absorbances at a given wave length λ of two samples of thicknesses x_1 and x_2.

For the direct identification of structural groups, sub-groups and groups with ionic character, IR absorption technique is

most useful. Apart from these, the extent to which the added cations enter the network of the basic glass or reside interstitially or help in the formation/breaking of the bonds in the network, can be assessed with better reliance. For example, in phosphate glasses (Co_3O_4-P_2O_5), IR analysis shows[45] that the bond in P=O is broken to produce P-Co-O-P cross linkages at high CoO contents and also shows the presence of ionized groups, such as PO_4^{3-}.

In the far infrared region , the results of IR absorption in v-B_2O_3 have been plotted[46] as α/ν^2 versus the frequency,ν (here α is the absorption per centimeter). This curve showed a maximum at ν=26 cm^{-1}which is exactly similar to the maximum observed in Raman scattering in v-B_2O_3 at room temperature. The absorption was calculated using the relation,

$$I/I_o = [(1-R)^2 \exp(-\alpha x)]/[(1-R^2) \exp(-2\alpha x) \qquad (1.12)$$

in which I/I_o is the transmission through a sample of thickness, x and R is given by

$$R = (n-1)^2/(n+1)^2 \qquad (1.13)$$

Minami et al[47] have investigated, by IR spectral analysis, the glass structure of (50AgBr.25Ag_2O.25B_2O_3) for samples obtained from both thin film (~ 5μm thick) and KBr pellet. It has been observed that the bands between 945-1010 cm^{-1}, characteristic of BO_4 groups (observed in thin film spectra), displayed almost no frequency shift in KBr matrix spectra whereas, those between 1310-1255 cm^{-1}, characteristic of BO_3 groups (observed in thin

film spectra), were shifted towards higher wavenumbers by about 100 cm^{-1} in KBr pellet spectra. This peak shift may be caused by the ionic exchange between Ag^+ ions and K^+ ions in the KBr powder in the pellet making process. Accompanying the ion exchange, the partial crystallization takes place and new absorption bands appear (in the above case, new bands at 880 and 1325 cm^{-1} appeared). K^+ ions have larger ionic radii than Ag^+ and the exchange of it with Ag^+ ions increases the ionic character between K^+ ions and non-bridging oxygens. In other words,strong partial covalency is present between the Ag^+ ions and the non-bridging oxygens and the bond strength of B-O bonds in BO_3 groups is weaker in original glasses than in ion exchanged samples. Similar ionic exchange have also been reported[48,49].

However, the fact that the peak shift was observed only in the absorption band characteristic of BO_3 groups suggests that non-bridging oxygens are present in BO_3 groups only but not in BO_4 groups. This is experimental evidence for Beekenkamp's postulation[50] that BO_4 groups have no non-bridging oxygens in borate glasses containing both BO_3 and BO_4 groups.

1.6 Theory of Raman scattering

In general, the scattering cross section is proportional to the space-time correlation function[51], G(r,t), which describes the correlation between the presence of a particle in position r'+r at time t'+t and the presence of a particle in position r' and

time t', averaged over r'. When t=Ø, the function becomes g(r). In light scattering, the variations in the local optical dielectric tensor $\varepsilon_{\alpha\beta}(r,t)$ of the medium are taken into consideration. Here the scattering cross sections for all possible experiments are proportional to linear combinations of the space-time Fourier components of the correlation functions of the dielectric fluctuations i.e.,

$$G_{\alpha\beta,\gamma\delta}(r,t) = \langle \Delta\varepsilon_{\alpha\beta}(r',t')\ \Delta\varepsilon_{\gamma\delta}(r'+r,t'+t) \rangle \qquad (1.14)$$

Expanding the dielectric tensor to first order in atomic displacements and expressing the displacements in terms of normal coordinates $Q_j(t)$ for the j^{th} mode, we have,

$$\Delta\varepsilon_{\alpha\beta}(r,t) = \sum_{j=1}^{3N} \{\partial\varepsilon_{\alpha\beta}(r)/\partial Q_j\}\ Q_j(t) \qquad (1.15)$$

Substituting equation (1.15) in equation (1.14), one finds,

$$G_{\alpha\beta,\gamma\delta}(r,t) = \sum_j R_{\alpha\beta,\gamma\delta}(r,j) \langle Q_j(t')\ Q_j(t'+t) \rangle \qquad (1.16)$$

where,

$$R_{\alpha\beta,\gamma\delta}(r,j) = \langle \{\partial\varepsilon_{\alpha\beta}(r')/\partial Q_j\}.\ \{\partial\varepsilon_{\gamma\delta}(r'+r)/\partial Q_j\} \rangle \qquad (1.17)$$

is the spatial correlation function and

$$\langle Q_j(t')\ Q_j(t'+t) \rangle = \hbar/2\omega_j\{n(\omega_j)\exp(i\omega_j t) + [1+n(\omega_j)]\exp(-i\omega_j t)\} \qquad (1.18)$$

Here, $n(\omega_j) = [\exp(\hbar\omega_j/KT) - 1]^{-1}$ is the Bose-Einstein population factor. The equation (1.18) is the time correlation function of the dielectric fluctuations. Equations (1.16-1.18) are quite general. It applies to any vibrational Raman scattering from solids whether crystalline or amorphous. The spatial correlation function R(r,j) of the dielectric fluctuations essentially reflects just

the spatial correlations of the atomic displacements of the normal modes. Hence the correlation range $R(r,j)$ will be that of the mode j.

For a crystal, the function $R(r,j)$ would have a sinusoidal dependence on r with wavelength, $\lambda_j = 2\Pi/q_j$. The light scattering spectrum can only show frequencies ω_j for which the mode j has a wave vector $\mathbf{q}_j$ equal to the scattering vector $\mathbf{q}$. This is the usual "momentum selection rule" for crystals which gives rise to the discrete set of lines seen in the spectra. In amorphous materials, translational symmetry is lost causing the correlation functions to be localized. For the vibrational modes in a glass, it is assumed that (i) the vibrations are harmonic, (ii) the vibrations are coupled to the light through the displacement dependence of the electronic polarizability of the material and (iii) the coherence length of the normal modes is short compared with optical wavelengths.

If it is assumed that the modes have coherence lengths of the order of 1/10th of the optical wavelengths or less, then such modes will not be characterized by a single wave vector and will not give a momentum selection rule. This assumption of a short range for $R(r,j)$ has the immediate consequence that its Fourier transform has a broad flat maximum around $\mathbf{q}=0$ instead of being sharply peaked at a particular wave vector $\mathbf{q}_j$. This will be true for all j, so that the modes of the material can give contribution to the light scattering spectrum.

The spatial Fourier transform of the correlation function, with range Λ_j in the limit $q\Lambda_j<<1$, has the limiting form,

$$\{R_{\alpha\beta,\gamma\delta}(r,j)\}_q = A_{\alpha\beta,\gamma\delta}(j)\Lambda_j^3 \qquad (1.19)$$

which is independent of q. Here A(j) measures the strength of the dielectric modulation of the mode and Λ_j^3 is essentially the volume of the region of coherence of the mode. With this approximation, the space-time components of the dielectric correlations for light scattering wave vectors become,

$$G_{\alpha\beta,\gamma\delta}(q,\omega) = \sum_{j=1}^{3n} A_{\alpha\beta,\gamma\delta}(j)\Lambda_j^3(h/2\omega_j)\{n(\omega_j)\delta(\omega+\omega_j)+[1+n(\omega_j)]\delta(\omega-\omega_j)\} \qquad (1.20)$$

The delta functions $\delta(\omega+\omega_j)$ give the anti-stokes components (upshifted scattered light) and the delta functions $\delta(\omega-\omega_j)$ give the stokes components (downshifted scattered light). The expression (1.20) shows that all modes will contribute to the Raman spectrum of the amorphous materials but with an unknown weighting factor, $[A_{\alpha\beta,\gamma\delta}(j)\Lambda_j^3(h/2\omega_j)]$.

The normal vibrations are expected to fall into broad bands having similar microscopic motions, optical coupling and correlation ranges etc. corresponding to stretching, bending, out of plane bending frequencies. Thus A(j) (Λ_j^3) can be approximated to be a constant for all the modes of a given band. Again, the frequencies are closely spaced. Thus the descrete sums in equation (1.20) can be replaced by the density-of-states functions for each band, where the density of states gives the number of modes per

unit frequency. With these assumptions, the intensity (I) of the stokes components of the Raman spectrum could be represented by the expressions,

$$I_{\alpha\beta,\gamma\delta}(\omega) = \sum_b C_b^{\alpha\beta,\gamma\delta}(1/\omega)\,[1+n(\omega,T)]g_b(\omega) \qquad (1.21)$$

The sum is over all the bands. The coupling constant C_b will depend on the band b. The labels $\alpha\beta$, $\gamma\delta$ indicate the polarization of the incident and the scattered light respectively and $g_b(\omega)$ is the band density of states.

1.6.1 Low frequency Raman scattering and M-B model

The low frequency Raman scattering in most oxide glasses is dominated by an unpolarized broad band known as the "boson peak" whose position varies in the range 25-100 cm^{-1} in borate glasses. It is a common belief that this low frequency peak is basically due to the thermal population increase with decreasing phonon frequency at room temperature counterbalanced with the decrease in the vibrational density of states.

The model of Martin-Brenig[17], applied by Nemanich[52] to some chalcogenide glasses and alloys, attributes this low frequency peak in glasses to structural disorder of the amorphous materials. The structural disorder affects the Raman coupling coefficient C_b of equation (1.21). The important consequence of the model is the direct relationship between the peak position and the coupling coefficient C_b which in turn is related to the structural correlation range (SCR). The M-B model description is as follows:

For solids having both electrical disorder (the spatial fluctuations of the photo-elastic tensor) and mechanical disorder (the spatial fluctuations of the strain tensor), the frequency (ω) dependence of the coupling coefficient C_b is expressed by

$$C_b^{\alpha\beta,\gamma\delta}(\omega) \propto x^2 [g_t(x) E_t^{\alpha\beta,\gamma\delta} + g_l(x) E_l^{\alpha\beta,\gamma\delta}] \quad (1.22)$$

where the variable x is linear in ω,

$$x = 2\pi c\omega\sigma/v_l \quad (1.23)$$

v_l is the longitudinal sound velocity and 2σ is the structural correlation range.

The terms E_t and E_l respectively contain the transverse and longitudinal fluctuations of the elastic and elasto-optic constants, weighted by the Gaussian functions $g_t(x)$ and $g_l(x)$, where,

$$g_l(x) = \exp(-x^2) \quad (1.24a)$$

$$g_t(x) = [v_l/v_t]^5 \exp\{-x^2[v_l/v_t]^2\}. \quad (1.24b)$$

Combining these equations, one obtains the ω dependence of C_b in VH scattering configuration as

$$C_{VH}(\omega) = A\omega^2[3(v_l/v_t)^5 \exp\{-(2\pi c\omega)^2\sigma^2/v_t^2\} + 2\exp\{-(2\pi c\omega)^2\sigma^2/v_l^2\}] \quad (1.25)$$

where A is a constant and v_t is the transverse sound velocity.

The expression (1.25) is derived under the condition that only phonons of wavenumber ω, with

$(2\pi c\omega/v_\mu)\sigma < 1$, for $\mu = l$ or t (1.26)

play a significant role in the scattering. Differentiating the function C_b with respect to ω, one obtains a maximum for C_b at

$$\omega = \omega_{max} = v_t/2\pi c\sigma \quad (1.27)$$

Thus the low frequency peak is attributed to the maximum in Raman coupling coefficient C_b which in turn is related to SCR in glass.

1.6.2 Vibrational density of states

The stokes Raman spectra $I_{obs}(\omega)$ (eqn.1.21), when reduced by the term $\{n(\omega,T)+1\}/\omega$, reflects the density of vibrational states $g_b(\omega)$ modulated by the coupling coefficient C_b:

$$I_{obs}(\omega)/[\{n(\omega,T)+1\}/\omega] = g_b(\omega).C_b(\omega) = I_R \quad (1.28)$$

where, I_R is the reduced Raman intensity,

$$\text{or,} \quad g_b(\omega) = I_{obs}(\omega)/[C_b\{n(\omega,T)+1\}/\omega] = I_R \quad (1.29)$$

Thus the vibrational density of states is expressed in terms of reduced Raman intensity I_R. Here I_R is dependent on the coupling coefficient C_b. If C_b is assumed to have the values 1 and ω^2, then the frequency reduced Raman spectra (I_R^F) would be defined as

$$I_R^F(C_b=\omega^2) = I_{obs}/\omega\{n(\omega,T)+1\} \quad \text{and} \quad (1.30a)$$

$$I_R^F(C_b=1) = I_{obs}.\omega/\{n(\omega,T)+1\} \quad (1.30b)$$

The temperature reduced Raman spectra (I_R^T) is defined, when $C_b=\omega$, as,

$$I_R^T = I_{obs}/\{n(\omega,T)+1\} \quad (1.30c)$$

1.6.3 Structural correlation range

The frequency dependence of Raman coupling coefficient C_b is expressed theoretically by equation (1.25), while experimental values of C_b can be obtained from the reduced Raman intensity I_R (eqn.1.29) as,

$$C_b = I_{obs}(\omega)/[\omega\{n(\omega,T)+1\}] \quad , \qquad (1.31)$$

in the Debye-approximation where the acoustical density of states g_b is proportional to ω^2.

Thus the value of structural correlation range (SCR) can be deduced by fitting the theoretical $C_b(\omega)$ from equation (1.25) to the experimental values (eqn.1.31) or SCR can also be approximated from equation (1.27).

1.7 Structure of borate glasses

Zachariasen[53,54] first proposed the continuous random network model for A_2X_3 system of glasses. In his model A atom is surrounded trigonally by three X atoms (Fig.1.3) and each X atom bridges between two A atoms with an A-X-A angle θ that varies over a large range. This disordered system of corner sharing of identical AX_3 triangles has the exact A_2X_3 stoichiometry and has a wide variation of ring sizes and configurations. He proposed that the nature of forces between atoms in glass and crystal are essentially the same. But he did not show any correspondence between glass and crystal.

Gunnar Hagg[55] assumed a correspondence between rapidly

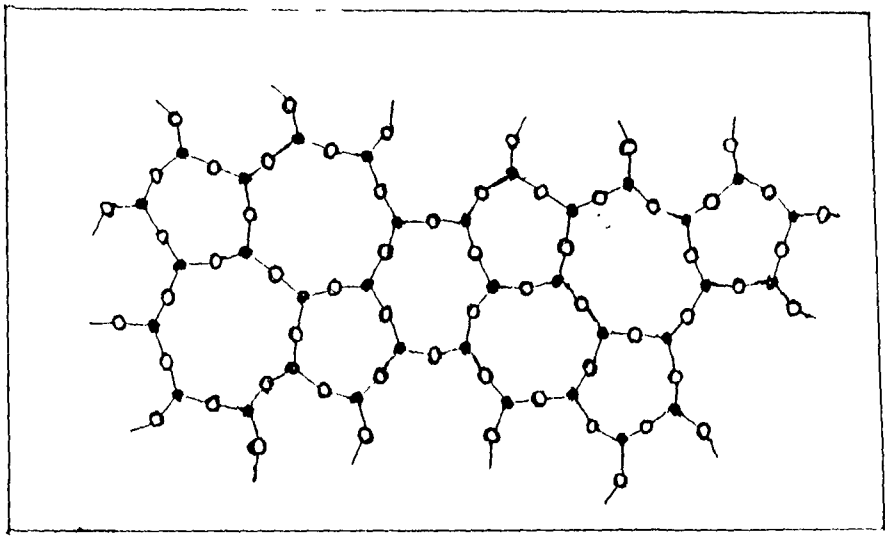

Fig.1.3 Schematic (Zachariasen) continuous random network model for the structure of AX_3 triangles in amorphous glass (A_2X_3). Here '●' is A and 'O' is X atom.

disintegrating and reforming groups present in the glass (viewed as a supercooled liquid) and the crystal of the same material. He gave examples of these groups in terms of rings, chains and other groups found in the crystalline compounds of borates and silicates. However he did not make any specific claim of identity between two systems i.e. glass and crystal.

Warren et al.[56] showed that B_2O_3 could be interpreted, by X-ray spectrum analysis, in terms of BO_3 triangles only. It was Jan Krogh-Moe[57], a pioneering investigator of glasses, who suggested a model in 1962 based on IR measurements that B_3O_3 boroxol rings rather than BO_3 triangles were the most probable structural units in glassy B_2O_3. He stated, as a general rule, an identity between the identifiable structural groupings in crystals and those postulated to be present in glasses. For borate glasses, the network should contain those structural groupings; i.e., boroxol, di-, tri-, penta-, ortho-borate etc. [Fig.1.4] that exist in the crystalline borate compounds.

However, concerning B_2O_3 glass structure, the BO_3 triangle – boroxol ring controversy continued until the X-ray studies of Mozzi and Warren[58]. They found that their data were better fitted to a picture (model) in which most of the BO_3 triangles were incorporated into boroxol rings. This also supports Krogh-Moe view points. The Krogh-Moe model was also supported by Griscom[59].

Though some contradictory views[60] against the Krogh-Moe model of borate glass structure have been expressed, some other

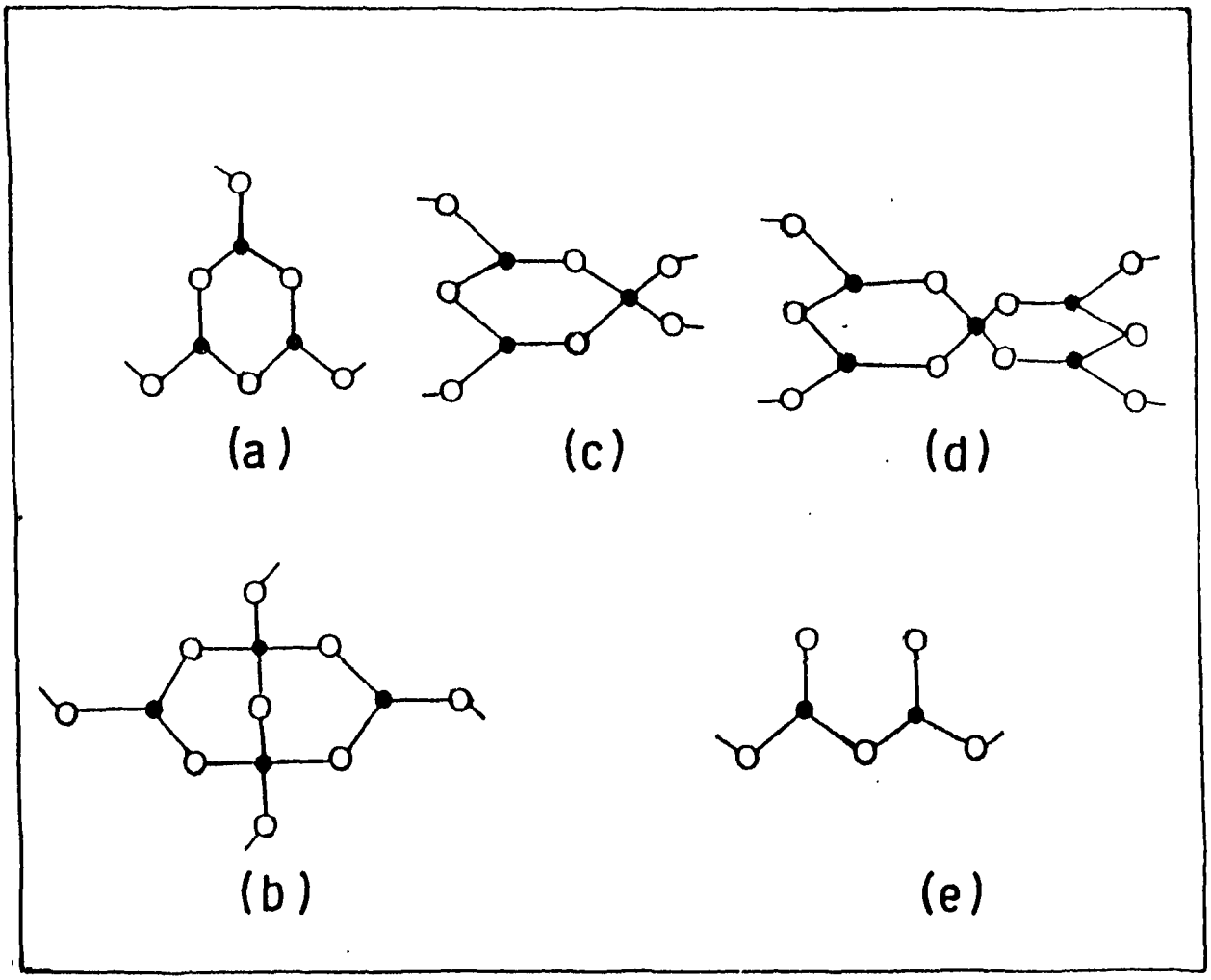

Fig.1.4 Structural groupings in borate glasses: (a) boroxol ring, (b) diborate, (c) triborate, (d) pentaborate and (e) orthoborate.

studies[61-65,12], both experimental and theoretical, confirm that the structure consists of 2/3 of the boron atoms in boroxol rings and 1/3 in BO_3 triangles.

1.8 Role of metal ions in glass

When metallic oxides are introduced in a glassy matrix, the oxides may enter into the structure in a number of ways (Fig.1.5):

(1) as a molecular entity in which the metallic ion is coordinated by oxygens which are not part of the glass network

(2) as a quasi-molecular complex in which the metallic ion is coordinated by non-bridging oxygens and which may result in the local re-arrangement of the glass structure.

(3) as a network modifier which occupies a site the geometry of which is determined by the glass structure, or

(4) as a network former either by substitution into network sites or by the polymerization of metal polyhedra.

The chromate and dichromate ions are examples of molecular entities in silicate and borate glasses[66]. Other molecular species have also been observed in these glasses, such as[67] AgO_4^{3-} in the system, $xAg_2O.(1-x)B_2O_3$.

In the case of network modifier, the metallic ion occupies a site which is determined by the configuration of the structural units present in the glass melt. Hence the sites could be of almost any size and would probably be asymmetric. Whatever may be their geometry, these sites can be expected to vary with

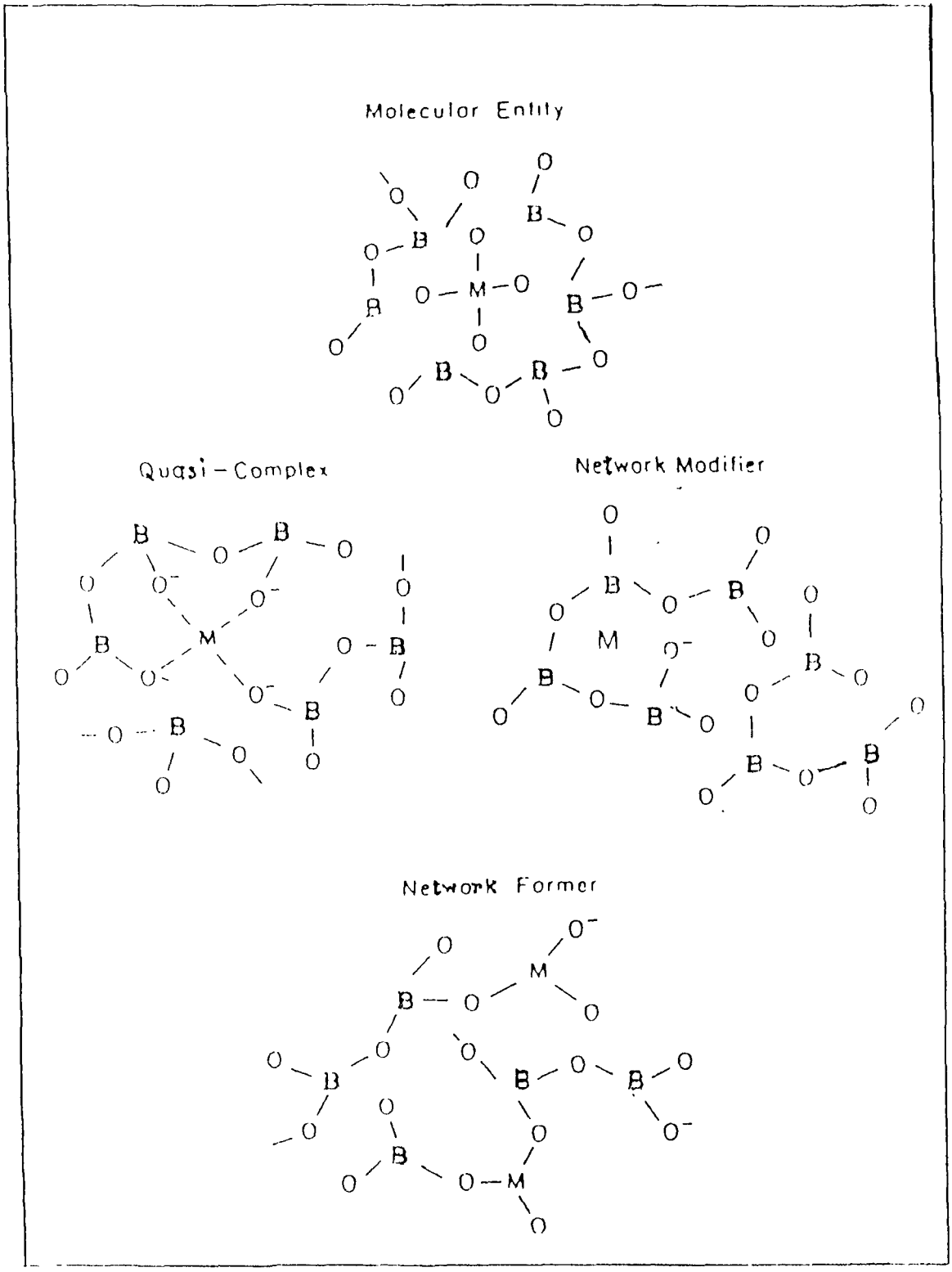

Fig.1.5 Schematic possible diagrams of borate glass complexes when metal ions (M) are introduced in the glass matrix. See also text.

melt composition and structure. On the other hand, in the formation of quasi-molecular complex, the metallic ion modifies the network locally to provide a more regular coordination polyhedron with adjusted bond lengths. Obviously these two cases are the end members of a continuous range of possibilities which depend upon the balance between the network bonding strength and the bonding requirements of the metallic ion (i.e., the field strength of the metal).

The way in which the metallic ions incorporate or take their places arranged in the glass matrix can be deduced from the position of Raman or IR bands arising from stretching and bending of e.g., boron-oxygen bonds. The position and shift of the vibrational frequencies as a function of metallic ion M, depends on three factors:

(a) coordination change of boron atom

(b) the electronegativity of M

(c) the M-O force constant

The addition of metallic oxide to the glass network causes a change (in the case of borate glasses) of boron atom coordination number following the scheme:

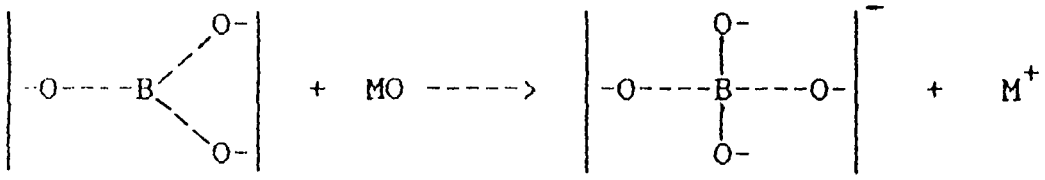

which liberates cations increasing the ionic conductivity of the glass.

The vibrations of the glass network may be divided into two classes:

(i) the vibrations involving network formers

(ii) the vibrations of the modifier-oxygen bonds

Again these two types may occur in two ways: those which consist mainly of motions of a boron atom and non-bridging oxygen atoms, such as,

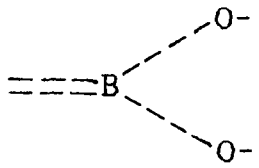

or $\equiv\equiv B\text{--}O^{-}$ *groups*

(Here O^{-} is specified as non-bridging oxygens) and those which are mainly due to motions of the boron atom and the bridging oxygens, such as,

$\equiv\equiv B\text{--}O\text{--}B\equiv\equiv$ *groups*

These two types of modes are considered especially for the streching modes.

Now, in order to discuss the effect of the modifier ion, M, on the B-O (bridging) and $B\text{-}O^{-}$ (non-bridging) vibrational modes of the borate network, consider the unit,

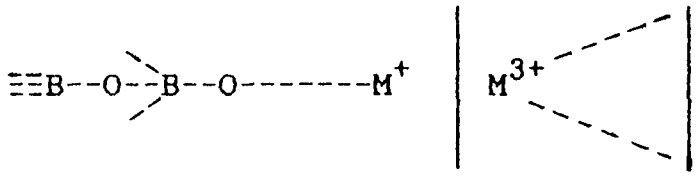

Upon variation of M, the vibrational frequencies of this unit will be influenced by two effects stated earlier i.e., the electronegativity of M and the change in the M-O force constant.

The electronegativity of M will have an influence on the bond strength of $B\text{-}O^-$ and hence the $B\text{-}O^-$ force constant. A large electronegativity will reduce the π-bonding of the bond $B\text{-}O^-$, giving rise to a decrease in the bond strength and the force constant[68]. Mainly the vibrational frequency of $B\text{-}O^-$ will vary with variation of M and to a lesser extent the B-O-B vibrations will also be affected, because the system is of coupled oscillators.

REFERENCES

1. D.F. Hornig, J. Chem.Phys.,**14** (1948) 1Ø63
2. R.A. Condrate Sr., "The infrared and Raman spectra of glasses" *in* "Introduction to glass science" Ed. by L.D.Pye, H.J.Stevens and W.C.Lacourse (Marcel Dekker, New York, 1972) p-1Ø1
3. J. Bock and G.J. Su , J. Am. Ceram. Soc.,**53** (197Ø) 69
4. E.B. Wilson Jr., J.C.Decious and P.C.Cross, *in* 'Molecular Vibrations' (Mc Graw Hill, New York , 1955)
5. H.Moore and P.W. Mcmillan, J.Soc. Glass Technol, **40** (1969) 661
6. R.V.Adams and R.W.Douglas, J. Soc. Glass Technol. **43** (1959) 1471
7. R.J. Bell, N.F.Bird and P Dean, J.Phys. C **1** (1968) 299
8. R.J. Bell and P Dean, *in* "Localization of phonons in vitreous silica and related glasses", *in* "Amorphous Materials", Ed by R.W. Douglas and B. Ellis (Wiley Inter-Science, London, 1972) p-443
9. H.Inoue and I.Yasui, J. Non-crystalline Solids, **95** (1987) 217
1Ø. G. Lucovsky and R. M. Martin , J. Non-Crystalline Solids, **8-10** (1972) 185
11. P.N. Sen and M.F. Thorpe, Phys. Rev. B **15** (1977) 4Ø3Ø
12. F.L. Galeener, G.Lucovsky and J.C.Mikkelson Jr.,Phys.Rev.B 22 (198Ø) 3983
13. J. Joannopoulos , A.I.P. Conference Proceedings, **31** (1976) 1Ø8
14. M.F.Thorpe , Phys. Rev. B **8** (1973) 5352

15. I.Simon, *in* "Modern aspects of the vitreous state", Ed. by J.D. Mackenzie and Butterworth (196Ø), p-138

16. J. Wong and C.A. Angell, Appl. Spectrosc.Rev.,**4** (1971) 155

17. A.J.Martin and W.Brenig, Phys. Status Solidi B **64** (1974) 163

18. Tsutomu Minami, Yujiro Ikeda and Masami Tanaka, J. Non-Crystalline Solids (North Holland), **52** (1982) 159

19. D.Kunze, *in* "Fast ion tranport in solids", Ed. by W.Van Gool (North Holland, Amsterdam, 1973) p-4Ø5

2Ø. N. Tohge, K. Kanda and T. Minami, Appl. Phys. Letters, **48** (1986) 1739

21. T. Minami, *in* "Matrials for solid state batteries", Ed. by B.V.R.Choudari and S.Radhakrishna (World Scientific, Singapore 1986) p-169

22. Solid State Ionics, **3/4** (1981), **9/10** (1983), **18/19** (1986) respectively the proceedings of each meeting

23. Y. Sakurai and J.Yamaki,J. Electrochem. Soc.,**132** (1985) 512

24. J.Wong and C.A.Angel, *in* "Glass-Structure by Spectroscopy" (Marcel Dekker, Inc, New York, 1976) p-2

25. Matrials Advisory Board , Nat-Acad, Sci.Res.Council, MAB-**243** (1968)

26. "Structure and Mobility in Molecular and Atomic Glasses", Ed. by J.M.O'Reily and M.Goldstein (The New York Academy of Sciences, New York, 1981)

27. E.A. Di Marzio and J.H. Gibbs, J. Chem. Phys., **28** (1958) 8Ø7

28. (i) M. Goldstein, J. Chem.Phys. **67** (1977) 2246

(ii) M. Goldstein, J. Chem. Phys.64 (1976) 4767

29. R.Zwanzig, Phys Rev. 156 (1967) 190

30. R.Shuker and R.W. Gammon, Phys. Rev. Letters, 25 (1970) 222

31. W.S. Gornall, H.E. Howard-Lock and B.P Stolen, Phys. Rev. A1 (1970) 1288

32. W.L.Konijnendijk, Philips Res. Rep. Suppl.,1 (1975)

33. T.W.Brill, Philips Res. Rep. Suppl. 2 (1976)

34. M.Irion, J. Solid state Chem. 31 (1980) 285

35. M.Sayer and A.Mansingh, Phys. Rev. B 6 (1972) 4629

36. Y.T.Quan and C.E. Adams,J. Phys. Chem., 70 (1966) 331

37. N.F.Borrelli and G.J.Su, Phys. Chem. Glasses, 4 (1963) 206

38. G.J.Su, N.F.Borrelli and A.R. Muller, Phys. Chem. Glasses 3 (s) (1962) 167

39. S.K.Shih and G.J.Su, Proceedings of the 7th International Congress on Glass, Brussels, paper 48 (1965) (Institut National du Veric, Charlevoi, Belgium, 1966)

40. N.F.Borrelli and G.J.Su, Mater.Res.Bull., 3 (1968) 181

41. I.Simon, *in* "Modern Aspects of the Vitreous State", Ed. by J.D.Mackenzie, Butterworth (1960) p-138

42. T.S.Moss, *in* "Optical properties of semiconductors" (Academic Press, New York ,1959)

43. F.L.Galeener, A.J.Leadbetter and M.W.Stringfellow, Phys.Rev.B 27 (1983) 1052

44. S.K.J.Al-ani, C.A.Hogarth and R.A.El-Malawany, J. Mater. Sci. (GB) 20 (1985) 661

45. A.A.Higazy and B.Bridge , Journal of Materials Science, 20 (1985) 2345

46. R.H.Stolen, Phys. and Chem.of Glasses, 11 (197Ø) 83

47. T.Minami, Y.Ikeda and M.Tanaka J. Non-Crystalline Solids, 52 (1982) 159

48. T.Minami, T.Katsuda and M.Tanaka, J. Non-Crystalline Solids, 29 (1978) 389

49. T.Minami, T.Katsuda and M.Tanaka, J. Phys. Chem. 83 (1979) 13Ø6

5Ø. P.Beekenkamp, *in* "Physics of Non-Crystalline Solids", Ed. by J.A.Prins (North Holland, Amsterdam, 1965) p-512

51. L.Vane Hove, Phys.Rev. 95 (1954) 249

52. R.J.Nemanich, Phys. Rev.B 16 (1977) 1655

53. W.H.Zachariasen, J. Am.Chem. Soc. 54 (1932) 3841

54. W.H.Zachariasen, J. Chem. Phys. 3 (1935) 162

55. G.Hagg, J.Chem. Phys. 3 (1935) 42 & 363

56. B.E.Warren, H.Krutter and O.Morningstar, J. Am. Ceram. Soc., 19 (1936) 2Ø2.

57. J. Krogh-Moe, Phys. Chem. Glasses, 3 (1962) 1Ø1

58. R.L.Mozzi and B.E.Warren ,J. Appl. Cryst. 3 (197Ø) 251

59. L.Griscom, *in* "Borate Glasses", Ed.by L,D.Pye, V.D.Frechette and N.K. Kreidl (plenum, New York, 1978)

6Ø. S.R.Elliott, Philos. Mag., B 37 (1978) 435

61. G.F.Jellison Jr., I.W.Panek, P.J.Bray and G.B.Rouse, J. Chem. Phys., 66 (1977) 8Ø2

62. L.C.Synder, G.F.Peterson, and C.R.Kurkjian, J. Chem. Phys. 64 (1976) 1569

63. P. A. V. Johnson,A. C. Wright, and R. N. Sinclair, J. Non-Crystalline Solids, 50 (1982) 281

64. C.F.Windisch and W.M.Risen Jr., J. Non-Crystalline Solids, 48 (1982) 307

65. C.F.Windisch and W.M.Risen Jr., J. Non-Crystalline Solids, 48 (1982) 325

66. S.A.Brawer and W.B.White, Mater. Res. Bull., 12 (1977) 281

67. W.L.Konijnendijk and J.H.J.M.Buster, J. Non-Crystalline Solids, 22 (1976) 379

68. W.P.Griffith, J. Chem. Soc. A, Inorg. Phys. Theor. 9 (1969) 1372

CHAPTER II

EXPERIMENTAL METHODS

2.1 Introduction

The samples studied in the present investigation by Raman technique are transparent glasses. In order to record Raman spectra in the 90° scattering geometry (Fig.2.4b), the samples should be made rectangular in shape (at least two faces should be smooth and vertical, one incident face and the other scattered face).

A typical laser Raman spectrometer needs an intense and highly monochromatic light source. An ideal monochromatic light beam (which is necessarily polarized and coherent) is one in which the frequency is identical at all points in space and time But a real beam always departs from this ideal situation in various ways depending on its method of production. However, the output of argon ion laser (that has been used here) is much closer to an ideal source. In this work, the Raman spectra of all the samples have been recorded using Jobin-Yvon Laser Raman Spectrometer (Models U 1000 & HG2S).

First order IR absorption spectra may be obtained using thin glass films whose thickness is of the order of the wavelength of the infrared light used. But in practice, laboratory preparation of thin glass films is difficult to

prepare in most of the cases and normally one utilizes the KBr pellet technique where a small quantity of glass sample (powdered) is dispersed in the transparent matrix of KBr. This procedure may have undesirable consequences such as dispersion at short wavelengths (Christiansen effect[1]), loss of spectral bandshape and intensity information, residual water from KBr pellet and difficulty in the determination of weak absorption bands. The infrared instrument normally used is a double beam grating spectrophotometer or a single beam Fourier transform spectrophotometer (FTIR). Perkin-Elmer 681 has been mainly used to record the IR spectra.

2.2 Sample preparation

(i) All the glass samples, for Raman study, were prepared by heating the chemicals under investigation through a range of temperature upto 1400 K using a home made electric furnace. China clay crucibles (boat types) were used. When the melts become transparent and bubble-free, these were poured on to a stainless steel mold kept at 300 K and then pressed by a stainless steel plate kept at 300 K to obtain homogeneous glass of desired thickness. The size of the glass samples were made rectangular (some were made circular) of the dimension of around (15 X 10 X 1.5) mm^3.

(ii) For scanning of IR spectra of the glasses, KBr pellets were prepared by using the pressed disc technique. A small piece

of each glass sample was grinded properly into fine powder by using morter-pestle of vitrosil. This minimizes the Christiansen effect which arises when the refractive indices of a solid particle and its surrounding medium differ appreciably. An amount of about 1 mg of glass powder was thoroughly mixed with ~ 300 mg of high purity KBr (KBr has no IR absorption[2] in the range of wavenumbers 400-3000 cm^{-1}). The mixture was then placed in a die and pressed by means of a laboratory press at a pressure of about 12000 pounds per square inch under vacuum to yield a transparent pellet or disc of particular shape and size. lack of evacuation makes the pellet (especially in v-B_2O_3) visually opaque in a short time even when stored in a dry atmosphere.

2.3 Care of sample materials

Among all the borate glasses, the boric oxide glass is highly hygroscopic material. Even at very high temperatures hydroxyl groups may be present in it. However, just after the preparation, the glass is kept in the desiccator which is provided with dry $CaCl_2$ to remove the last traces of water from inside. Whenever the sample is used for scanning of the Raman spectra, the faces of the glass were smoothened with carborandum powder of 800 mesh and then polished with soft cloths. The binary and ternary borate glasses were also kept in the desiccator, though they were comparatively less hygroscopic.

KBr pellet samples for IR spectra were prepared just at the time of scanning the spectra using the previously grinded glass samples.

2.4 Raman Instrument

In the basic Raman spectrometer, the sample under investigation is subjected to irradiation from a suitable monochromatic light source and the Raman spectrum is observed by the use of a system comprising: (i) a monochromatic light source, (ii) a sampling compartment, (iii) a monochromator dispersing system, (iv) a detecting system, (v) a recording system, (vi) a scan control unit.

The block diagram of Fig. 2.1 shows the components of the basic Raman spectrometer.

2.4.1 Monochromatic light source

The essential requirements of a light source for the excitation of Raman spectra are that it should be highly monochromatic (i.e.,having a narrow line width) and capable of giving high irradiance at the sample. An argon ion laser meets these requirements. The Spectra Physics model 171 (9 watt) argon ion laser[3], equipped with model 27Ø power supply unit, 171 laser head and power meter, provides a stable high power excitation line. The green line at 5145 A^{O} has been used here. The laser head contains the optical cavity resonator structure, the

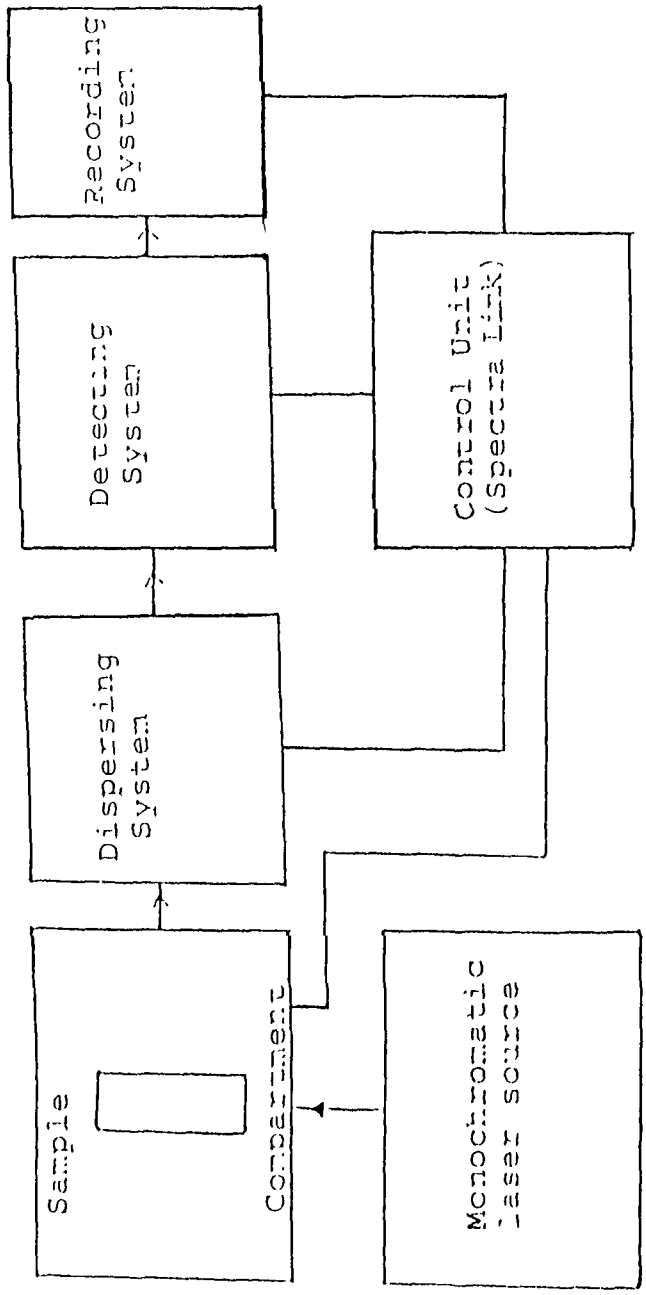

Fig.2.1 Block diagram of basic laser Raman spectrometer

beryllium oxide plasma tube and the plasma tube solenoid. The energy level diagram of singly ionized argon can be seen from the Fig.2.2. The two ground state sub levels of the $4s^2$ P states of argon ion have very high probabilities of emitting radiations and dropping to the ground state. The population at any given time in an ionic ground state is not very large so that there is no tendency for self absorption . The energy separation between the lower laser levels and the ground state of the ion is very large (about 17 eV) so that , even though the plasma is at a higher temperature, there is no tendency for a Boltzmann population equilibrium to be established between the ionic ground state and the lower laser levels.

A magnetic field is generated by a solenoid surrounding the plasma tube. It tends to force the electrons away from the walls of the tube. Since the electrons are not lost as quickly to the walls, there is a shift of energy distribution of the free electrons towards higher values. The atomic levels can only be populated through collisions with electrons having at least the energy of the state being excited. Therefore, the result of the magnetic field is a stronger population inversion.

The plasma tube is conduction-cooled and all the heat is carried away by cooling water which is in direct contact with the plasma tube. The cooling system (Fig.2.3) operates at $35^{\circ}C$ and requires a flow rate of Ø.22 litres per second when operating at full power.

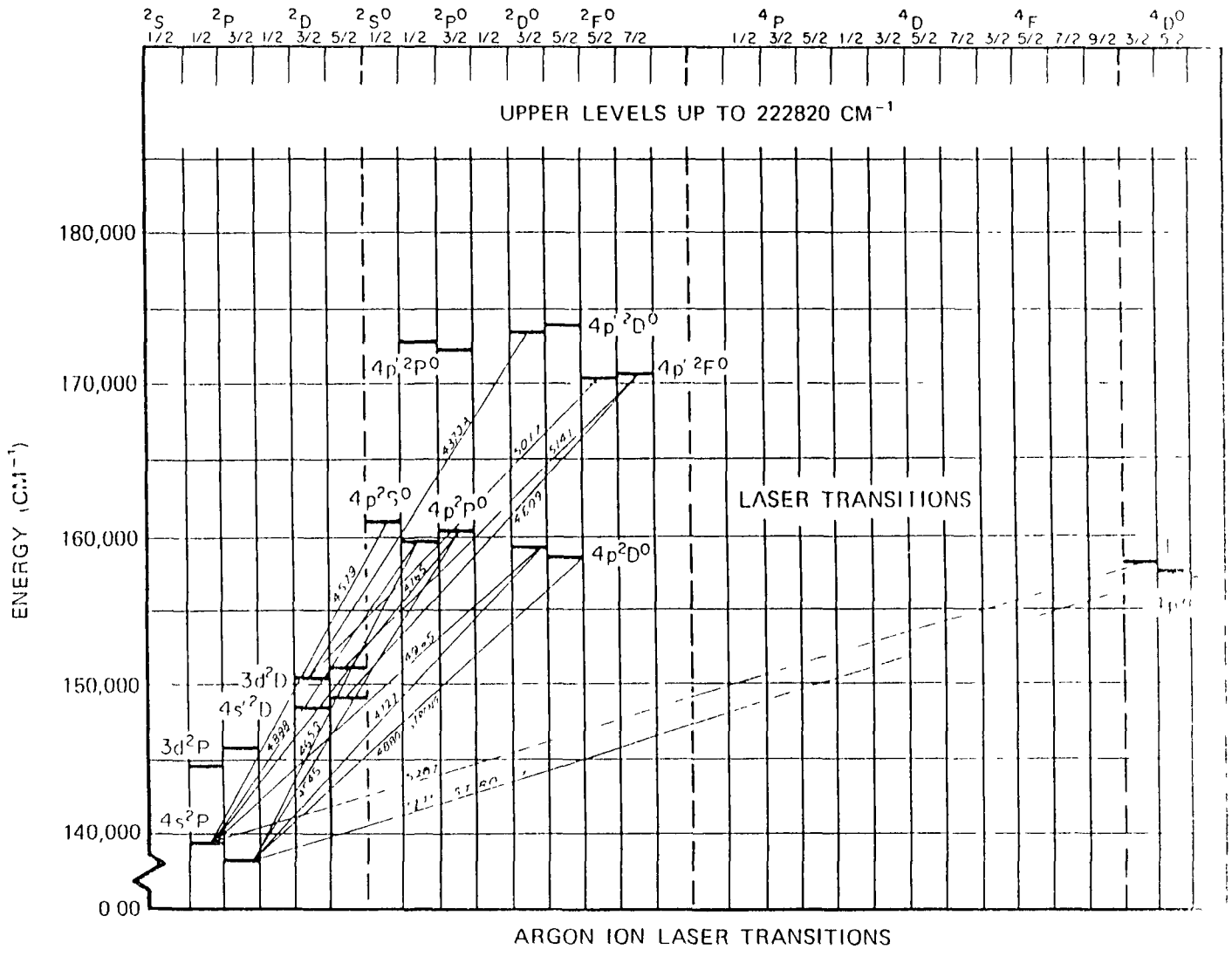

Fig.2.2 Energy level diagram of the singly ionized argon atom

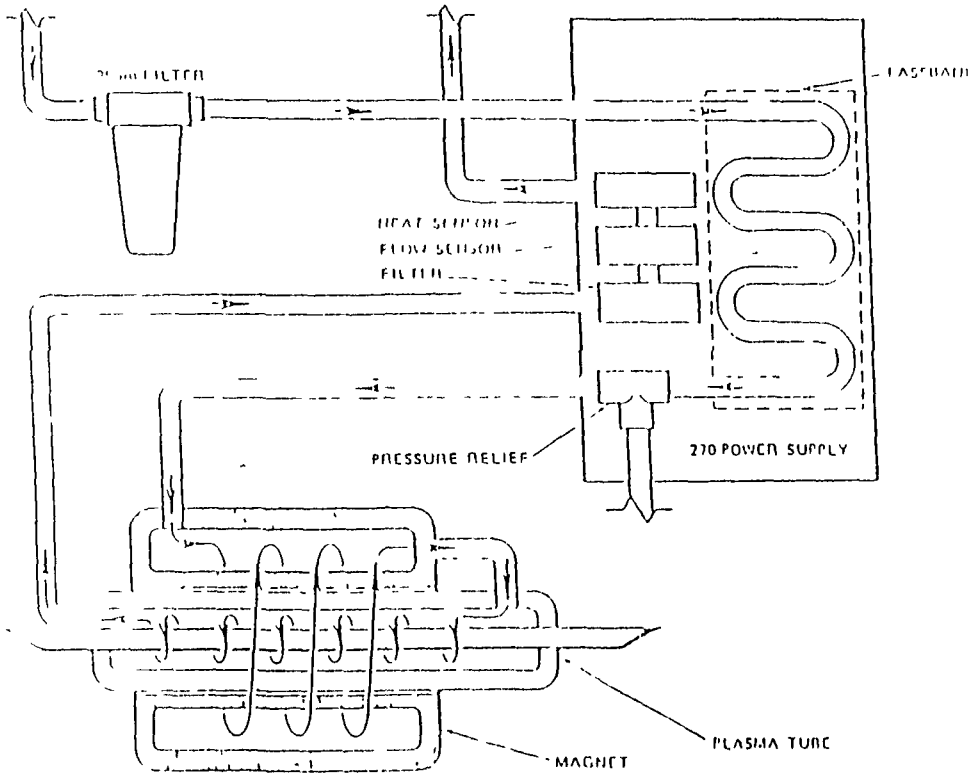

Fig.2.3 Water cooling system for 171 argon ion laser source

2.4.2 Sample compartment

Every laser Raman instrument has its own system of sampling and pre-slit optics. However, the sample is to be illuminated in such a way that an acceptable image is produced at the entrance slit of the monochromator. In the present experimental set up, the conventional 90^{o} scattering geometry in which the laser beam passes normally to the direction of view is used. The sample compartment and the related optical ray diagram are as shown in the Fig.2.4(a&b).

2.4.3 Monochromator Dispersing System

Jobin-Yvon Ramanor U 1000 is a typical double monochromator designed for spectroscopic applications that require high resolution and extreme stray light rejection. The optical layout[4] of the monochromator dispersing system is shown in Fig.2.5. The two identical monochromators are in an additive mount equipped with plane holographic gratings. Each monochromator features an asymmetric Czerney-Turner mountings equipped with two slits which open symmetrically . The two gratings are mounted and rotated on a single horizontal shaft which is parallel to the grating grooves. The exit slit F_2 of the first monochromator is imaged on the entrance slit F_3 of the second monochromator. Finally the exit slit F_4 allows, from the dispersed beam, only a narrow wave number band to reach the detecting system. The model Ramanor U1000 has the following

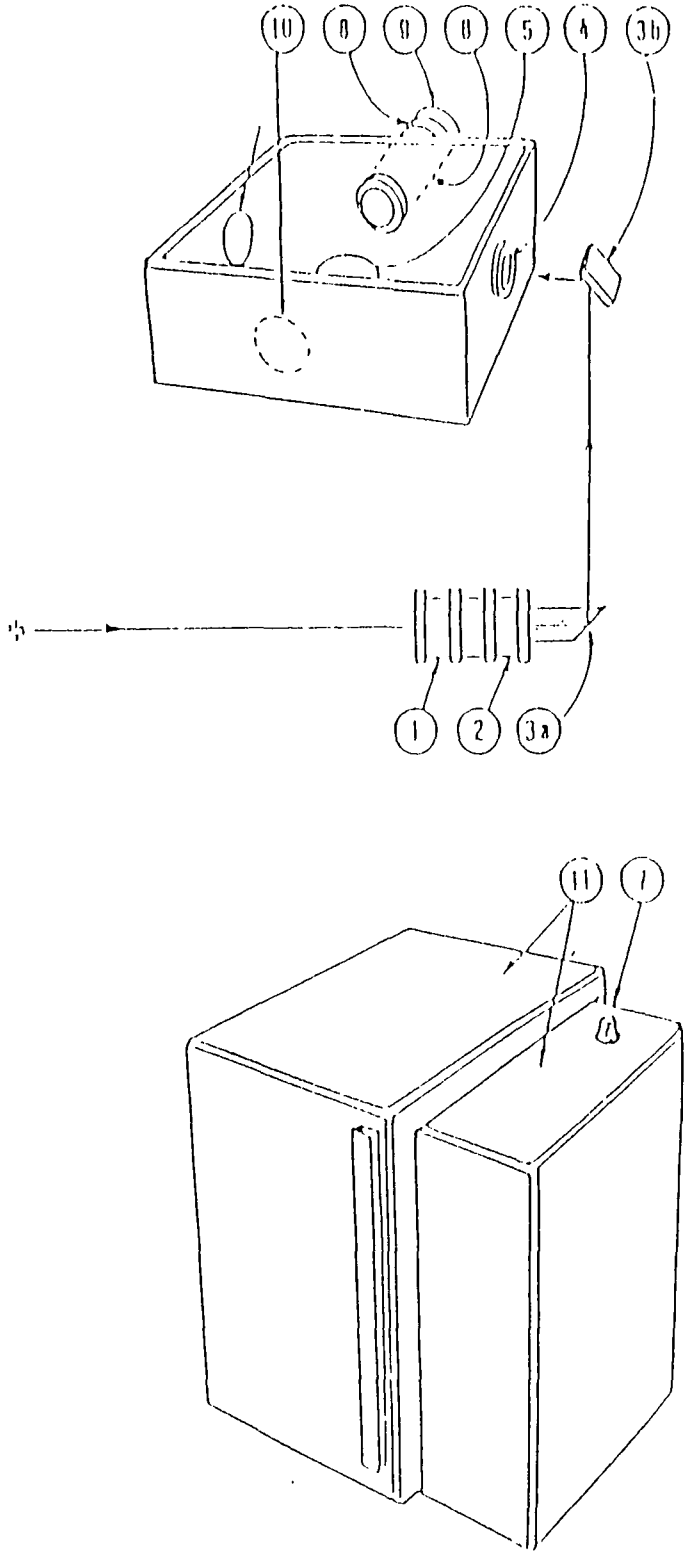

Fig.2.4(a) Sample compartment for the laser Raman spectrometer.

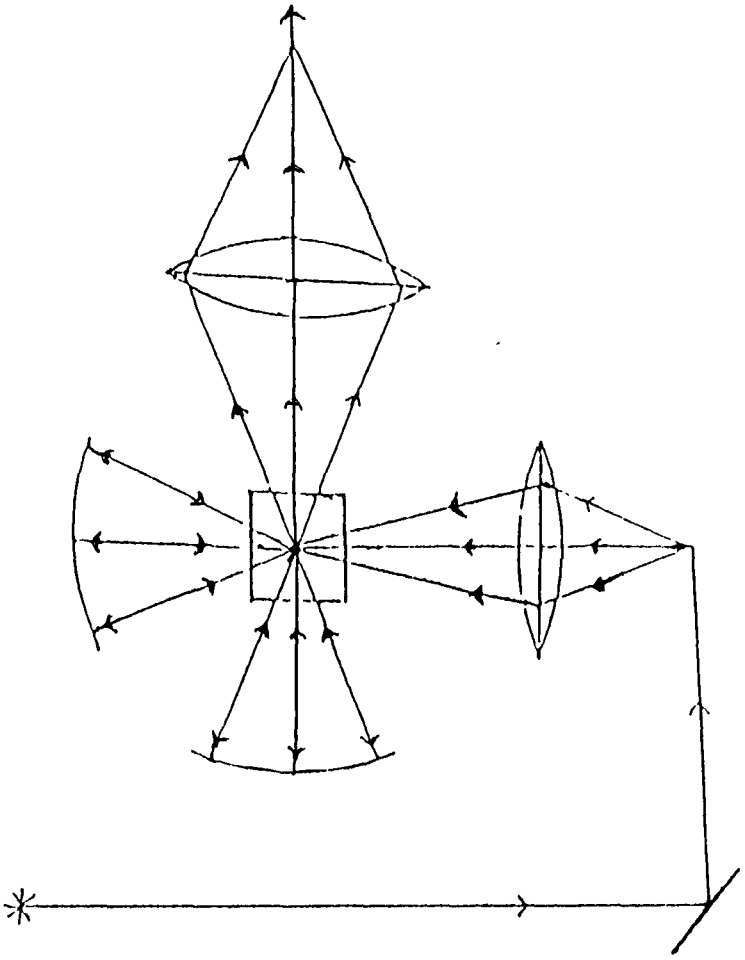

Fig.2.4(b) Optical ray diagram for the sample compartment of Fig.2.4(a).

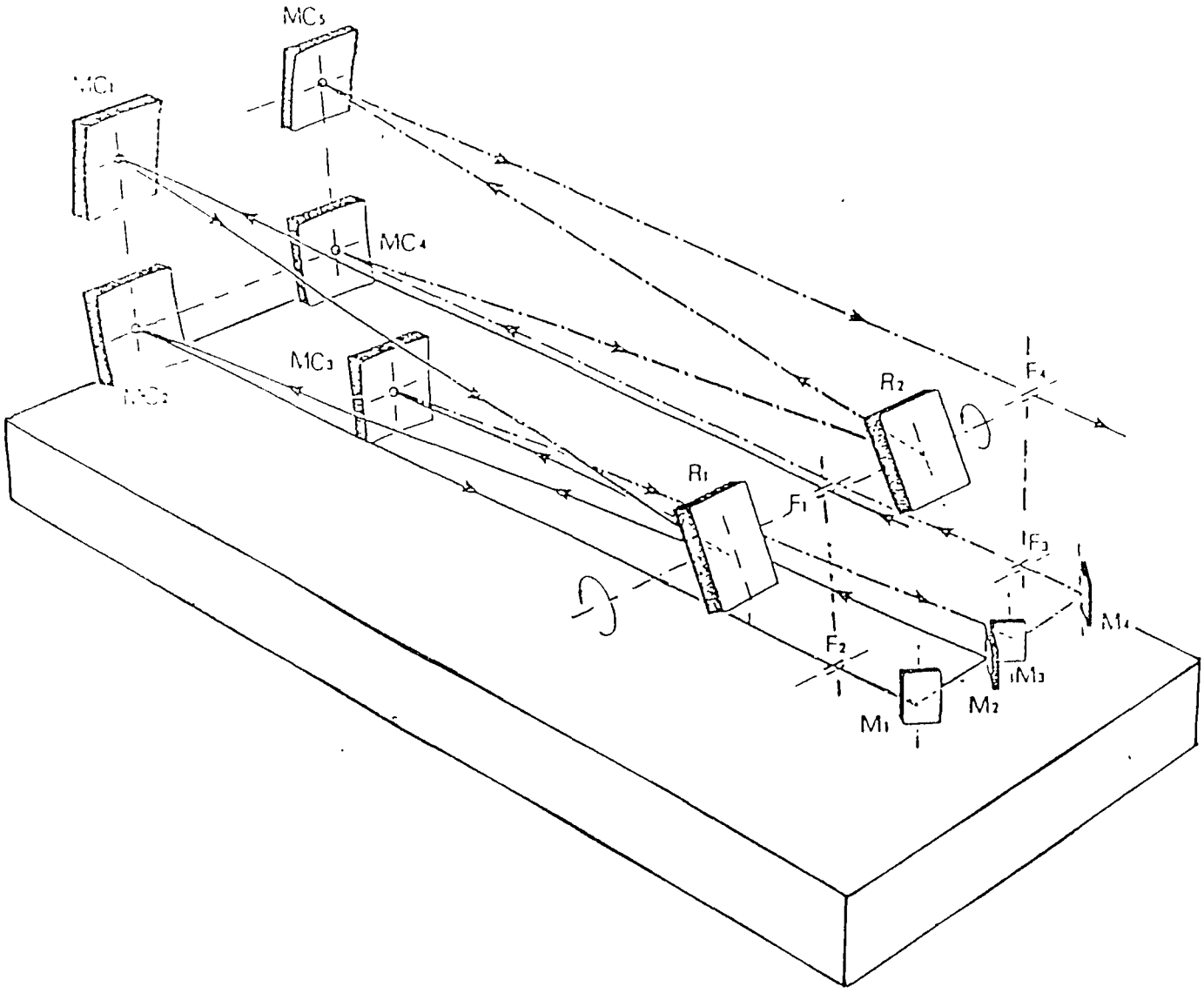

Fig.2.5 Monochromator dispersing system of the Raman spectrometer (model Ramanor U 1000).

specifications:

Grating grooves: 1800/mm, Grating size: 110x110 mm^2,

Resolution: 0.15 cm^{-1} on Hg line at 5791A°,

Dispersion: 9.2 cm^{-1} per mm at 514,5 nm line,

Spectral range: 440-750 nm (22700-13500 cm^{-1}),

Scanning wave number accuracy: 1 cm^{-1} over 5000 cm^{-1},

Reproducibility: Better than 0.1 cm^{-1},

Slits: 4 (four) slits manually adjustable from 0 upto 3 mm.

2.4.4 Detecting and Recording System

For spectral intensity measurement, the photo-emissive cell is the best of all and is linear over widely different intensities of illumination. In the form of the electron multiplier, the photo-emissive cell is equipped with electronic DC amplifier in a single envelope. The basic principle (Fig.2.6) is the phenomenon of secondary electron emission from a treated metal surface. A single primary electron ejected by the photon falling on the cathode C from the exit slit of the monochromator may give rise to a large number of secondary electrons. These electrons are accelerated towards a number of electrodes at which increasing voltages are applied. The electrons from the final electrode are collected at the anode A whence they are conducted away and measured as photo current signals. The over all amplification may be about a million for a typical photo-multiplier tube. The photo current signals are converted

electronically into digital counts which show up on the counter display.

Synchronous scanning of the monochromator and of X-Y recorder is accomplished through stepping motors and scan controller which generate the drive pulses for both the operations. By selecting the scan rate and scan range , the logic circuit supplies proper pulse rate to each motor, thus obtaining the Raman spectra on a recording sheet.

2.4.5 Scan Control Unit

The wave number scanning is controlled by the microprocessor based scan controller (spectra link) including the following:

(i) Absolute or relative wave number display, (ii) Wave number scan speed selection in cm^{-1}/min, (iii) Repeatative scan, (iv) Recorder control and (v) Laser shutter control.

2.5 Ramanor HG2S

It is a littrow configuration in which the entrance and exit slits are horizontal and mounted in a plane parallel to the rotation axis. The square sized (11Ø x 11Ø mm^2) concave holographic gratings are used as dispersors. The straight and horizontal slits of length 2Ø mm and width upto 2 mm are operated independently by vernier or stepping motor. The resolution of the instrument is Ø.5 cm^{-1} at 5145 A^{o},

reproducibility is ± Ø.2 cm^{-1} and wave number accuracy is ± 1 cm^{-1} over 5ØØØ cm^{-1}. The instrument is simultaneously supported by two detection systems, photomultiplier and a multi-channel analyzer . The optimum range of the instrument in the visible version is 22720-12500 cm^{-1} where as in the ultra violet version is 31008-17391 cm^{-1}.

2.6 IR Instrument

The Perkin Elmer model 681 works on the principle of optical null method in the range 6ØØ-4ØØØ cm^{-1}. The optical system is shown as in the Fig.2.7. The system[5] automatically records the percent transmittance of the sample at different wave numbers . An IR radiation emitted from the source is divided into two beams, the sample beam and the reference beam. The sample beam passes through the sample, then through a trimmer. In the reference beam, there is a wedge-type attenuator. Both the beams pass through an identical path and are dispersed by diffraction grating G. Then both the beams are alternately focussed on a receiving surface of the detector. If certain sample has a characteristic absorption in a particular range of wave number, the intensity of the sample beam will be attenuated by the absorption and it causes an optical unbalance of energy between the two beams, which produces an alternating current signal corresponding to the rotational frequency of the sector mirror. This signal is amplified, then synchronously

Fig.2.6

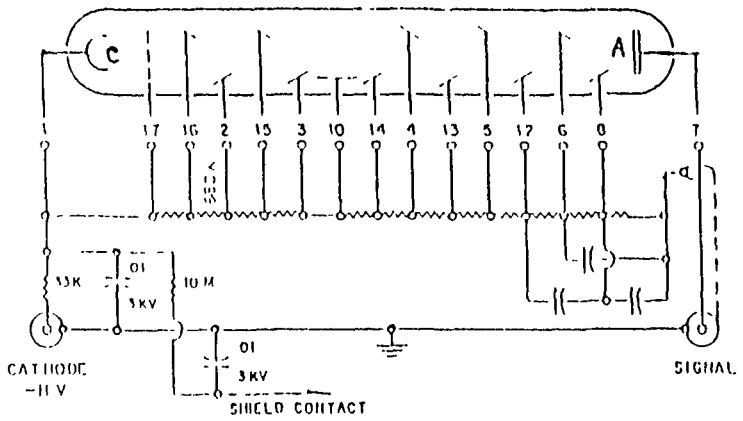

Fig.2.7

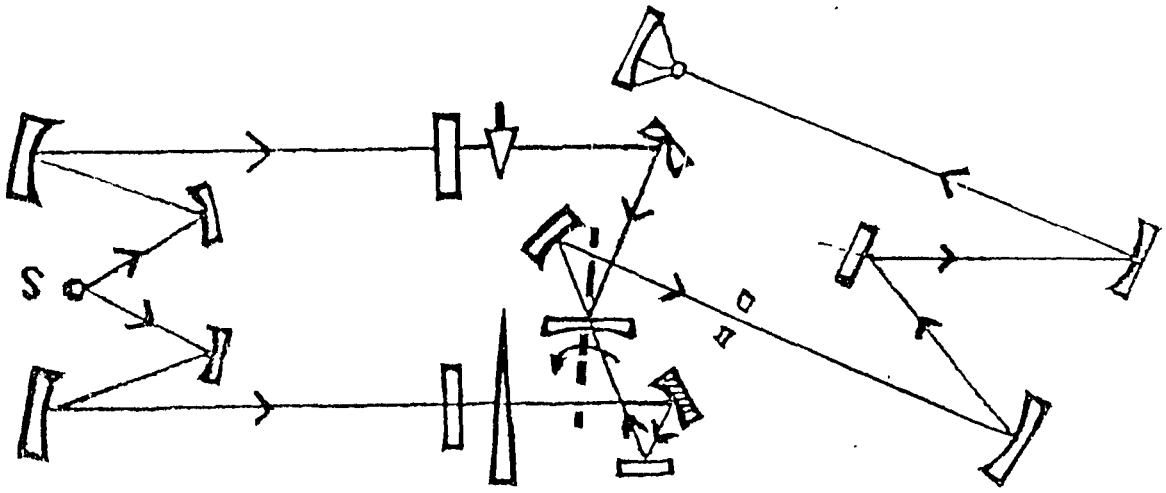

Fig.2.6 Photomultiplier tube for the detecting system of the Raman spectrometer.

Fig.2.7 Basic optical ray diagram of IR spectrophotometer (model Perkin-Elmer 681).

rectified by a reference signal produced synchronously with the rotation of the sector mirror. The servo motor runs until an optical unbalance of energy between the two beams disappears; then stops at a position where the alternate current signal from the detector becomes zero.

The light source used is Globar (silicon carbide). The temperature of the source is about 1300 K and power consumption is 65 W. The detector, a high sensitive vacuum thermo-couple, converts incident photon to an electrical signal. The wave number accuracy is ± 3 cm^{-1} in the range 600-2000 cm^{-1} and reproducibility is ± 0.5 cm^{-1} (approximately).

REFERENCES

1. David N. Kendall, ''Applied Infrared Spectroscopy'', p-137 (Reinold Publishing Corporation, Chapman & Hall, Ltd, London,1966)
2. Robert P. Bauman, ''Absorption Spectroscopy'', p-182 (John Wiley & Sons, Inc.,New York,1962)
3. Laboratory Instruction Manual (Spectra Physics model 171 argon ion laser)
4. Laboratory Instruction Manual (Jobin-Yvon Ramanor U1ØØØ)
5. Laboratory Instruction Manual (Perkin Elmer model 681)

CHAPTER III

SPECTRAL INVESTIGATION OF BORIC OXIDE GLASS

3.1 Introduction

The structure of vitreous B_2O_3 has been under investigation for a long time . There is increasing evidence, experimental as well as theoretical, that the structure consists of a network of planar BO_3 triangles, many of them grouped together in threes, in the form of planar hexagonal "boroxol" (B_3O_3) rings. The amorphous nature of this structure is illustrated in Fig.3.1. Three types of bridging connections between boroxol rings are shown in the Figure. Site (i) shows a single oxygen atom connecting two rings. The B-O-B bridging angle θ varies generally from site to site. The site (ii) in the Figure represents the next complicated connection between rings. Here a BO_3 triangle forms a bridge among the three boroxol rings with varying values of θ at three oxygen atoms. The site (iii) indicates four boroxol rings joined by two BO_3 triangles having varying angles of θ at the oxygen atoms. A dihedral angle δ is also required to specify the relative orientation of the two neighboring rings joined at different sites and δ is assumed to vary randomly from site to site. Following the above scheme, a large number of rings might be joined by randomly oriented triangles and it is consistent to assume that when three

Fig.3.1

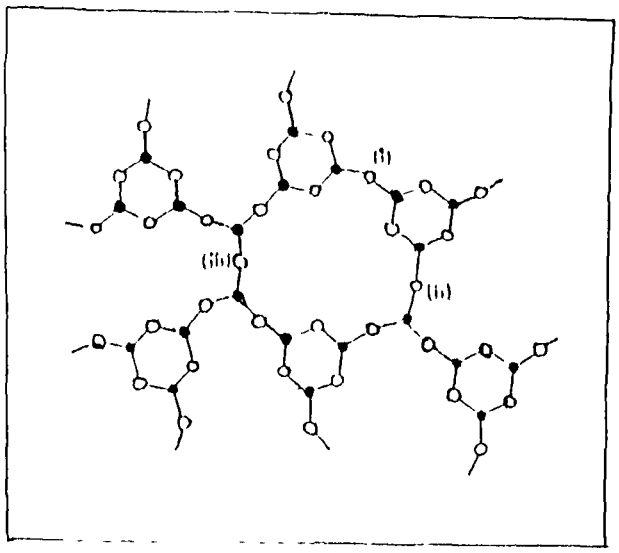

Fig.3.2

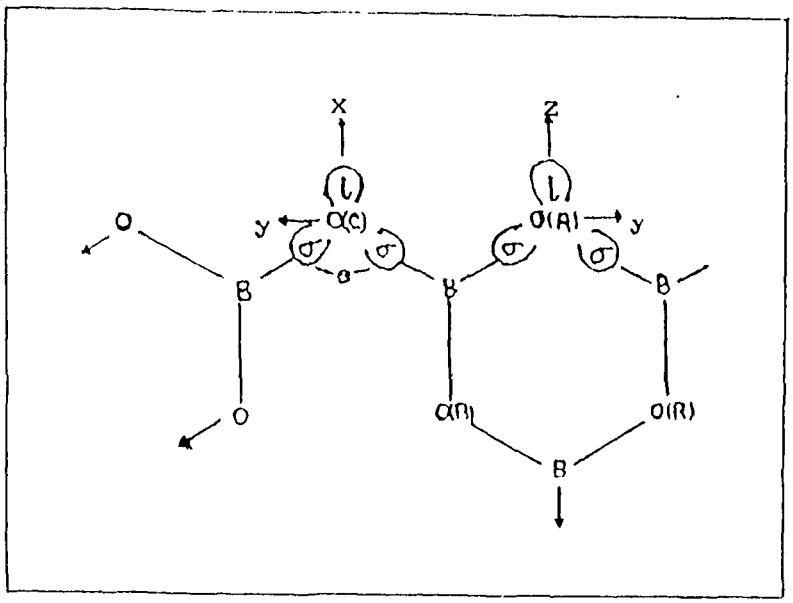

Fig.3.1 Schematic (planarized) diagram of the possible network in v-B_2O_3 based on B_3O_3 (boroxol) rings. Here, 'O' is an oxygen atom and '●' is a boron atom.

Fig.3.2 Boroxol model for the B_2O_3 glass. σ refers to the oxygen σ bonds and l refers to the non-bridging oxygen lone pair orbitals. The π bonds are perpendicular to the page (not shown). B-O-B angle is θ. The principal axes for O(R) and O(C) are shown , excepting the z-axis for O(C) and the x-axis for O(R) (these are perpendicular to the page.

triangles unite together, they will become[1,2] planar leading to a boroxol ring.

The model showing many boroxol rings was first proposed by Goubeau and Keller[3] which was further supported by Krogh-Moe[4]. In 1965, Krogh-Moe[5], on the basis of the infrared study, proposed that the B_2O_3 glass network consists exclusively of boroxol rings, while, in 1969, he[4] further extended these investigations and, combining them with those carried out by others, came to the conclusion that the BO_3 triangles prefer to form planar hexagonal boroxol rings. Mozzi and Warren[6] found that their X-ray radial distribution function (RDF) data on v-B_2O_3 could best be explained by a mixture of independently oriented rings and triangles, much like that of Fig.3.1.

Jellision et al[7] and Bray et al[8] estimated through NMR studies that 82% of the B atoms are in B_3O_3 rings. The computer simulation of the B_2O_3 (O^{17}) NMR spectrum indicates that two distinct oxygen sites are present in the structure : (i) a ring oxygen site O(R), which is an oxygen atom contained in a boroxol ring, and (ii) a connecting oxygen site O(C), which is an oxygen atom that bridges between two boroxol rings (Fig.3.2)[9]. For the B_2O_3 glass enriched with ^{17}O, the NMR line shapes displaying second order quadroupole effects were obtained by Bray et al[9]. The quadroupole parameters, which characterize those oxygen sites, O(R) & O(C), present in the glass structure were obtained by computer simulation of the

spectra and these parameters were related to the occupation number and geometry of the oxygen electronic orbitals by simple calculation. In the Fig.3.2, the label σ corresponds to the oxygen σ bonds and the label 1 refers to the non-bridging oxygen lone pair orbitals. The π bonds are perpendicular to the plane of the paper. Thus the presence of the two oxygen sites, O(R) and O(C), indicates that B_2O_3 glass consists of a majority of randomly oriented boroxol rings.

The situation upto 1978 was reviewed by Griscom[10] supporting the boroxol ring model of the B_2O_3 structure. Neutron diffraction measurements[11] also show that 60% of the B atoms are in boroxol rings. Walrafen et al[12] obtained Raman data as a function of temperature and calculated the energy required to break a boroxol ring. This energy (6.4 ± 0.4 K cal/mol boroxol) was in good in agreement with Krogh-Moe's estimate and Synder's **ab initio**[27] quantum mechanical calculation for the energy difference between BO_3 groups in boroxol rings and those in the random network. Thus BO_3 triangles in boroxol rings are favoured energetically over BO_3 triangles in the random network. Galeener et al[13] have suggested, through vibrational spectral study of v-B_2O_3, that the extraordinary narrowness (~ 15 cm^{-1}) of the dominant Raman line at 806 cm^{-1} was a clear indicator of the fact that the B-O-B angles were tightly controlled to 120±0.8° within boroxol rings. They showed a comparison of the Raman spectra of v-B_2O_3 with the vibrational frequencies reported for

"triangular" molecules of BF_3[14] and "boroxol ring" molecules of $H_3B_3O_6$. This comparison provides important evidence for the presence of boroxol rings as well as triangles which are not part of boroxol rings.

In the computer calculated Raman spectral study from a ball-and-stick model[15] containing boroxol rings, it has been found to account reasonably well for the large polarization ratio (I_{HH}/I_{HV}=28) observed for the dominant Raman line at 8Ø6 cm^{-1}. Thus there prevails a wide spread understanding that v-B_2O_3 structure consists largely of a network of remarkably regular and planar three-fold (so called boroxol) rings with some fraction of BO_3 triangles.

It could be mentioned here that these boroxol rings are known to occur in various alkali borate crystals[16] but not in crystalline B_2O_3[1Ø]; although some other authors[17] claimed that the band near 8ØØ cm^{-1} was also found in crystalline B_2O_3. However, the existence of boroxol rings in v-B_2O_3 structure has been seriously questioned . Elliot[18] has calculated radial distribution functions (RDF) from computer-generated structures and concluded that X-ray data could be better understood by a continuous random network (CRN) of BO_3 triangles having no planar boroxol rings. He suggested that the rings in the structure are of rather high order (six to eight fold).

Molecular dynamics (MD) calculations, in which equations of motions for a small collection of interacting atoms or molecules

in a cube are solved, have been applied to study the structure of v-B_2O_3 [19-22]. The structural analysis of the network by MD simulation reveals that almost all the boron atoms are coordinated to three oxygen atoms, while each oxygen atom is coordinated to two boron atoms which shows that boron and oxygen atoms form planar BO_3 triangles. The average O-B-O angle [2Ø] is 119±6°. The distribution of B-O-B angles is very broad with an average of 154° which indicates the predominance of six- and higher-fold rings in the system, supporting Elliot's suggestion. Again Soppe[22] considered B-O-B angles to be fixed at 12Ø° and performed MD calculations to conclude that the glass structure consists of BO_3 triangles only.

Very recently[23] vibrations of v-B_2O_3 system have been investigated theoretically using Bethe lattice approximation to handle an infinite system along with that of an isolated boroxol molecule. They have shown by their explicit calculations that 8Ø6 cm^{-1} (A_1') mode of the boroxol group remains sharp even when an infinite network is formed which confirms that this mode involves mainly the breathing motion of oxygen atoms inside the ring while boroxol-boroxol coupling on network formation involves mainly the motion of the boron atoms and the external (bridging) oxygen atoms.

The studies relating the frequency shifts in the vibrational spectra of isotopically substituted forms of v-B_2O_3 are also noteworthy. Galeener and Geisberger[24] have reported measurements

of the $^{10}B \rightarrow ^{11}B$ isotope shifts in v-B_2O_3 and found almost zero shifts for 806 cm^{-1} band. An experiment of similar nature has also been performed by Windisch and Risen[25] who measured the $^{16}O \rightarrow ^{18}O$ isotope shift to be 48 cm^{-1} for this band. The fact that 806 cm^{-1} band shifts on oxygen mass change but not on boron mass change, shows that the mode involves essentially only oxygen motion. Also the fact that it is replaced by four bands (one at 806 cm^{-1}) in the intensity ratio 1 : 3 : 3 : 1 instead of by one band in $^{11}B_4{}^{16}O_3{}^{18}O_3$, is strong evidence that the mode is highly localized one.

In this chapter, Raman and IR spectral measurements on v-B_2O_3 structure have been reviewed . Especially, low frequency Raman spectral measurements have been performed on the basis of Martin-Brenig model . These measurements confirm that the dominant Raman feature at 806 cm^{-1} mainly represents v-B_2O_3 structure and supports Krogh-Moe model of boroxol rings with some fraction of BO_3 triangles.

3.2 Experimental

The oxide B_2O_3 (or H_3BO_3) in powder form obtained from BDH, England, was first dehydrated by heatng upto 180 °C in a china clay crucible and then heated at 1000 °C continuously for twenty four hours. The clear bubble-free melt was then quenched rapidly to room temperature and pressed between two preheated (at about 100°C) stainless steel plates to prepare glass of thickness

about 2mm for Raman study. Just before recording the spectra the faces of the glass were grinded and polished with carborundum powder in three stages using different meshes of lower grades and then with 800 mesh and finally smoothened with soft cloths.

For IR study, the glass was grinded into powder by morter-pestle made of stainless steel and transparent pellet was prepared with KBr using pressed disc method.

Raman spectra were recorded on Ramanor U-1000 double monochromator using 5145 A° line of the argon ion laser as the exciting radiation in the 90° scattering geometry, while IR spectra were recorded on Perkin-Elmer model-681.

3.3 Raman spectra of v-B_2O_3

The Fig.3.3(a&b) shows the Raman spectra of v-B_2O_3 at room temperature in the range 100 — 1600 cm^{-1}. It has been observed through many trials that lower laser power could excite mainly the dominant Raman line at 806 cm^{-1} whose sharpness and position has been confirmed (Fig.3.3a). The band is assigned to the totally symmetric stretching mode, also known as the breathing motion, of the boroxol ring with major contribution arising due to oxygen atom vibration and very little boron motion involved in it. Its full width at half maximum is found to be 16 cm^{-1}. The peak is strongly polarized as expected for such a symmetric vibration. Since this mode involves the vibrations of the internal oxygen atoms within rings only, it is entirely

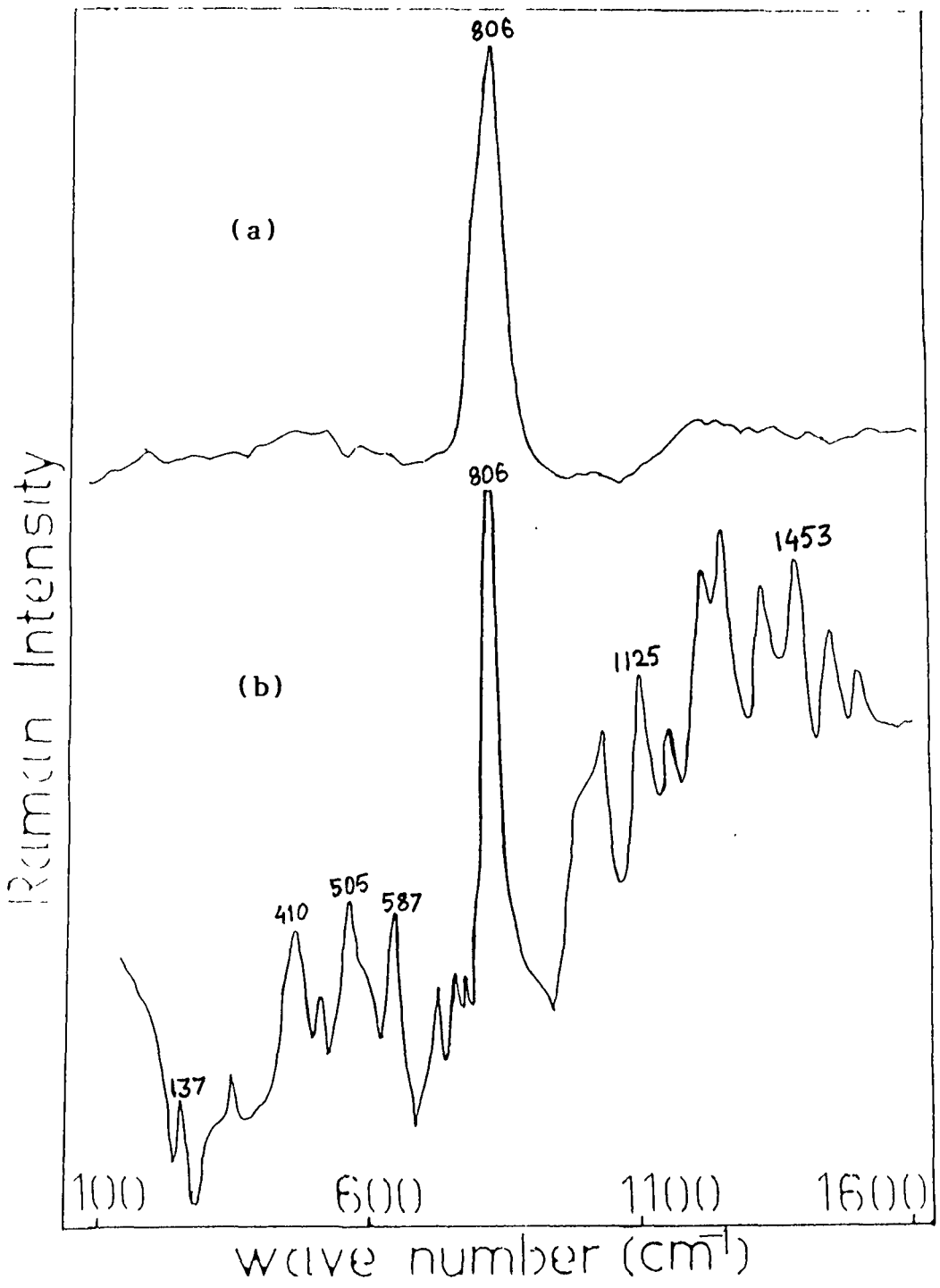

Fig.3.3 (a) Raman spectrum for v-B_2O_3 using laser output power of 400 mW.
(b) Raman spectrum for v-B_2O_3 using laser output power of 800 mW.

localized on each ring and can account for the small line width observed. The temperature dependence[12,26] of this band shows that its intensity starts decreasing as the glass transition temperature is approached and this tendency is attributed to a rapid breakdown of boroxol rings with increasing temperature. The integrated Raman intensity of 806 cm^{-1} band refers primarily to boroxol ring concentration and the total integrated contour intensity in the region 300-800 cm^{-1} almost certainly refers to the contribution arising from the BO_3 triangles linked to form boroxol rings as well as BO_3 triangles in random network configurations. With temperature rise, the intensity of the band at 806 cm^{-1} decreases, while an enhancement in intensity of the band near 587 cm^{-1} with respect to other bands is observed. This band at 587 cm^{-1} is assigned to the deformation mode of BO_3 triangles involved in the random network, not in boroxol rings. Of course, a number of vibrations are included in the region 300-800 cm^{-1}, such as B-O-B bending (720 cm^{-1}), B-O-B rocking (505 cm^{-1}) etc., in addition to the modes involving the boroxol rings.

The heat energy involved in the breakdown of boroxol ring has been calculated to be 6.4±0.4 K cal/mole boroxol. This estimate is in good agreement with Krogh-Moe's estimation and *ab initio* quantum mechanical calculations[27] of the energy difference between BO_3 groups in boroxol rings and those in random network. These measurements show that BO_3 triangles in

boroxol rings are favored energetically over BO_3 triangles in a random network. All the Raman bands observed for v-B_2O_3 are shown in table 3.1 with their assignments. Table 3.1 also shows the relative peak intensities observed for all the Raman bands in the scale of 1ØØ assigned to the 8Ø6 cm^{-1} band. The low frequency bands below 3ØØ cm^{-1} have been attributed to the cooperative motions of the whole structure comprising a mixed BO_3 triangular and boroxol ring network, whereas 8Ø6 cm^{-1} band is an internal mode. The band at 137 cm^{-1} is associated with librational motion of boroxol rings.

3.3.1 Low frequency Raman spectra of v-B_2O_3

Fig.3.4a shows the experimental Raman spectrum of v-B_2O_3 in the range (12—15Ø cm^{-1}) and Fig.3.4(b,c&d) show the reduced (see section, 1.6.2) Raman spectra with $C_b \sim \omega^n$, for n= 2,1 & Ø respectively. The experimental Raman spectrum (Fig.3.4a) reveals two broad bands ; one at 26 cm^{-1} and the other at about 137 cm^{-1}. For the reduced spectra, the position of the second peak remains nearly constant, where as the first peak shifts to 5Ø cm^{-1} for n=1. This peak (known as boson peak) is observed in most of the borate glasses. This band may arise or be enhanced in intensity due to

(i) an increase in the Bose-Einstein thermal phonon population number, $n(\omega) = 1/[\exp(\hbar\omega/kT)-1]$, where ω is the Raman shift.

(ii) an increase in the Raman scattering intensity proportional

Table 3.1 Raman bands observed in v-B_2O_3 with assignments, intensities and comparison with those obtained by others

Ref.13 Wave$_1$Nos. (cm^{-1})	Ref.12 Wave$_1$Nos. (cm^{-1})	Present Wave$_1$Nos. (cm^{-1})	peak* intensity (arb.units)	Assignments
145	12Ø	137	1Ø	Libration of boroxol rings
26Ø	26Ø	262	Ø7	Cooperative motions of the whole structure
-	4ØØ	41Ø	12	-----
47Ø	46Ø	46Ø	Ø7	Ring bending
5ØØ	49Ø	5Ø5	14	Rocking of B-O-B
61Ø	585	587	25	Deformation of BO_3
67Ø	65Ø	685	19	Bond bending of B-O-B
-	725	72Ø	Ø4	Wagging of B-O-B
75Ø	-	755	Ø5	B-O rtetch in complex cyclic groups
8Ø8	8Ø1	8Ø6	1ØØ	Totally symmetric stretch in B_3O_6 rings
1Ø3Ø	1Ø4Ø	1Ø44	11	Symmetric stretch in BO_4
-	-	1125	25	Asymmetric stretch in BO_4 groups
121Ø	12ØØ	1195	1Ø	Triangular B-O stretch
126Ø	125Ø	1245	Ø5	Stretch on boron oxygen sub lattice
1325	132Ø	13Ø5	17	Three coordinated boron motion
-	-	1375	23	Bending and stretching of O-H groups
1475	147Ø	1453	28	Strech of >B-O$^-$ groups
-	156Ø	1534	17	Motion due to boric acid formed at the surface
1615	1615	158Ø	14	BOH bending motion

* Intensities are calculated in comparison with that of 8Ø6 cm^{-1} band

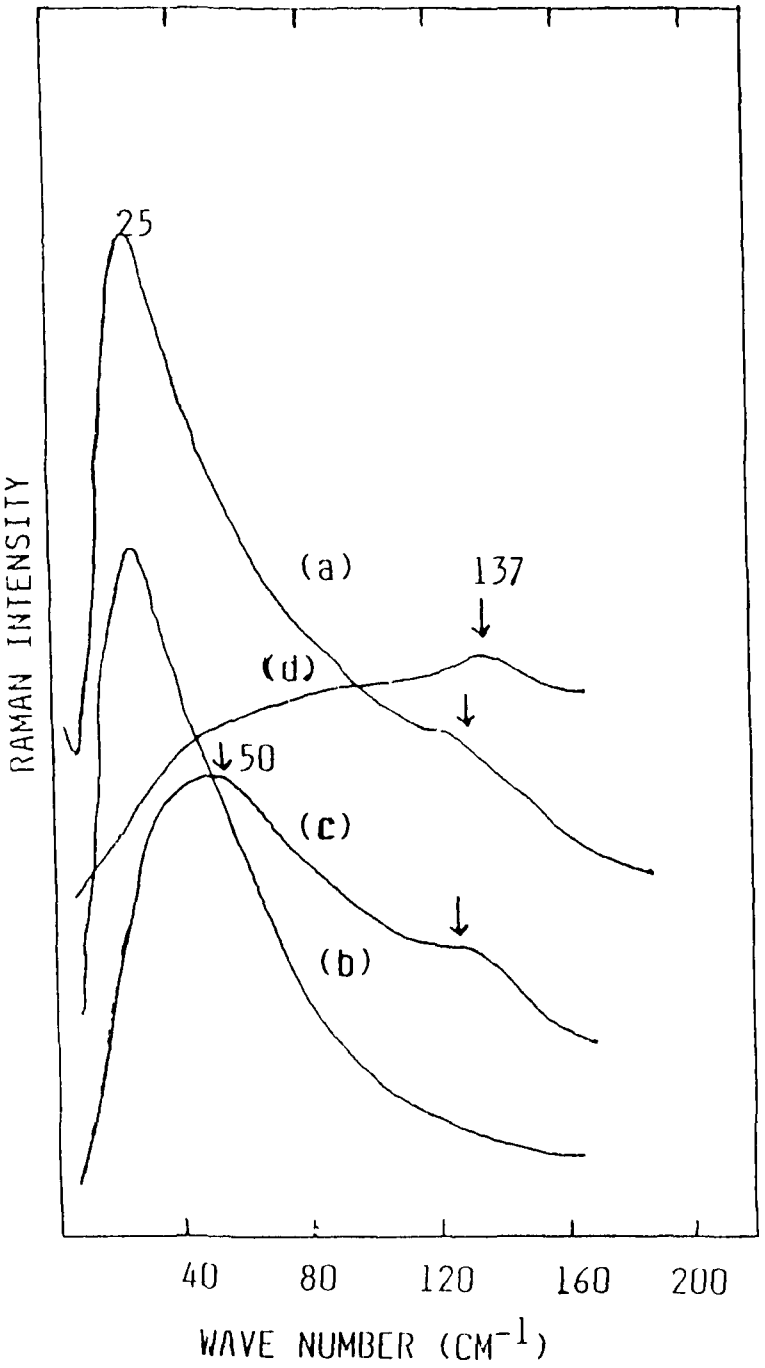

Fig. 3.4 (a) Low frequency Raman (experimental) raw spectrum I(obs) of v-B_2O_3.
The reduced Raman spectrum, $[I(obs)/C_b\{n(\omega,T)+1\}]=I_R$ with (b) $C_b=\omega^2$, (c) $C_b=\omega$ and (d) $C_b=1$.

to $(\omega_L - \omega)^4$, ω_L being the frequency of the exciting laser line.
(iii) the elastically scattered Rayleigh radiation and sometimes, Mie or Tyndal scattered stray light.
(iv) low frequency light scattering from long wavelength acoustic modes of disordered solids and
(v) low frequency Raman spectral feature termed as 'Light Scattering Excess' (LSE) attributed to the defect states which are invoked[28,29] to describe the linear temperature-dependent specific heat of glasses at low temperature[30,31].

According to Almeida[32], certain Raman active low frequency modes in glasses containing ions of large polarizability probably have major contribution towards the so called boson peak. Similar low frequency wings observed in the Raman spectra of gases [33] and liquids[34,35], have been interpreted as being due to binary collisions[36,33]. It is also to be noted that the low frequency peak was also observed in the Raman spectra of surfaces consisting of the silver particles[37]. The diameter, d~100 A°, of these particles estimated from the value of the energy corresponding to the maximum of boson peak position in the reduced Raman intensity, $[I(obs)/\omega\{n(\omega,T)+1\}]=I_R$ was equal to that one obtained from the electron micrography[37]. It is a direct evidence of the presence of the size effect in Raman scattering.

A critical evaluation of the continuous spectra of amorphous materials in the low frequency region when extended[38,39] to

v-B_2O_3 glass and its melt shows that the vibrational spectrum in the liquid state of the glass is quite similar to that of the glass phase. This suggests that the low frequency wing B_2O_3 of the glass spectrum can be thought of as due to low frequency vibrational density of states. In the disordered system of amorphous materials, in which the periodic atomic arrangement inherent in crystalline state lies only within few coordination spheres, the Raman process is characterized by inelastic light scattering which does not conserve momentum. This shows that the ordered micro region or short correlation range (SCR) in the disordered system leads to a breakdown of the crystal momentum selection rule[38] and the continuous Raman spectra in glasses are ascribed to this disorder-induced scattering. Thus the low frequency light scattering from long wavelength acoustic modes of disordered solids might be responsible for the appearance of boson peak in the spectra of v-B_2O_3.

Temperature variation[40] of low frequency Raman spectrum of v-B_2O_3 shows that, at very low temperature ~ 8 K, the two broad bands are centered near about 50 cm^{-1}(boson) and 137 cm^{-1}. At 70 K, the boson peak shifts to 28 cm^{-1} and its position remains constant upto 500 K. It is further shifted to 10 cm^{-1} at 673 K. This shows that,with rising temperature, the band shifts towards lower frequencies. The density of states, g_b, of the temperature reduced Raman spectra (Fig.3.4c) also indicates two bands at 50 and 137 cm^{-1} at room temperature.

3.3.2 M-B model and short range order in v-B_2O_3

Martin and Brenig[41] attributes the low frequency boson peak to structural disorder which affects the Raman coupling coefficient C_b appearing in the Stokes Raman intensity expression (equation 1.21, chapter I),

$$I(obs) = C_b [n(\omega,T) + 1] g_b/\omega \quad (3.1)$$

The expresssion for C_b given as (equation 1.25),

$$C_{VH}=A\omega^2[3(v_l/v_t)^5\exp\{-(2\pi c\omega)^2\sigma^2/v_t^2\}+2\exp\{-(2\pi c\omega)^2\sigma^2/v_l^2\}] \quad (3.2)$$

shows the dependence of C_b on frequency ω and corresponds to the maximum values of C_b at $\omega = \omega_{max} = v_t/2\pi c\sigma$, where ω_{max} is the boson peak position , v_t is the transverse sound velocity and (2σ) is the structural correlation range (SCR) of glass structure. The SCR value estimated from the relation $2\sigma = v_t/\pi c\omega_{max}$ for v-B_2O_3 is found to be 7.267 A°. The transverse and longitudinal sound velocity values (v_l and v_t) are obtained from reference 42. The Fig.3.5 shows the comparison of the theoretical C_b values (calculated from the equation 3.2) with the experimental values of C_b (obtained from equation 1.31),

$$C_b = I(obs)/\omega \{n(\omega,T)+1\}, \quad (3.3)$$

in the Debye density of states $g_b=\omega^2$ approximation. There is close agreement between theory and experiment at room temperature. Guha and Walrafen[40] have conducted Raman studies of vitreous B_2O_3 in the low frequency region as a function of

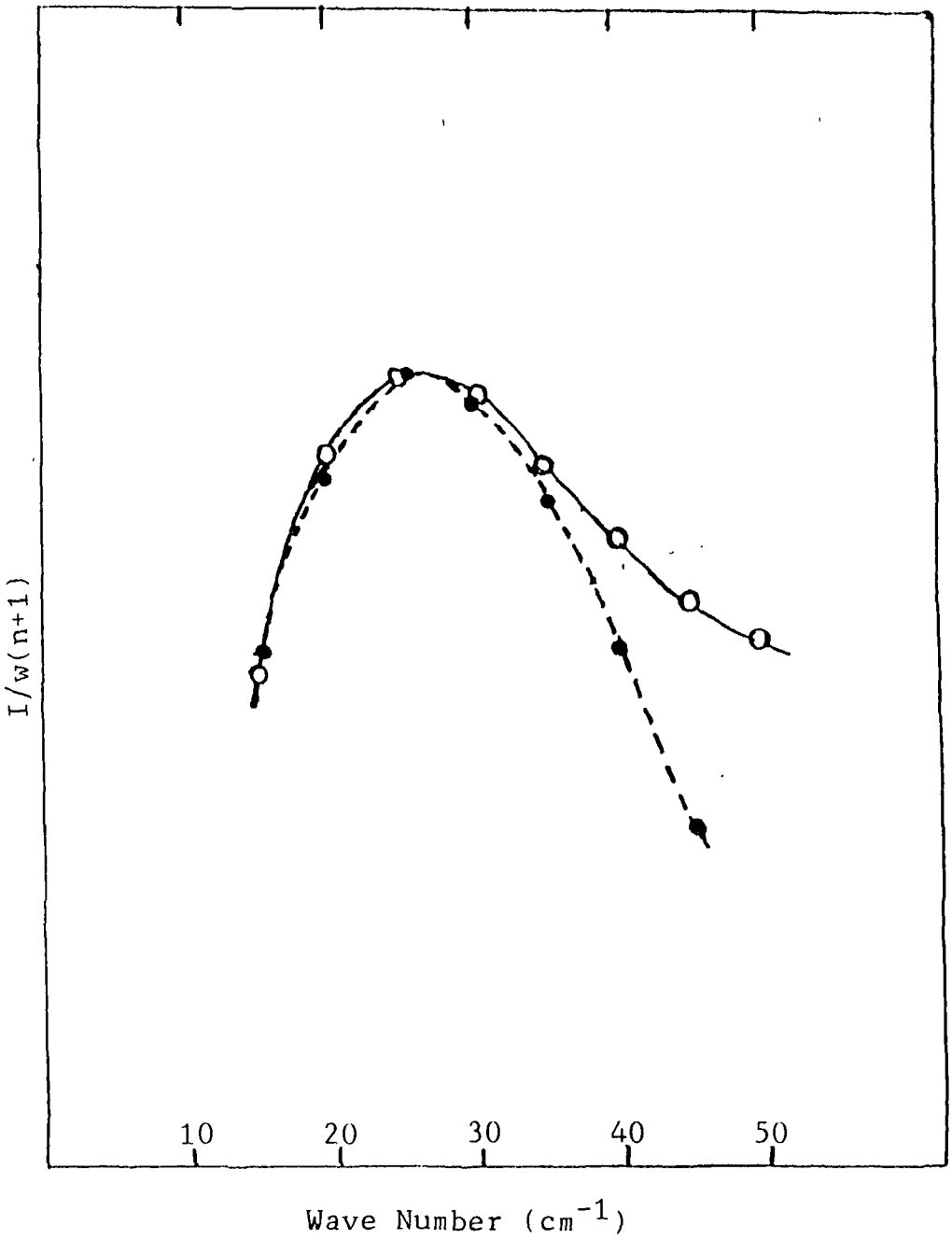

Fig. 3.5 Fitting of Martin-Brenig model. The dotted curve shows the theoretical C_b values (equation, 1.25) and the solid curve shows the experimental values of C_b (equation, 1.31).

temperature between 8 and 7ØØ K. They calculated vibrational density of states g_b using the equation (3.1) with presumed values of C_b as 1, ω and ω^2 in the low frequency region (<3ØØ cm^{-1}). They also performed the fitting of equation (3.2) (theoretical) with equation (1.31) (experimental) at different temperatures; which shows that the choice of $C_b=\omega^2$ is not valid above 28 cm^{-1} below T_g (573 K) and 2Ø cm^{-1} above melting temperature (723 K). Near the glass transition temperature T_g, the boson peak in the temperature reduced as well as in the experimental Raman spectra, shifts suddenly to lower frequencies. This is expected because this change at T_g is associated with a change in mass distribution and force constants near the glass transition temperature. The frequency reduced spectrum does not exhibit such a sharp decrease in frequency. So the temperature reduced Raman spectrum in which C_b varies as ω is probably the true representation of the vibrational density of states between 3Ø and 3ØØ cm^{-1}. Following the equation (1.29), we see that the representation of the vibrational density of states in v-B_2O_3 is dependent on the Raman coupling coefficient C_b. Here it is found that C_b varies as ω^2 below 3Ø cm^{-1} and as ω between $3Ø<\omega<3ØØ$ cm^{-1}. Thus in general, either the frequency reduced or the temperature reduced Raman spectrum could represent vibrational density of states in v-B_2O_3.

3.4 Glass transition in v-B_2O_3

We follow the discussions about the glass transition phenomenon described in section 1.3 and assume that the clusters of atoms within the cages shown by the shaded areas in Fig.3.6a undergo librational motion . They are trapped in one of the potential wells below T_g and the librational motions of clusters of atoms of various sizes may be responsible for the observed low frequency peaks. The force constants associated with the 26 and 137 cm^{-1} bands are comparable[16] to each other and therefore, these librational motions are probably decoupled motions around the centre of mass of each cage. If we increase the temperature, the large amplitude of motions of individual bonds broaden the vibrational spectrum; but the vibrational density of states would not change unless the structure is not changed.

Near T_g, a number of boroxol rings are broken extending the polymeric network of the BO_3 triangles, thereby decreasing the density of atoms. Therefore, there will be a weakening of the force constants between atoms. Since the potential wells are closely spaced together, the system would seek a new equilibrium position at a different configurational state. The potential minima associated with different configurational states are likely to have different curvatures because of the variations in the force constants. All these effects would result in a shift of scattering spectra to lower frequencies. At higher temperatures (above melting point), the viscosity of the melt is

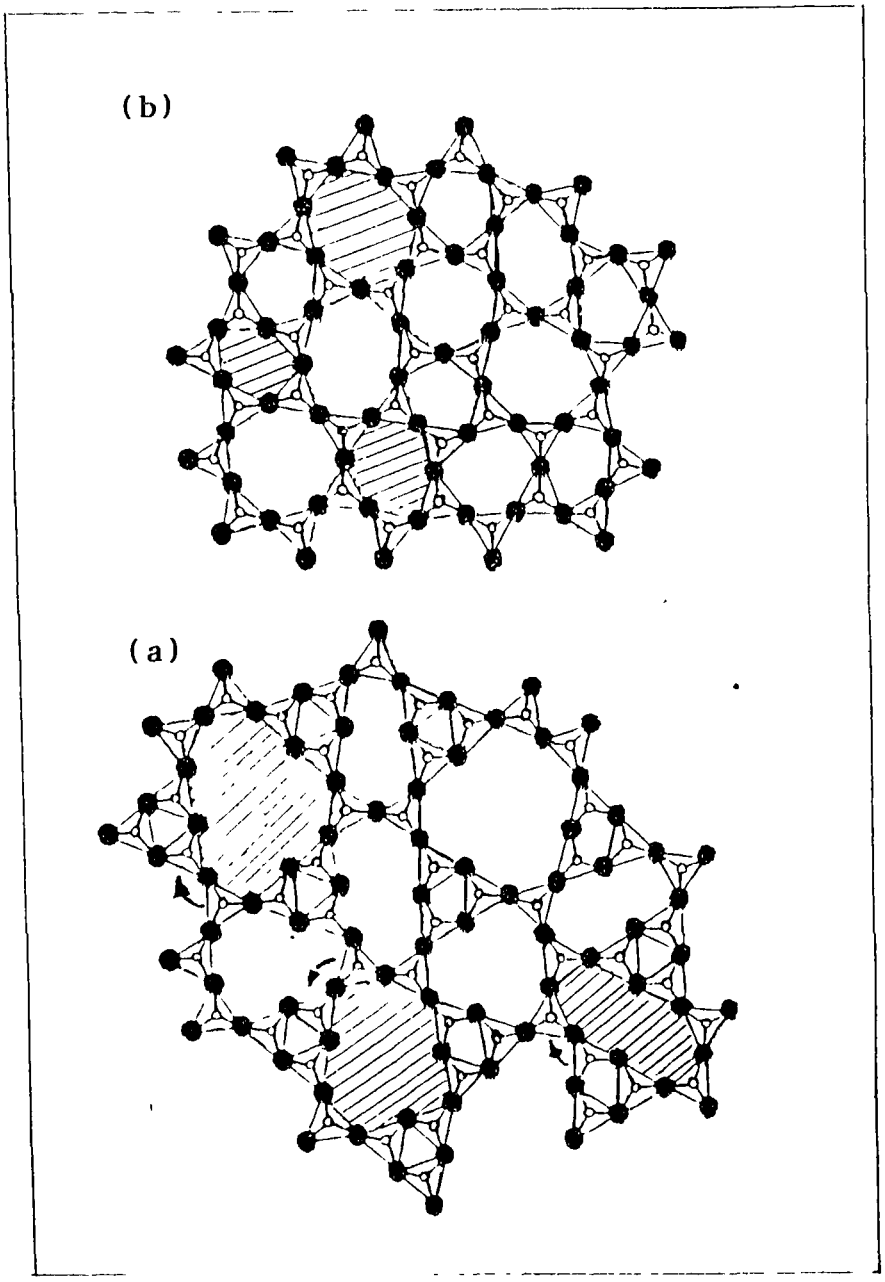

Fig.3.6(a) A possible v-B_2O_3 structure at room temperature containing high proportion of boroxol rings. Arrows indicate possible librational motions.

(b) The v-B_2O_3 structure in the molten state containing only BO_3 units. The density of glass is reduced due to the replacement of boroxol rings with BO_3 units.

lowered. Therefore, instead of linking the ruptured bonds of boroxol rings to the same network, one can think of regrouping of atoms which would lead to a more open structure (Fig.3.6b). These clusters of atoms are still harmonically bound to their neighbors but with a much weaker force constants than the glassy state. With further rise of temperature, the number of these atomic clusters increases, while the number of boroxol rings decreases. The integrated intensity of the whole contour will remain constant unless there is marked change in free volume.

3.5 Structure of v-B_2O_3

Based on the various observations reported earlier it could reasonably be stated that the Stoke's Raman shift in v-B_2O_3 at 8Ø6 cm^{-1} could be associated with the oxygen motion of boroxol rings. Brill[16] has reported values for various force constants associated with different motions of the B_3O_6 ring. He calculated the force constant for the 26 cm^{-1} band to be 2 N/m from the relation $\omega = \sqrt{k/m}$, m being the mass (~ 23ØØ amu) corresponding to ~ 169 atoms. Thus he suggested that the band at 26 cm^{-1} might represent the motion of a cluster of atoms. The force constant corresponding to 137 cm^{-1} band was calculated to be ~ 2.5 N/m by using the mass of a single boroxol unit (~ 8Ø amu). This band at 137 cm^{-1} is due to the librational motion of boroxol rings. The vibrational features which appear below 3ØØ cm^{-1}, arise from the cooperative motions of the whole structure

comprising a mixed BO_3 triangular and boroxol ring network.

A random boron-oxygen network with high proportion of boroxol rings is shown in Fig.3.6a. This two dimensional network can be extended to a three dimensional network. It is assumed that cage like structures, as shown by shaded areas in Fig.3.6a of various shapes and sizes, can be constructed in v-B_2O_3 and this random distribution of mass simulates the disorder in the glassy state. Above T_g, a random open structure is formed by reorganization of BO_3 triangles from boroxol rings (Fig.3.6b).

3.6 IR spectra of v-B_2O_3

The infrared spectrum of v-B_2O_3 is displayed in Fig.3.7 in the range 600-2000 cm^{-1}. The band near 800 cm^{-1} is very broad. In the Raman spectrum, this band peaks at 806 cm^{-1}. Here this band is attributed to the internal stretching mode of boron-oxygen hexagonal ring structure. According to Sharma et al[17] this IR band is also observed in crystalline B_2O_3 near 740-800 cm^{-1}. The sharp peak at 1210 cm^{-1} has been assigned as B-O bond stretching of the boron sub lattice against the oxygen sub lattice. The broad band around 1443 cm^{-1} is observed in both v-B_2O_3 and crystalline B_2O_3[17]. Here it is very broad in the region (1380-1500 cm^{-1}) and has been assigned to the characteristic B-O stretching vibration of different large borate groups. Among the other bands, 655 cm^{-1} is assigned to the bond bending vibration

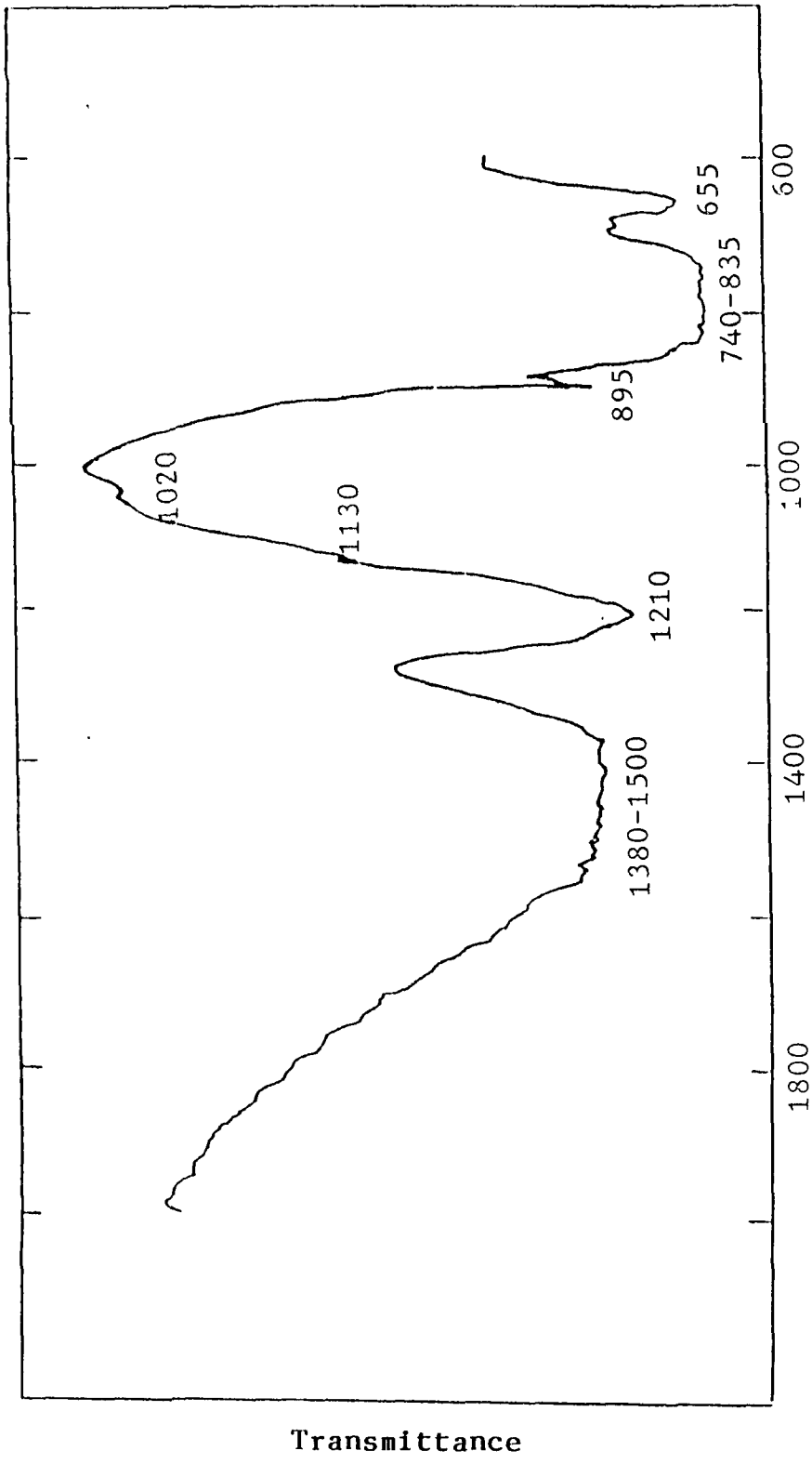

Fig.3.7 Infrared spectrum of v-B_2O_3 in the range of wave numbers 600-1600 cm^{-1}.

of B-O-B linkage, 1020 and 1130 cm^{-1} bands correspond to the motion of BO_4 groups.The observed IR and Raman bands are tabulated in Table 3.2 for comparison.

Table 3.2 IR bands observed in v-B_2O_3 and comparison with Raman bands and other reference

Raman bands (cm^{-1})	IR bands (cm^{-1}) Reference 43	present	
137			
262			
410			
460	464		
505	500		
587			
685		655	(ws)
720	717-727	690	(vw)
755			
806	808	740-835	(vb)
	947	895	(w)
1044	1035	1020	(vw)
1125	1094	1130	(vw)
1195		1210	(s)
1245	1266		
1305			
1375	1400	1380-1500	(vb)
1453			
1534			
1580			

w -->weak ; vw--> very weak ; vb--> very broad ; s--> sharp

REFERENCES

1. F.L. Galeener, J. Non-Crystalline Solids, **49** (1982) 53
2. F.L. Galeener, J. Non-Crystalline Solids, **44** (1982) 1Ø37
3. J. Goubeau and H.Z.Keller, Inorg. Chem. 272 (1953) 3Ø3
4. J. Krogh-Moe, J. Non-Crystalline Solids, **1** (1969) 269
5. J. Krogh-Moe, Phys. Chem. Glasses, **6** (1965) 46
6. R.L.Mozzi and B.E.Warren, J.Appl.Crystallogr.3 (197Ø) 251
7. G.E.Jellison Jr, L.W.Panek, P.J.Bray and G.B.Rouse, J. Chem. Phys. **66** (1977) 8Ø2
8. P.J.Bray, S.A.Feller, G.E.Jellison Jr. and Y.H.Yun, J. Non-Crystalline Solids, **38-39** (198Ø) 93
9. P.J.Bray, .E.A.Geissberger, F.Bucholtz and I.A.Harris, J. Non-Crystalline Solids (North Holland), **52** (1982) 45
10. L.Griscom, in 'Borate Glasses' Ed. by L.D.Pye, V.D.Frechette and N.K. Kreidl (Plenum, New York,1978) p-11
11. R.N.Sinclair, J.A.E.Desa, G.Etherington, P.A.V.Johnson and A.C.Wright, J. Non-Crystalline Solids, **42** (198Ø) 1Ø7
12. G.E.Walrafen, S.R.Samanta and P.N.Krishnan, J. Chem. Phys. 72 (198Ø) 113
13. F.L.Galeener, G.Lucovsky and J.C.Mikkelson Jr., Phys. Rev.B 22 (198Ø) 3983
14. K.Nakamoto, 'Infrared and Raman Spectra of Inorganic and Boron and its coordination compounds'(Wiley,New York,1973) p-97
15. R.J.Bell and A. Carnevale, Philos. Mag. B **43** (1981) 389

16. T.W.Brill, Philips Res. Rep. Suppl.No. 2 (1976) 1

17. B.K.Sharma, D.C.Dube and Abhai Mansingh, J. Non-Crystalline Solids, 65 (1984) 39

18. S.R.Elliot, Philos. Mag.B 37 (1978) 435

19. T.F.Soules, J. Chem. Phys. 73 (1980) 4032

20. M.Amini, S.K.Mitra and R.W.Hockney, J. Phys.C,14 (1981) 3689

21. W. Soppe, C. Vander Marel and H. W. den Hartog, J. Non-Crystalline Solids, 101 (1988) 101

22. W.Soppe and H.W. den Hartog, J. Phys.C 21 (1988) L 689

23. M.A.Kanehisa and R.Elliot, Materials Science and Engg., B3 (1989) 163

24. F.L.Galeener and A.E.Geisberger, J. Phys.(Paris) Colloq. 44 (1983) c 9-343

25. C.F.Windich and W.M.Risen Jr., J. Non-Crystalline Solids, 48 (1982) 307

26. (i) T.F.Young and R.P. Westerdale, ARL 135, Aero Space research, U.S.Air Force,1961

(ii) S.L.Strong, Dissertation, MIT,1965-66

27. L.C.Synder, 'Quantum Mechanical Studies of the Structure and Thermo Chemistry of Species Postulated to exist in Borate glasses', Am. Ceram. Soc. Mig. Bedford Springs, P.A., Oct. 12, (1978)

28. P.W.Anderson , B.I.Halperin and C.M.Verma, Philos. Mag. 25 (1972) 1

29..W.A.Philips, J. Low Temp. Phys., 7 (1972) 351

30. R.C.Zeller and R.O. Pohl, Phys. Rev. B **4** (1971) 2029

31. R.B.Stephens, Phys. Rev. B **8** (1973) 2896

32. R.M.Almeida, J. Non-Crystalline Solids, **106** (1988) 347

33. J.P.Mc Tague and G.Birnbaum, Phys. Rev. Letters, **21** (1968) 661

34. W.S.Gornall, H.E.Howardlock and B.P.Stoicheff, Phys. Rev, **A1** (1970) 1288

35. J.P.Mc. Tague, P.A.Fleurry and D.B.Dupre, Phys. Rev.**188** (1969) 303

36. J. Bucaro and T.A.Litovitz, J. Chem.Phys. **54** (1971) 3846 Also see reference 32

37. Gigantskoe Kombintsionnce-- Rasseyanic Sveta, Ed. by R. Cheng and T.Furtak, Mir Moskva,p-342

38. R.Shuker and R.W.Gammon, Phys. Rev. Letters **25** (1970) 222

39. R.Shuker and R.W.Gammon, J. Chem Phys. **55** (1971) 4784

40. S.Guha and G.E. Walrafen, J. Chem. Phys.,**80** (1984) 3807

41. A.J.Martin and W.Brenig, Phys.Status Solidi B **64** (1974) 163

42. Vskaya, *in* 'Hand book of glass data, part B, Single Component and Binary Nonsilicate Oxide Glasses, (Elsevier, Amsterdam,1985)

43. J.L.Parsons and M.E.Milberg, J.Am. Chem. Soc., **43** (1960) 326

CHAPTER IV

VIBRATIONAL STUDIES OF ALKALINE-EARTH BORATE GLASSES

4.1 Introduction

When a boron atom of electronic configuration $1s^2\ 2s^2\ 2p^1$ forms a bond with an oxygen atom of electronic configuration $1s^2\ 2s^2\ 2p^4$, they form triangular planar bonds by hybridized sp^2 orbital and the transition from triangular to tetrahedral (through sp^3 orbital hybridization) is facilitated by easy acceptance of an electron-pair from a base into the low-energy fourth orbital of the boron valence shell. The measured B-O bond distances in trigonal borates range from 1.28 to 1.44 A° while tetrahedral bond lengths vary from 1.42 to 1.54 A°. Moreover, there is evidence[1] based on IR measurements for B =O stretching motion in gaseous borates. Here the boron coordination by oxygen is two-fold and linear, that is, -O-B= . The structural analysis of the borates by Raman and IR spectroscopy would permit the determination of boron oxygen linkage involving triangular BO_3, tetrahedral BO_4 or any other form of B-O bonding in which the fundamental frequencies are established by comparison with chemically analogous or known borate configurations.

Spectroscopically, Krogh-Moe[2-4] studied alkali borate glasses and proposed that alkali borate glasses should contain

those structural units (pertaining to the ranges of alkali oxide concentrations) which occur in related crystalline compounds. Konijnendijk[5] recorded Raman and infrared spectra of alkali and alkaline earth borate glasses and obtained similar results as was predicted by Krogh-Moe. In general, BO_3 and BO_4 units appear in larger structural groups whose type and distribution change with changing composition. Also in the transition from triangular BO_3 to three dimensional BO_4 tetrahedra, there occurs a decrease of the expansion coefficient, while the introduction of alkali or alkaline-earth ions increases it. For the concentration range, 16 $<Na_2O<$33 mol% in sodium borate binary glasses, interstices have been proposed[6] to develop among the BO_4 tetrhedral units. Thus the density of the glass should change due to the formation of such interstices.

In this chapter, alkaline-earth binary and ternary glasses have been studied by Raman and infrared techniques. The binary glasses are specified as $xMO.(1-x)B_2O_3$ for M=Ca,Sr,Ba and Cd, where x represents the concentration in the range $Ø.2Ø \leq x \leq Ø.5Ø$. The alkali borate glasses $xM_2O.(1-x)B_2O_3$ (where M=alkali metal) are currently being used, besides other technological applications, as vitreous matrices for the realization of ionic conductors[7-1Ø]. In a similar way, the alkaline earth borate glasses might offer the valuable possibility of behaving as ionic conductors by a systematic variation of the nature of the

metal cation over a wide concentration range. Moreover, the study of the structural changes that may result in the borate network by the addition of metal cations is of interest for understanding the vitreous networks. With this end in view, ternary borate glasses $(MCl_2)_y.[(MO)_x.(B_2O_3)_{1-y-x}]_{1-y}$, where M=Ba & Sr for different values of x and y, have also been studied in this chapter. A substantial effect of MCl_2 (M=Ba & Sr) introduced into the binary $xMO.(1-x)B_2O_3$ glass has been observed in the low frequency region. The identification of the glass forming structural units are made qualitatively from the analysis of the high frequency part of the Raman spectra (in conjunction with IR spectra) following the concentration dependence of the dopant in the basic glass network. Special mention is made to the low frequency part of the Raman spectra which includes the so called "boson" peak.

The structure of disorderd solids would be systematically unravelled with the help of the data made available by the light scattering experiments in the low frequency region or by Brillouin scattering. Theoretically Martin and Brenig[11] had described the feature of the low frequency Raman spectra in terms of structural properties of the amorphous solids. This low frequency region of Raman spectra of disordered solids has been investigated by Nemanich[12] to determine not only the general features associated with the light scattering from acoustic

modes but also to ascertain structural properties of specific glasses. In this chapter, we specially apply Martin and Brenig (MB) model to interpret the low frequency wing of Raman spectra of the strontium borate glasses leading thereby to the estimation of the structural correlation ranges (SCR) in these systems.

4.2 Experimental

For the preparation of alkaline earth borate glasses in the system $xMO.(1-x)B_2O_3$, where M = Ca, Sr, Ba & Cd, for concentration range $Ø.2Ø \leq x \leq Ø.5Ø$, appropriate amounts of MCO_3 (obtained from sd. Fine Chem, Bombay, India) were mixed properly with dehydrated boric acid powder and the mixture was heated upto 12ØØ°C for two hours in a china clay crucible and the glass samples of about 1.5 mm thickness were prepared following the procedure described in section 2.2 of chapter-II. All these binary glass samples were transparent, homogeneous and colourless except at higher concentrations of calcium borate glasses which were slightly redish. The ternary borate glasses were prepared in the system $(MCl_2)_y.[(MO)_x.(B_2O_3)_{1-y-x}]_{1-y}$, where M=Ba & Sr for $Ø.2Ø \leq y \leq Ø.4Ø$ and x=Ø.2Ø & Ø.35, by mixing the appropriate amounts of MCl_2 (M=Ba & Sr) with MCO_3 and dehydrated boric acid powder and then by heating the mixture upto 12ØØ°C for one hour in the same way as described above.

These ternary glasses were transparent and slightly greenish in colour.

For IR spectral measurements, a part of the above glasses were grinded into fine powder by morter-pestle and mixed with analar grade KBr powder using the pressed disc technique (see chapter-II) and transparent KBr pellets were prepared. These samples were used for recording the IR spectra with the help of the Perkin-Elmer model-681 spectrophotometer. Raman spectra of all the glass samples were recorded on both the HG2S and Ramanor U-1000 double monochromator equipped with argon ion laser using 514.5 nm line.

4.3 Chemical mechanism

The Raman spectrum of pure v-B_2O_3 is characterized by a strong and narrow (full width at half maximum ~ 15 cm^{-1}) peak near 806 cm^{-1} which is now unambiguously assigned to the boroxol ring oxygen atom breathing vibrations with little boron motion involved. Though the v-B_2O_3 structure mainly comprises of a matrix (network) of boroxol rings (Fig.3.1), it essentially consists of BO_3 triangles. The introduction of MO (M=Ca,Sr,Ba & Cd) to the v-B_2O_3 matrix causes a change of the boron atom coordination number from 3 to 4 according to the following scheme:

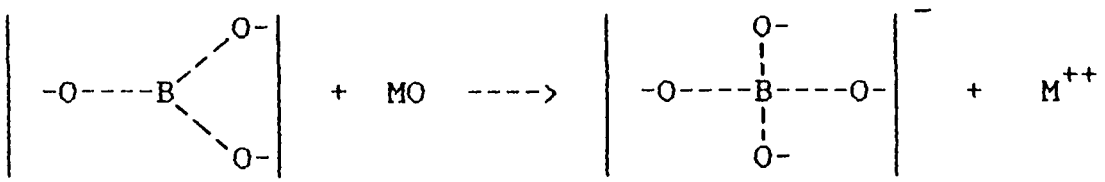

This mechanism liberates cations (M^{++}) to increase the ionic conductivity of the glass. The experimental evidence of such a process is the appearance of a Raman band around (780-755 cm^{-1}) in the borate glasses with corresponding disappearance of the band at 806 cm^{-1}.

4.4 Calcium borate glasses' spectra

(A) Raman results:

Fig.4.1(a-f) shows the Raman spectra of calcium borate glasses in the system $xCaO.(1-x)B_2O_3$ for $0.20 \leq x \leq 0.50$ in the range 12-1600 cm^{-1}. Fig.4.1(a) shows a splitting of the band at 806 cm^{-1} for v-B_2O_3, giving rise to a new band at 778 cm^{-1} along with the band at 800 cm^{-1} slightly displaced from 806 cm^{-1}. With gradual increase of concentration (x) of CaO, the intensity of the new band at 778 cm^{-1} increases causing a corresponding decrease in intensity of the band at 800 cm^{-1}. At concentration x=0.35 (Fig.4.1d), the band at 800 cm^{-1} disappears completely and the band at 778 cm^{-1} shifts towards lower wave number at 773 cm^{-1}. The variation in position of 778 cm^{-1} band with concentration (x) is shown in Fig.4.2a, while the corresponding

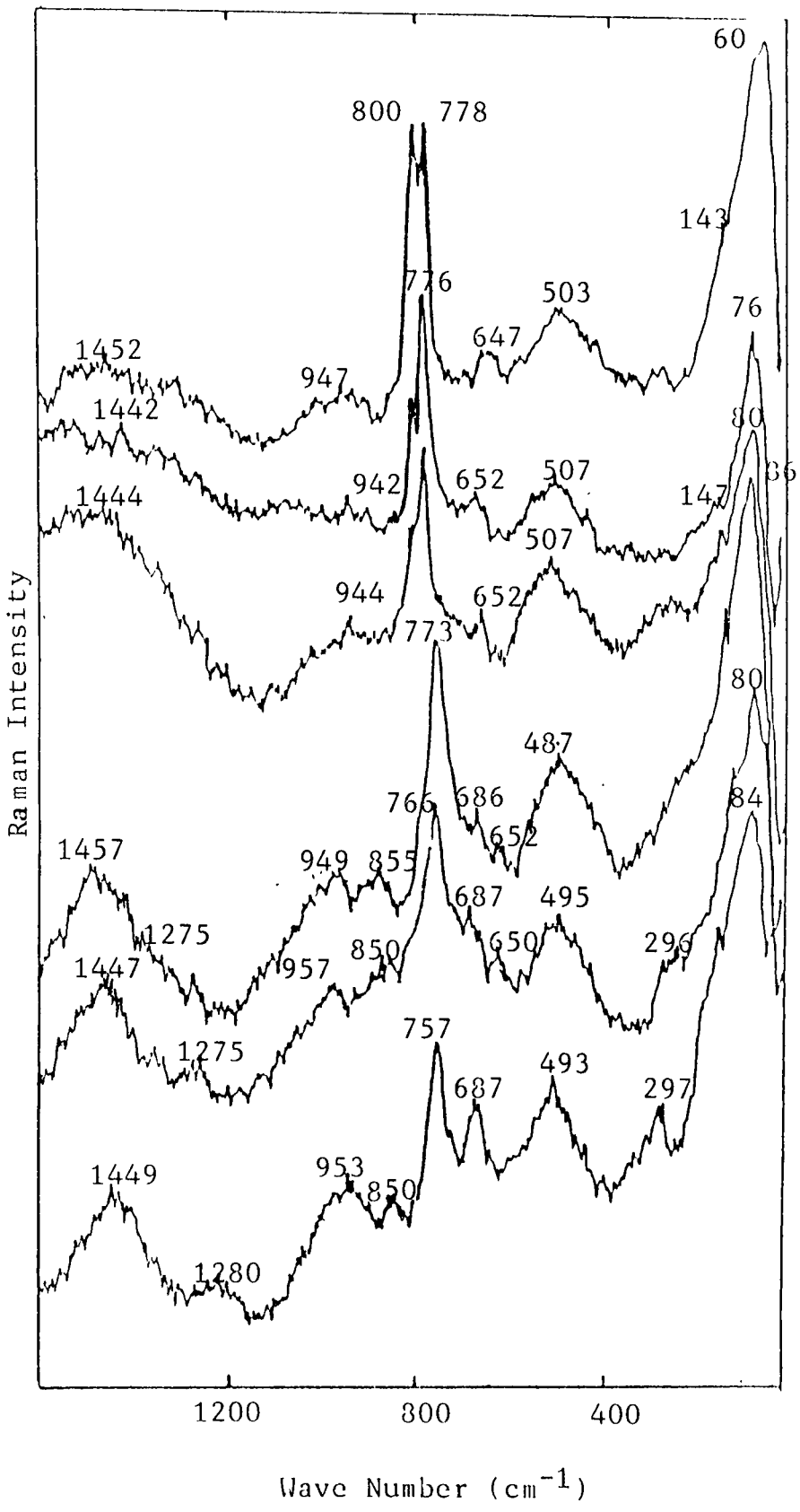

Fig. 4.1 Raman spectrum of calcium borate glasses in the system $xCaO.(1-x)B_2O_3$ for concentration x:
(a) Ø.2Ø, (b) Ø.25, (c) Ø.3Ø, (d) Ø.35, (e) Ø.4Ø and

change in intensity of 778 cm^{-1} band with x is shown in Fig.4.2b. We see that as a result of addition of CaO to v-B_2O_3, the trigonal coordination of boron within boroxol ring is changed into tetragonal, forming borate cyclic rings with one BO_4 at lower concentration (x) of CaO. A similar situation is observed in alkali borate[13,14] and silver borate glasses[15]. The appearance of the band at 778 cm^{-1} at the cost of the band at 8Ø6 cm^{-1} is attributed to the symmetric breathing vibration of borate rings containing BO_4 and BO_3 units. Schematic representation of the change of boroxol ring is as given below:

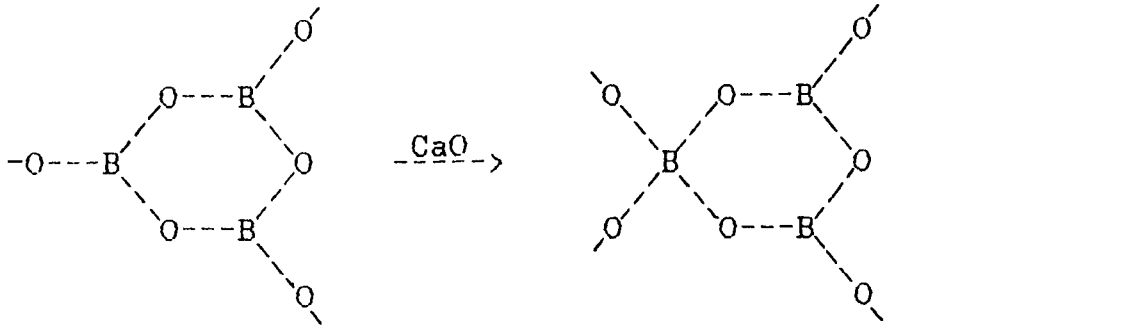

(8Ø6 cm^{-1}, boroxol ring) (773 cm^{-1}, triborate ring[14])

The vibrational band at 78Ø cm^{-1} is characteristic[16] of the tetraborate groups which are formed when triborate and pentaborate groups are paired. So upto x=Ø.35, tetraborate groups are predominantly present in the calcium borate glasses. All the extra oxygen atoms begin to form bridge between boron atoms. The gradual addition of CaO to v-B_2O_3 increases the network coherence degree i.e., the formation rate of BO_4 units

rises with concentration and at x=Ø.35, the network is saturated in its coherence degree since the intensity of 773 cm^{-1} band becomes maximum (Fig.4.2b) at this concentration of CaO. The disappearance of the band at 8Ø6 cm^{-1} at x=Ø.35 indicates that the boroxol rings are all converted into borate cyclic groups containing BO_3 and BO_4 units. At concentration x > Ø.35, the intensity of the band at 773 cm^{-1} diminishes gradually with increasing concentration x and its position is shifted to 757 cm^{-1} at x=Ø.5Ø indicating the formation of six membered borate rings with two BO_4 units (e.g. ditri- or dipentaborate groups)[16]. Schematically,

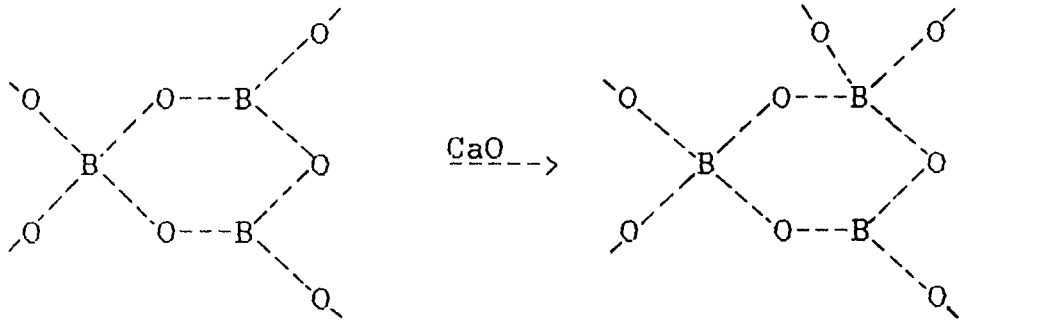

(773 cm^{-1}, triborate) (757 cm^{-1}, ditriborate)

Here the breakdown of the network coherence occurs and the relative number of tetragonal boron ions decreases, causing the formation of non-bridging oxygens (NBO) i.e., the oxygen atoms which are not involved in B-O-B linkages. The shifting of the band at 773 cm^{-1} towards lower wavenumbers is also due to the formation of NBO's. The calcium ions (Ca^{++}) become localized in

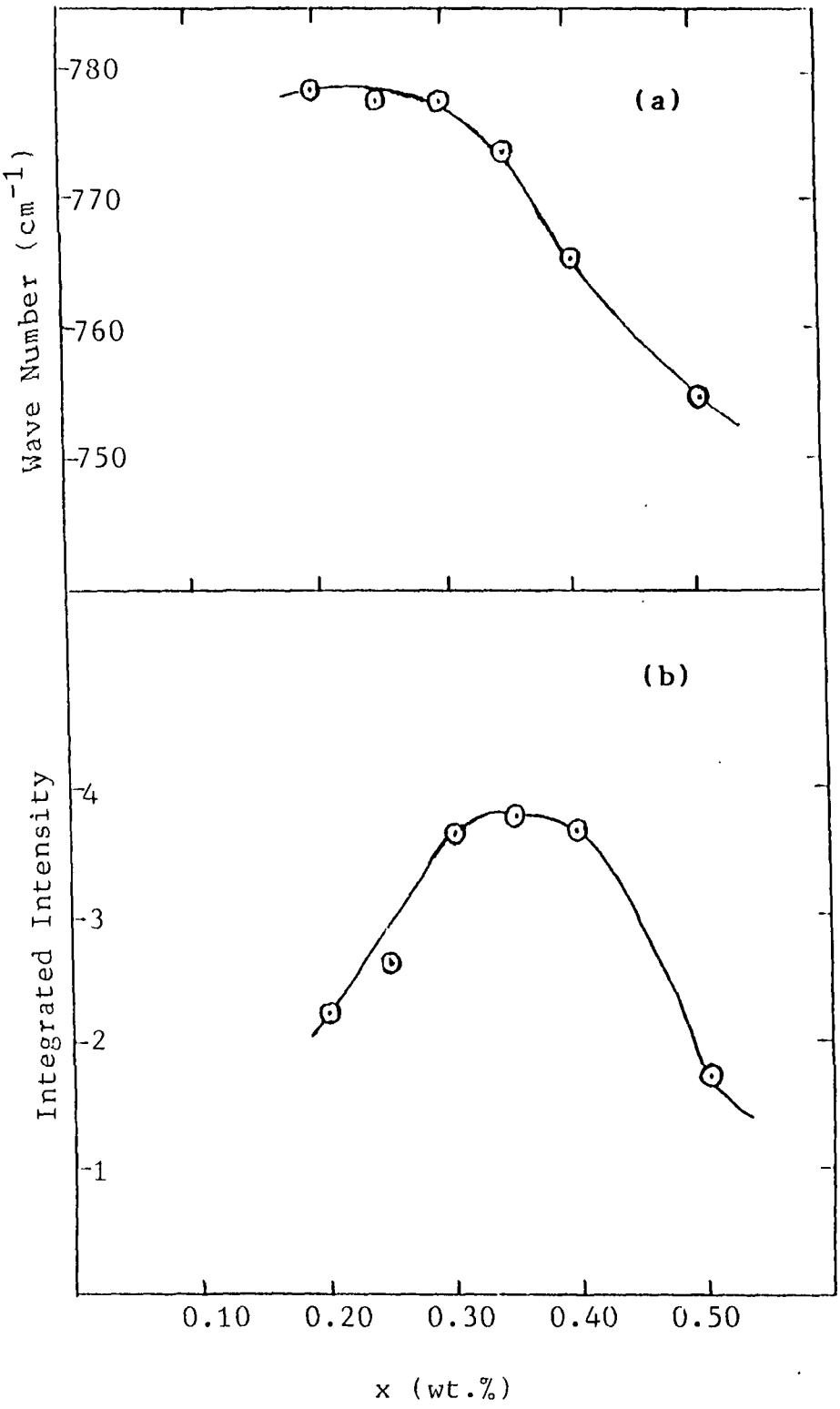

Fig. 4.2 Variation in (a) position and (b) integrated intensity (peak height x full width at half maximum) of the 778 cm^{-1} band with concentration (x) in calcium borate glasses.

the interstices of the network near BO_3 groups or the NBO's to ensure the charge neutrality. The positions of all the observed Raman bands in calcium borate glasses' spectra at different values of x are tabulated in Table-4.1. The second stronger feature in the high frequency region appears as a broad band contour in the region 1442-1457 cm^{-1}. This band whose intensity increases with concentration x of CaO is mainly due to different types of boron-oxygen stretching vibrations associated with $>B-O^-$ groups,similar to those observed in $Na_2O.B_2O_3$ glasses[17,18]. At higher concentration (x),this band involves non-bridging oxygens and may be associated with large borate groups with dangling $>B-O^-$ bonds[19,20]. For example, triborate group with one NBO represents typical borate group containing NBO bond:

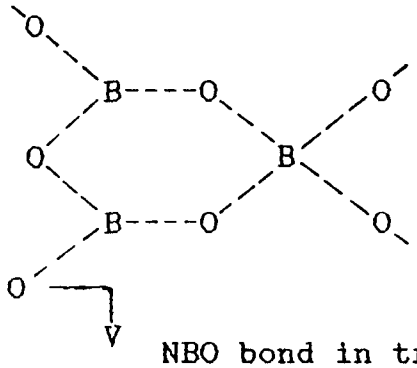

NBO bond in triborate with one NBO

A very weak broad band at 1275 cm^{-1} appears at higher concentrations (x) of CaO. This band is associated with pyroborate groups[16]. Raman bands in the region 900-1100 cm^{-1}

Table 4.1 The observed Raman bands in alkaline earth borate glasses in the system $xMO.(1-x)B_2O_3$ (for M=Ca, Sr and Ba) at various values of (x)

System	Conc. (x)	Wave numbers (cm^{-1})										
Calcium borate	Ø.2Ø	6Ø	143		5Ø3	647		778	8ØØ	947		1452
	Ø.25	76	147		5Ø7	652		776	799	942		1442
	Ø.3Ø	8Ø	145		5Ø7	652		776	799	944		1444
	Ø.35	86	14Ø		487	652	686	773	855	949	1275	1457
	Ø.4Ø	8Ø	139	296	495	65Ø	687	766	85Ø	957	1275	1447
	Ø.5Ø	84	146	297	493	-	687	757	85Ø	953	128Ø	1449
Strontium borate	Ø.2Ø	58			487	662		772	8Ø1	942		1427
	Ø.25	63			497	665		772	-	939		1462
	Ø.3Ø	67			5Ø2	662		772	-	932		1437
	Ø.35	71			5Ø2	662		767	-	942		1437
	Ø.4Ø	73			497	667		765	-	942		1442
	Ø.5Ø	79			5Ø7	673		762	-	953		1452
Barium borate	Ø.2Ø	44			474	654		775	8Ø2	912		15ØØ
	Ø.25	5Ø			475	655		774	8Ø3	937		1437
	Ø.3Ø	5Ø			476	657		771	8Ø2	932		1462
	Ø.35	51			469	659		767	-	937		1447
	Ø.4Ø	51		424	47Ø	654		765	-	957		1445
	Ø.5Ø	56		424	487	645		763	-	88Ø	96Ø 11ØØ	1433

appears in borate glasses containing tetragonal borons[21]. Thus the weak band around 942-957 cm^{-1} can be attributed to the boron-oxygen stretching of tetragonally coordinated borons associated with the group ≡B-O-B≡ at lower concentration (x). At higher concentration (x≥Ø.35) the band around 94Ø cm^{-1} is attributed to the stretching vibration of orthoborate units[14,16]. This assignment is supported by the fact that a similar band is observed in the spectra of crystalline orthoborates[5]. The adjacent band around 85Ø cm^{-1} which develops in the spectrum at x≥Ø.35, is the characteristic feature associated with the pyroborate groups. Comparison of the 85Ø and 942 cm^{-1} bands observed in crystalline magnesium pyro- and orthoborate compounds respectively[16] with those observed in calcium borate glasses, also confirms the above assignments. The band at 1275 cm^{-1} may also be due to the stretching vibration of the terminal $B-O^-$ bonds in $B_2O_5^{4-}$ anions.

The Raman band at 487-5Ø7 cm^{-1} may be associated with the bending motion of free BO_4 units or one (BO_4 unit) that is attached very weakly to a ring type structure. In pure v-B_2O_3, the band at 47Ø cm^{-1} has been assigned to the ring bending mode of the boroxol ring[22]. For alkali borate glasses this band is observed at higher wavenumber[14,23]. A less intense band can be seen in the spectra of Fig.4.1 around 647-687 cm^{-1}. This band originates from the vibrations of ring/chain type metaborate

groups[14,24]. At concentration x=Ø.5Ø (Fig.4.1f), this band is more intense than at lower concentration and is shifted to higher wavenumbers indicating the formation of chain type metaborate.

On the basis of these assignments of all the Raman bands in the high frequency region, the structural changes upon gradual introduction of CaO to v-B_2O_3 are obvious. We see that for x≥Ø.35 no boroxol rings exist, while the number of tetraborate groups which are predominant upto x≤Ø.35 (characterized by the band contour around 78Ø-773 cm^{-1}) decreases progressively with rise of concentration x. For the glass of composition Ø.35 CaO.Ø.65B_2O_3, the tetraborate groups along with tri- and pentaborate groups are expected to be appreciable which can be ascertained by a strong band at 773 cm^{-1}. However, it is not possible to distinguish from the Raman spectra alone which group is really present in the glass since tri- and pentaborate groups are paired to form tetraborate:

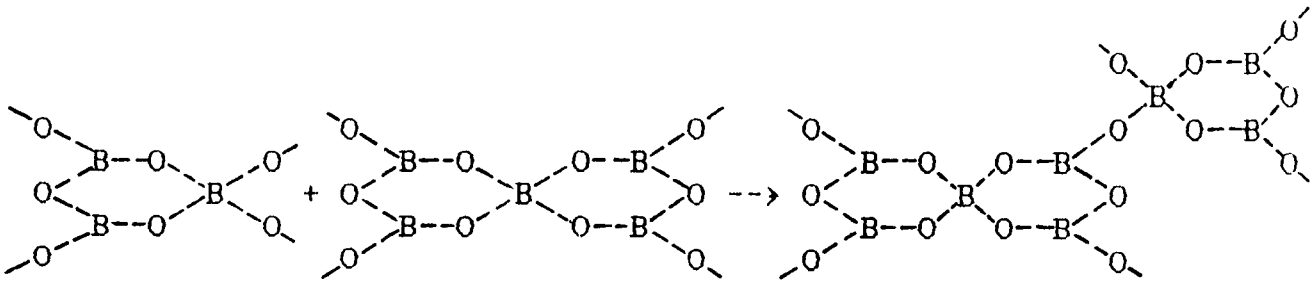

At x=Ø.35, the development of very weak bands (Fig.4.1d) at 1275

and 855 cm^{-1} shows the formation of pyroborate groups while 949 and 652 cm^{-1} bands indicate the presence of small number of ortho- and metaborate groups respectively. The developement of another weak band at 686 cm^{-1} at x=Ø.35 (Fig.4.1d) shows the formation of chain type metaborate. With rise of concentration x of CaO, this band at 686 cm^{-1} rises in intensity which shows that the number of chain type metaborates increases while the corresponding decrease in intensity of the band at 757 cm^{-1} shows the reduced number of di-triborate rings. So for the glass of composition Ø.5ØCaO.Ø.5ØB_2O_3, chain type metaborates [along with some small percentages of ortho- (953 cm^{-1}) and pyroborate (128Ø, 85Ø cm^{-1}) groups] are formed at the expense of the di-triborate rings:

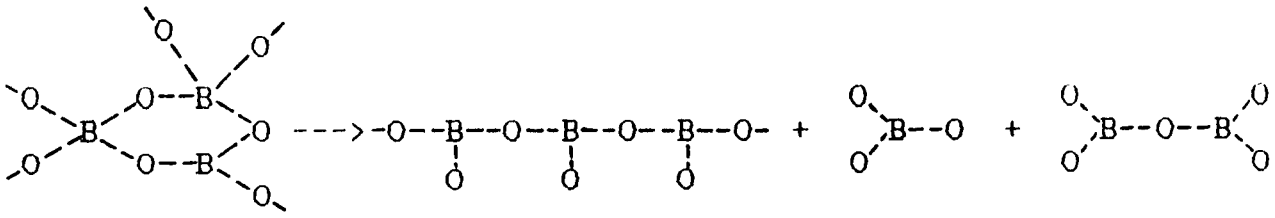

Ditriborate 757 cm^{-1} | *chain type meta-* 687 cm^{-1} | *ortho-* 953 cm^{-1} | *pyroborate* 850 & 1280 cm^{-1}

The chain type metaborate is also formed in the crystalline $CaO.B_2O_3$ compound[14].

In the low frequency region of calcium borate spectra (Fig.4.1), we see a broad band at 6Ø cm^{-1} (Fig.4.1a) together with a shoulder at 143 cm^{-1} and a weak band near 296 cm^{-1} at

high concentration (x). For pure v-B_2O_3, we observe also a similar band known as boson peak centering at 26 cm^{-1}. Upon introduction of CaO to v-B_2O_3 the band is shifted to 6Ø cm^{-1} and with gradual addition of (x) CaO, the band shifts towards higher wavenumbers (Fig.4.3a) while its intensity first rises (Fig.4.3b) and then decreases with concentration (x). The shoulder at 143 cm^{-1} remains nearly undisturbed in the spectra of these glasses. According to Brill[25], the force constants of O-B-O, B-O-B bendings and O-B-O-B torsion are about 3Ø-8Ø N/m. This corresponds to a cluster mass of 3Ø-8Ø amu. As the masses of BO_3 and BO_4 units are respectively 6Ø and 76 amu, it could be proposed that 143 cm^{-1} band corresponds to the librational modes of BO_3 and BO_4 units. The bands at 296 cm^{-1} for x=Ø.4Ø and 297 cm^{-1} for x=Ø.5Ø may be associated with the motions of Ca^{++} ions at the oxygen sites. Here the calcium ions may interact with the local oxygen (mainly NBO's) environments depending on the type of such oxygen sites such as tetrahedral, traingular or octahedral groups.

The origin of boson peak has been discussed in strontium borate glasses in section 4.5 and also for v-B_2O_3 spectra (chapter-III, sec.3.3.1). This band is the characteristic of all borate glasses and arises due to the limited structural correlation range in the glass structure. For a disordered system, where the periodic atomic arrangement lies only within

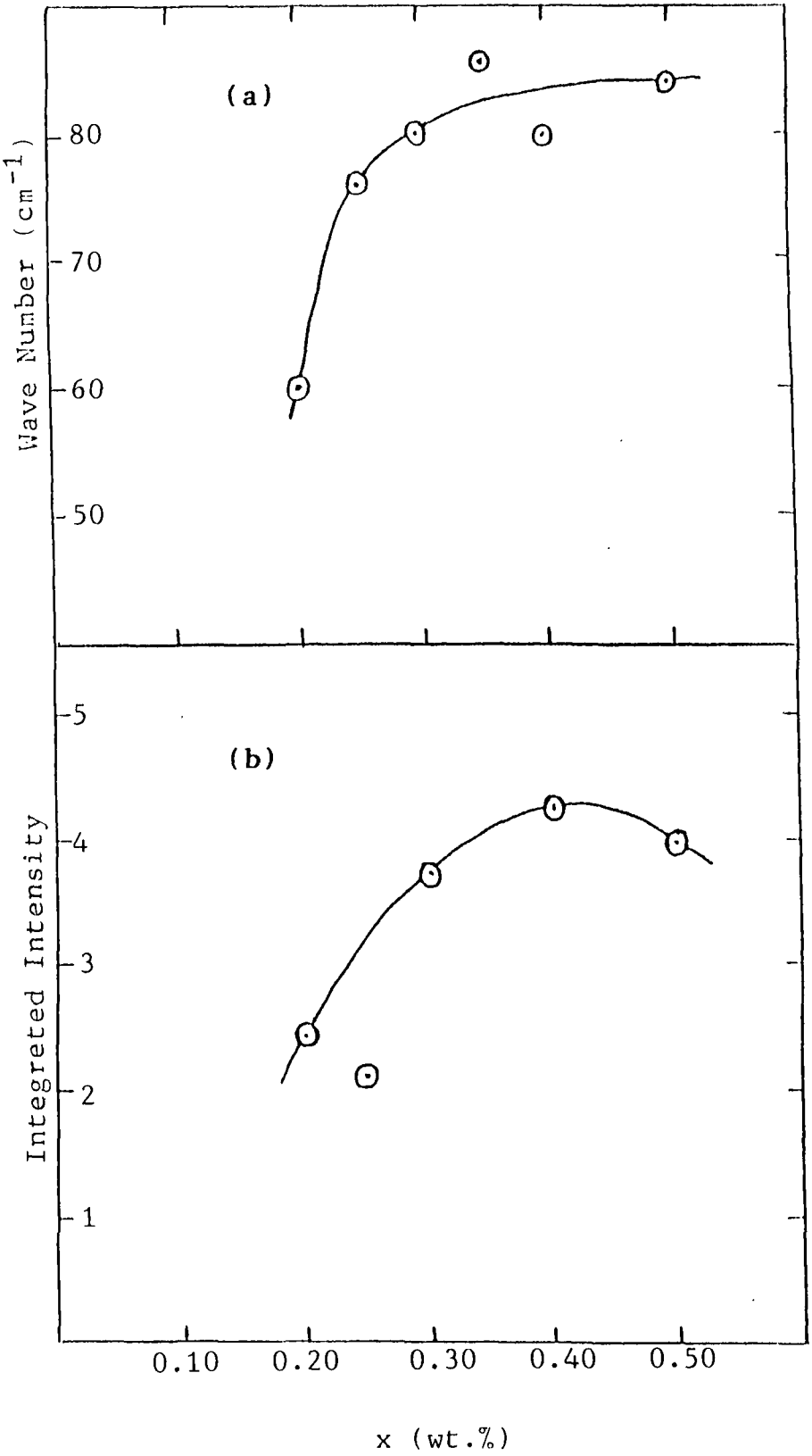

Fig. 4.3 Variation in (a) position and (b) integrated intensity (peak height x full width at half maximum) of the boson peak with concentration (x) in calcium borate binary glasses.

few coordination spheres, the low frequency light scattering from long wavelength acoustic modes is responsible for the appearance of the boson peak in the Raman spectra.

(B) IR results

Fig.4.4 shows the infrared spectra of calcium borate glasses in the system $xCaO.(1-x)B_2O_3$ for x=Ø,Ø.2Ø,Ø.35 and Ø.5Ø in the range of wave numbers 6ØØ-16ØØ cm^{-1}. The splitted band (Fig.4.4b) at 79Ø-82Ø cm^{-1}, also observed in the Raman spectrum for x=Ø.2Ø (Fig.4.1a) at 778 and 8ØØ cm^{-1}, is attributed to the stretching of boron oxygen cyclic ring containing BO_3 and BO_4 units. Fig4.4a shows the spectrum for $v\text{-}B_2O_3$ (x=Ø) where the band around 8ØØ cm^{-1} is broad and corresponds to boroxol ring. A detailed explanation of the IR spectra of borate glasses is found to be difficult due to the complexity originating from the glassy nature of the materials coupled with the large number of possible structural groups found in borate glasses. However, it is generally accepted that the broad absorption band around 12ØØ-145Ø cm^{-1} is attributed to B-O bond stretching of trigonal BO_3 units, while that in the region around 85Ø-11ØØ cm^{-1} originates from B-O bond stretching of tetrahedral BO_4 units. The 65Ø-7ØØ cm^{-1} band contour is assigned to the out of plane bending vibration of B-O-B linkages of boron oxygen network[6,22,26]. The shift of the band at 665 to 71Ø cm^{-1} with increase of concentration (x) along with the increase in its

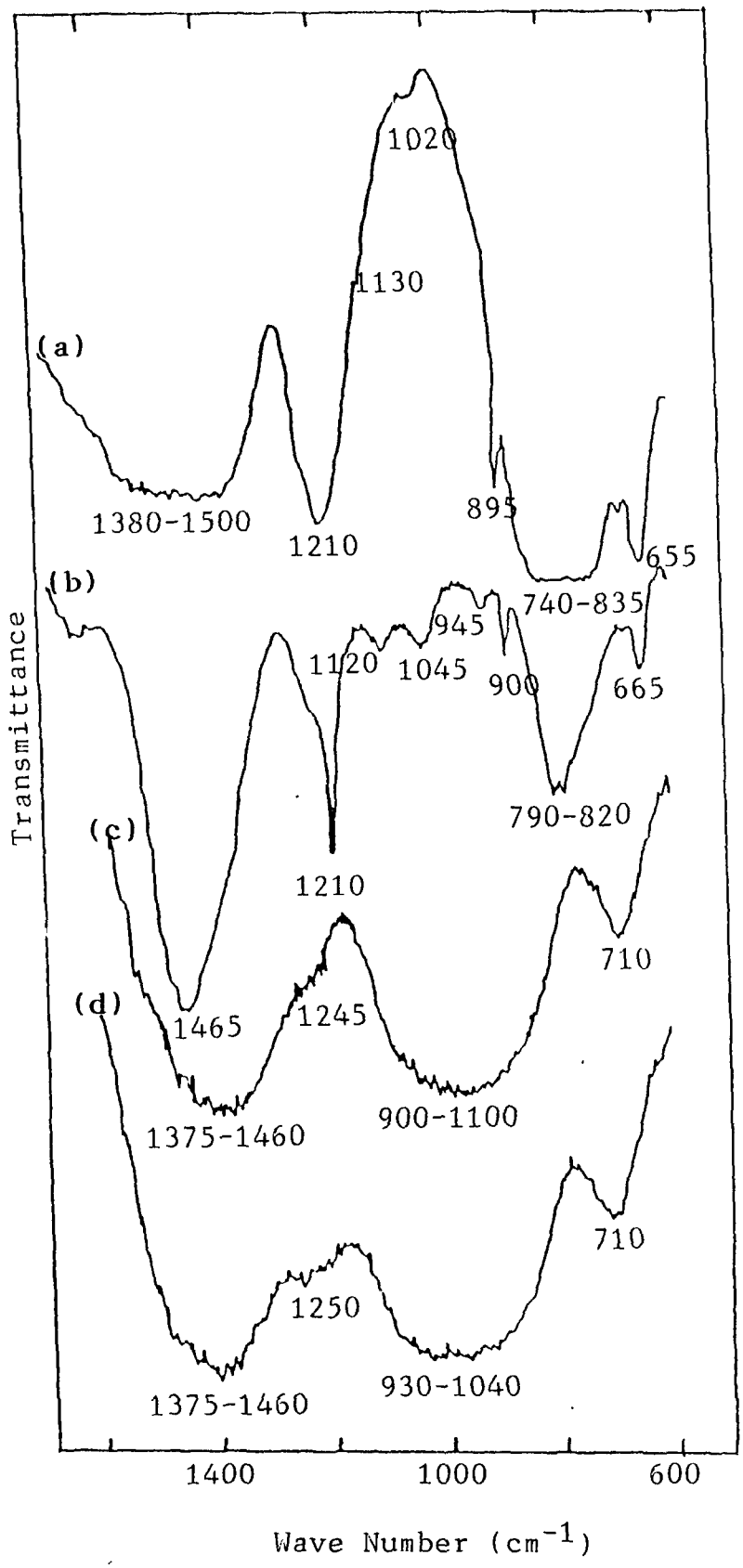

Fig. 4.4 IR spectra of calcium borate glasses in the system $xCaO.(1-x)B_2O_3$ for the values of x:
(a) Ø, (b) Ø.2Ø, (c) Ø.35 and (d) Ø.5Ø.

intensity shows the formation of chain type metaborate groups. However, all the above classifications give no account of the specific borate groups containing BO_3 and BO_4 units, even though each of the absorption band contours clearly exhibits structural changes. On the basis of the original work of Krogh-Moe[22,26] as well as the observed trends in the IR spectra of alkali borate glasses[17-19,27], the assignments of the present bands may be made. The band at 1210 cm^{-1} is observed in the IR spectra of both v-B_2O_3 (Fig.4.4a) and calcium borate (Fig.4.4b). Its intensity decreases upon increasing concentration of CaO and finally the band disappears. For v-B_2O_3, this band is assigned to the B-O stretching vibration involving mainly BO_3 triangles. In alkali borate glasses, it is assigned to the B-O stretching involving the linkage oxygen connecting different groups[22]. In the present system where no boroxol rings are present, the band at 1210-1245 cm^{-1} indicate that tetraborate groups also contribute to this absorption.

The broad band contour at 1375-1460 cm^{-1} is observed in v-B_2O_3, alkali and alkaline earth borate glasses. This band corresponds to the B-O stretch of different borate groups. At higher concentration of modifier cations, this band involves non-bridging oxygens. In the absorption region associated with BO_4 units, three main bands appear at 900-945, 1045 and 1120cm^{-1} (Fig.4.4b). Crystalline tetraborate[16] compounds show strong

bands at 1020 and 880 cm^{-1}. Thus the bands at 1045 and 900 cm^{-1} in the present experiment are associated with the BO_4 vibration of tetraborate (triborate,pentaborate) groups. The absorption in the region 900-1000 cm^{-1} is associated with vibrations of BO_4 tetrahedra belonging to diborate groups[16]. Crystalline $ZnO.2B_2O_3$ gives a strong band at 1115 cm^{-1} while $LiO.2B_2O_3$ compound gives[5] peaks at 1170 and 1035 cm^{-1}. The comparison of the IR spectra of calcium borate glass with the above crystalline diborates suggests that the 1120 cm^{-1} band may be assigned to the characteristic vibration of diborate groups. At higher concentrations (x) of CaO, all these bands merge and form a broad and intense envelope. Table 4.2 shows the comparison of the bands observed in Raman and IR spectra of calcium borate binary glasses.

4.5 Strontium borate glasses' spectra

(A) Raman results

Raman spectral measurements on strontium borate glasses in the systems of $xSrO.(1-x)B_2O_3$ and $(SrCl_2)_y.[xSrO.(1-y-x)B_2O_3]_{1-y}$ as functions of x and y of SrO and $SrCl_2$ respectively have been performed and the effect of temperature variation has also been studied in the binary system. Figure 4.5 shows the Raman spectra of strontium borate glasses in the system $xSrO.(1-x)B_2O_3$ for concentrations of x=0.20, 0.25,0.30,0.35,0.40 and 0.50 at room

Table 4.2 The bands observed in the Raman and IR spectra of the glasses in the system $xCaO.(1-x)B_2O_3$ for x=Ø.2Ø, Ø.35 and Ø.5Ø and their assignments.

Conc. (x)	Raman bands (cm^{-1})	IR bands (cm^{-1})	Assignments**
Ø.2Ø	1452 (wb)*	1465 (vb,i)	B-O stretch in different borates
	-*-	121Ø (vsh)	B-O stretch in BO_3 triangles
	-*-	112Ø (vw)	Stretching in diborate groups
	-*-	1Ø45 (vw)	
	947 (vw,b)	9ØØ-945 (vw)	BO_4 vibration in tetraborate
	8ØØ (sh,i)	79Ø-82Ø (b,i)	Symmetric stretch in boroxol ring
	778 (sh,i)	-*-	Stretching in triborate groups
	647 (vw)	665 (w,sh)	Due to metaborate groups
Ø.35	1457 (b,i)	1375-146Ø (b,i)	
	1275 (vw)	-*-	Due to pyroborate groups
	-*-	1245 (vw)	Due to tetraborate groups
	949 (vw)	9ØØ-11ØØ (vb,i)	
	855 (vw)	-*-	Due to pyroborate groups
	773 (sh,s)	-*-	Stretch in groups with one BO_4
	686 (vw)	-*-	Due to chain type metaborate
	652 (vw)	710	
Ø.5Ø	1449 (b,i)	1375-146Ø (b,i)	Due to borate groups with non-bridged oxygens
	128Ø (w)	125Ø (vw)	Due to pyroborate groups
	953 (w,b)	1Ø4Ø-93Ø (vb,i)	
	85Ø (vw)	-*-	
	757 (sh,w)	-*-	Stretch in di-triborate groups
	687 (w,sh)	710	Due to chain type metaborate

* w-->weak, b-->broad, vw-->very weak, sh-->sharp, i-->intense, s-->strong vb-->very broad, vsh--> very sharp ** For detailed assignments, see text

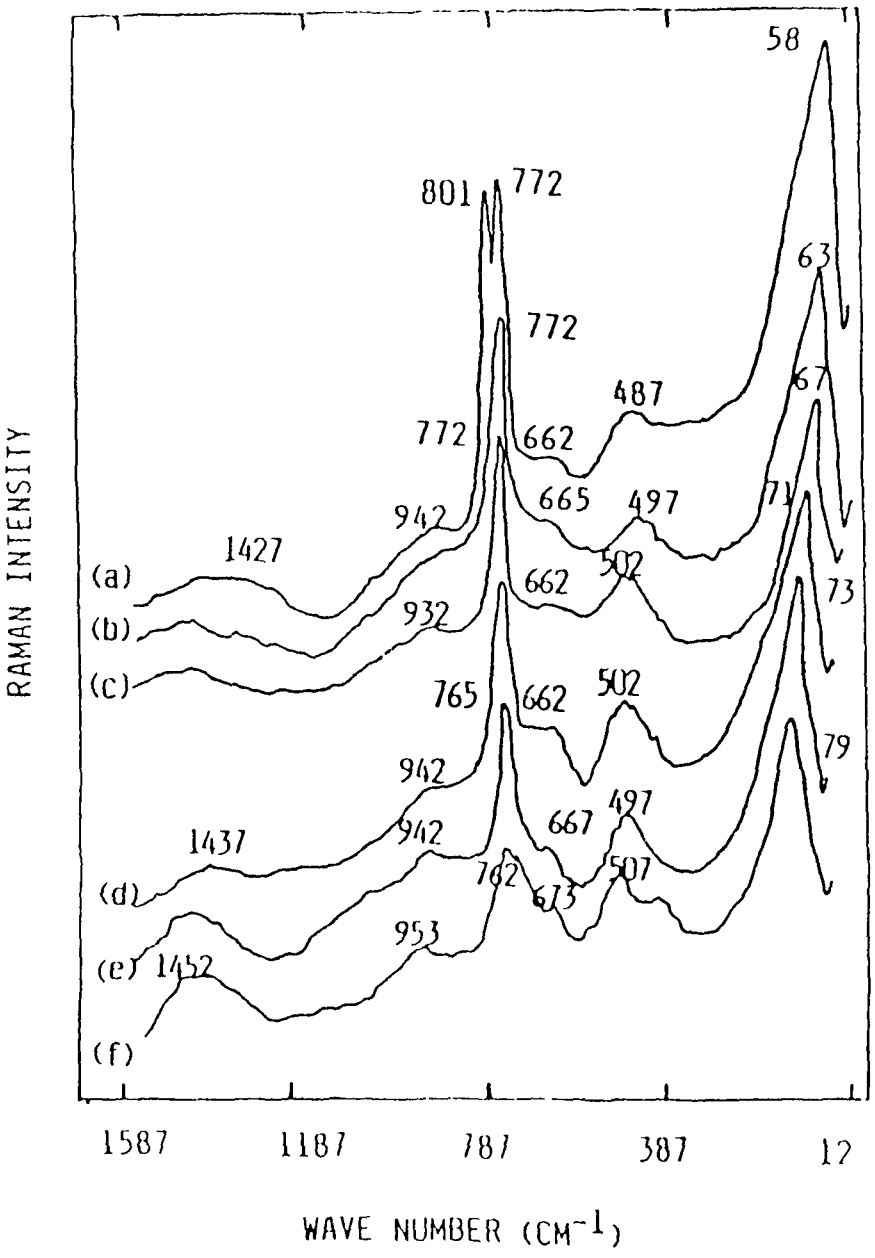

Fig. 4.5 Raman spectra of strontium borate glasses in the system $xSrO.(1-x)B_2O_3$ for the values of x:
(a) Ø.2Ø, (b) Ø.25, (c) Ø.3Ø, (d) Ø.35, (e) Ø.4Ø and (f) Ø.5Ø.

temperature. Two spectral regions are important for understanding the results:

(i) The region above 3ØØ cm^{-1}, where two intense bands are evident at 772 and 8Ø1 cm^{-1} and

(ii)The region below 3ØØ cm^{-1}, where a broad and intense band known as boson peak appears in all the spectra.

The introduction of strontium oxide into the matrix of boric oxide glass causes a breakdown of some of the boroxol rings resulting in a change of boron atom coordination number from 3 to 4. This indicates the modifying nature of SrO as a result of which (Sr^{++}) cations are liberated. The evidence of such a process is the appearance of the Raman band (Fig.4.5a) at 772 cm^{-1} with a corresponding decrease in intensity of the band at 8Ø6 cm^{-1} for v-B_2O_3. Fig.4.5a shows a clear splitting of the band at 8Ø6 cm^{-1} as a result of the addition of xSrO with x=Ø.2Ø, giving rise to an additional band at 772 cm^{-1}. The 8Ø6 cm^{-1} band is slightly displaced to 8Ø1 cm^{-1}. The intensities of the splitted bands at x=Ø.2Ø are nearly equal which shows the presence of equal proportion of boroxol rings and triborate groups in the glass of composition Ø.2ØSrO.Ø.8ØB_2O_3. The 772 cm^{-1} band is attributed to the symmetric breathing mode in cyclic borate ring containing one BO_4 unit. The band at 8Ø1 cm^{-1} disappears at the concentration x=Ø.25 (Fig,4.5b) , while the 772 cm^{-1} band remains in the same position with change of

concentration upto x=Ø.3Ø.

The formation of BO_4 groups as a result of addition of SrO, starts at a concentration x <Ø.2Ø and reaches the saturation value of glass network coherence at the concentration of x=Ø.25. This behaviour in strontium borate glasses is different in nature from that of other alkaline earth borate glasses where the formation of BO_4 groups starts at concentration of x <Ø.2Ø but reaches the saturation value of network coherence at concentration x=Ø.35 (in calcium and barium borate glasses). With increasing concentrations (Fig.4.5c-f), the intensity of the band at 772 cm^{-1} diminishes and the band position is shifted towards lower wave number at 762 cm^{-1}. This lowering may be interpreted in terms of the appearance of non-bridging oxygens which are not involved in B-O-B linkages[28,29]. At higher concentration (x), the shifting of 772 cm^{-1} band to 762 cm^{-1} (at x=Ø.5Ø) is associated with the formation of six membered borate rings containing two tetrahedrally coordinated borons. The variation in position of 772 cm^{-1} band with change of concentration (x) is shown in Fig.4.6a, while the corresponding variation in its integrated intensity (peak intensity X full width at half maximum) is shown in Fig.4.7a. We see that upto x=Ø.3Ø, the 772 cm^{-1} band position remains constant but its intensity decreases which indicates that the number of borate cyclic groups formed at 772 cm^{-1} is reduced. At higher

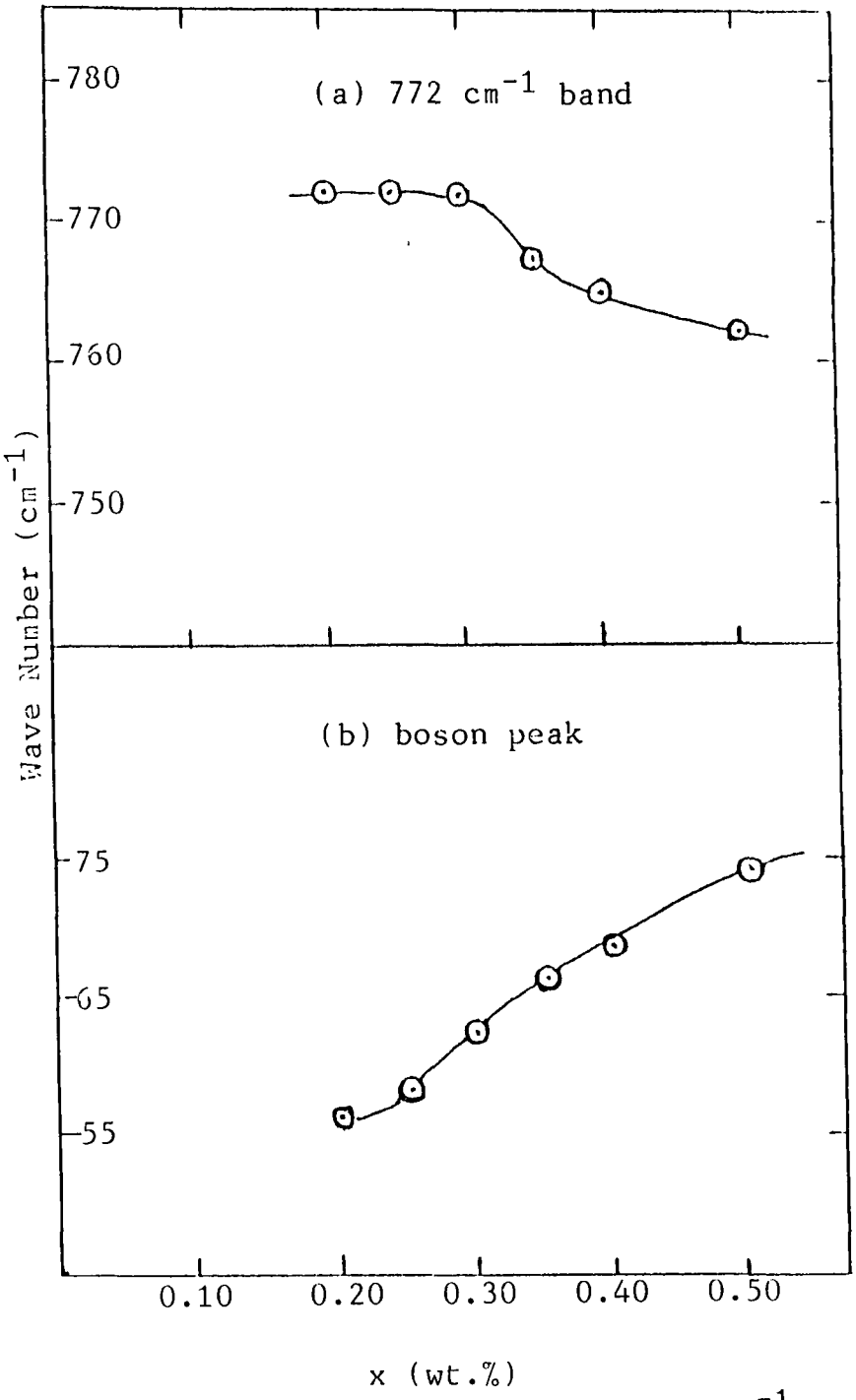

Fig. 4.6 Variation in position of (a) the 772 cm^{-1} band and (b) the boson peak with concentration (x) in the strontium borate binary glasses' spectra.

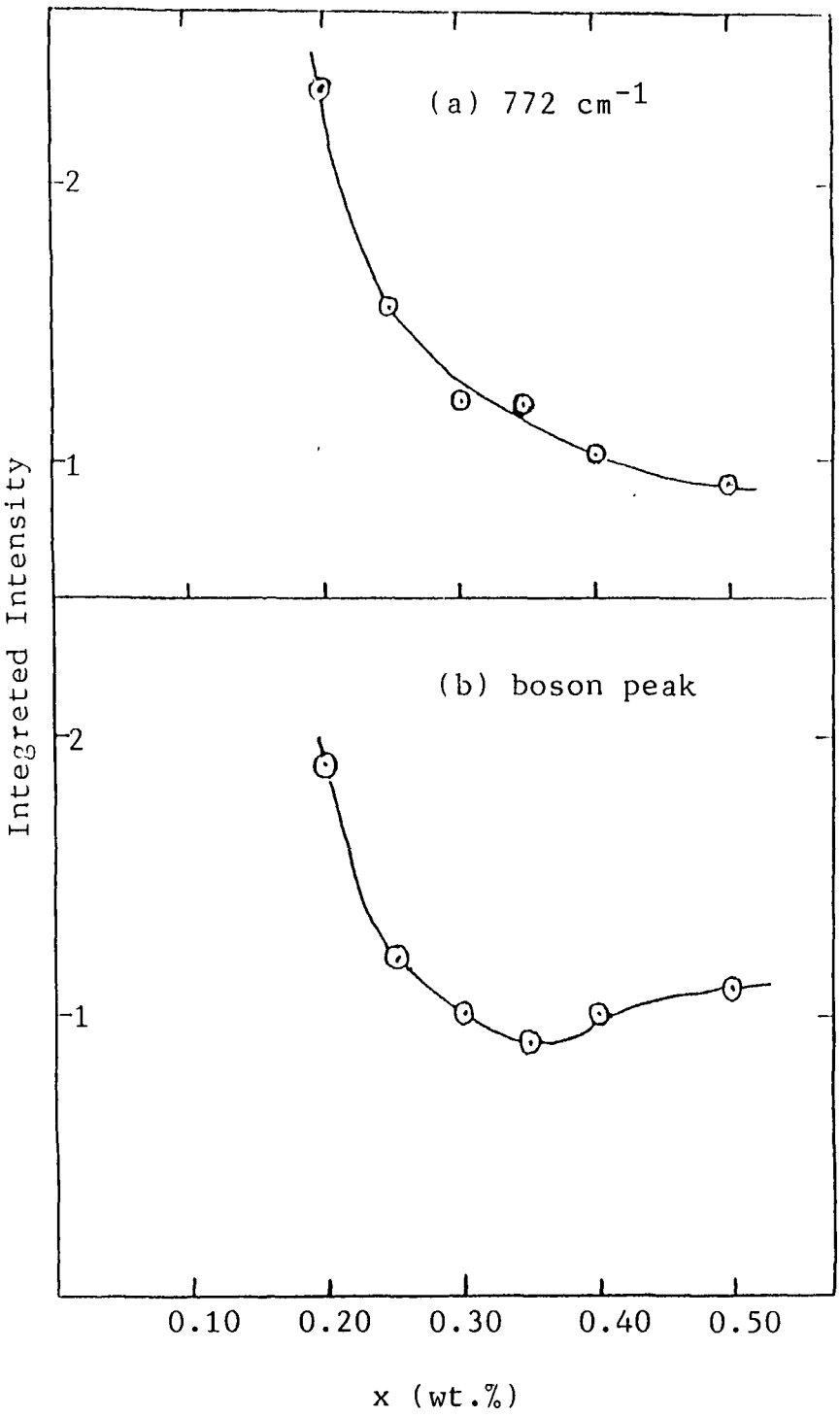

Fig. 4.7 Variation in integrated intensity of (a) the 772 cm^{-1} band and (b) the boson peak with concentration (x) in strontium borate binary glasses' spectra.

concentrations, however, the position of 772 cm^{-1} band is shifted towards lower wave number along with decrease in intensity of the band; the number of BO_4 units diminishes and BO_3 groups with NBO's are formed . The strontium ions (Sr^{++}) do not seem to be easily accomodated in the glass structure, tending to break up the network. These findings are corroborated by the increase in intensity (at x >Ø.3Ø) of the broad bands at 1452 and 953 cm^{-1} which are associated with the large borate groups with dangling $>B-O^-$ bonds. It is expected that the strontium borate glass of composition $Ø.5ØSrO.Ø.5ØB_2O_3$ contains pyro- and orthoborates having dangling $>B-O^-$ sub groups which involve NBO's (O^-).

The wave numbers of all the observed Raman bands are shown in Table 4.1. The assignments of these bands are nearly similar to those in calcium borate glasses. From the general appearance of the spectra(Fig.4.5)of strontium borate binary glasses, it can be seen that the band at 487-5Ø7 cm^{-1} is more or less insensitive to the concentration changes. The minor changes in intensity with concentration are also observed in the bands near 662 and 94Ø cm^{-1}.

In summary, it is difficult to predict the cyclic groups which would appear at the specified composition by means of Raman spectral analysis since the crystalline state of the strontium borate glasses (in some composition) show spectra dissimilar to those observed in the vitreous state[14]. However,

the presence of cyclic borate groups with non-bridging oxygens, such as pyro- and orthoborate groups is confirmed from the results of ESR, optical absorption and Mossbauer spectra in these glasses with high (x~ Ø.5Ø) SrO contents[3Ø].

In the low frequency region <3ØØ cm^{-1}, the important feature is characterized by a broad band (Fig.4.5) whose position in strontium borate glasses varies from 58 to 79 cm^{-1} at various concentrations (x) in the glass (Fig.4.6b). The intregrated intensities of this band (boson peak) at various concentrations (x) are shown in Fig.4.7b. The origin of the band has been discussed in chapter 3 for v-B_2O_3. However, according to Almeida[31], certain Raman active low frequency modes in glasses containing ions of large polarizability probably have major contribution towards the so called low frequency wing. The interpretation of this low frequency region could provide better information about the short range order in the disordered system of glasses (see later sections)by means of Martin-Brenig model[11].

(i) Effect of temperature on binary glass

Figure 4.8 shows the spectra of strontium borate binary glasses for concentrations x=Ø.2Ø and Ø.35 at different temperatures, while the variations in position and intensity (peak intensity and full width at half maximum) for the two

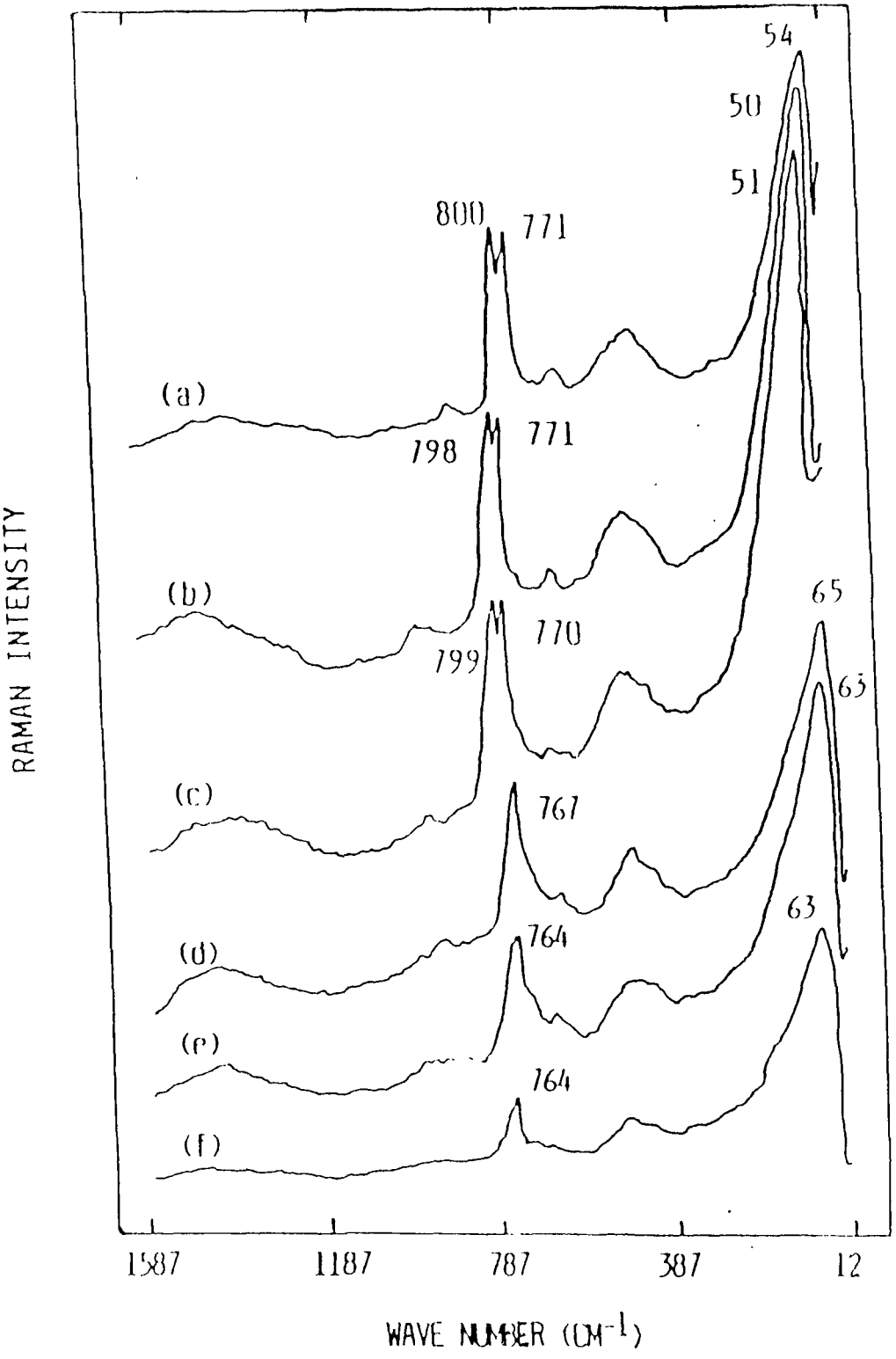

Fig. 4.8 Raman spectra of strontium borate glasses in the system $xSrO.(1-x)B_2O_3$ as a function of temperature T with x=Ø.2Ø and T:
(a) 2Ø °C, (b) 1ØØ °C, (c) 25Ø °C, (d) 39Ø °C and with x=Ø.35 and T:
(e) 2Ø°C, (f) 1ØØ °C (g) 25Ø °C, (h) 39Ø °C.

important bands i.e., boson peak and 772 cm^{-1} band with temperature at the corresponding concentrations are shown respectively in the Figures 4.9 and 4.1Ø. We see that the position of boson peak shifts towards lower wave number where as its overall intensity increases appreciably. The other important band at 772 cm^{-1} shows a minor change in its position, while there is a considerable change in the peak intensity and full width at half maximum.

With rising temperature, cyclic borate rings are broken extending the polymeric network of BO_3 triangles, thereby decreasing the density of atoms. So there will be a weakening of the force constants between atoms resulting in a shift of the Raman spectra towards lower frequencies. Since the potential wells are closely spaced together, the system would seek a new equilibrium position at different configurational states. The potential minima associated with these states will have different curvatures because of weakening of force constants.

(ii) Effect of $SrCl_2$ on binary

The effect of the addition of $SrCl_2$ into the strontium borate binary glasses can be studied from the spectra observed for the ternary system of glasses $(SrCl_2)_y.[xSrO.(1-y-x)B_2O_3]_{1-y}$ (Fig.4.11). We see that the presence of $SrCl_2$ in the glass matrix does not substantially modify the vibrational dynamics of

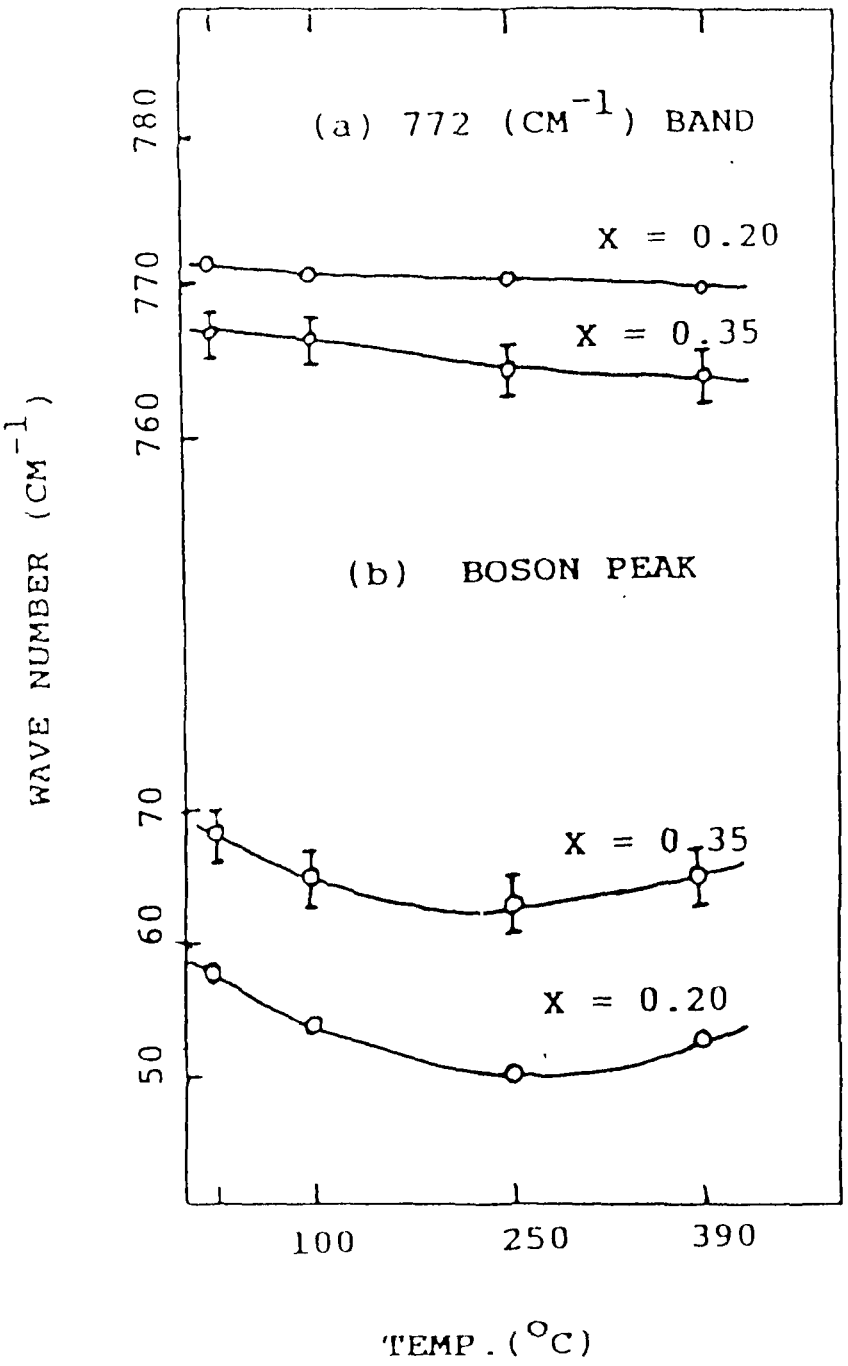

Fig. 4.9 Variation in position of (a) the 772 cm^{-1} band and (b) the boson peak with concentration x (=Ø.2Ø & Ø.35) as a function of temperature T in strontium borate binary glasses' spectra.

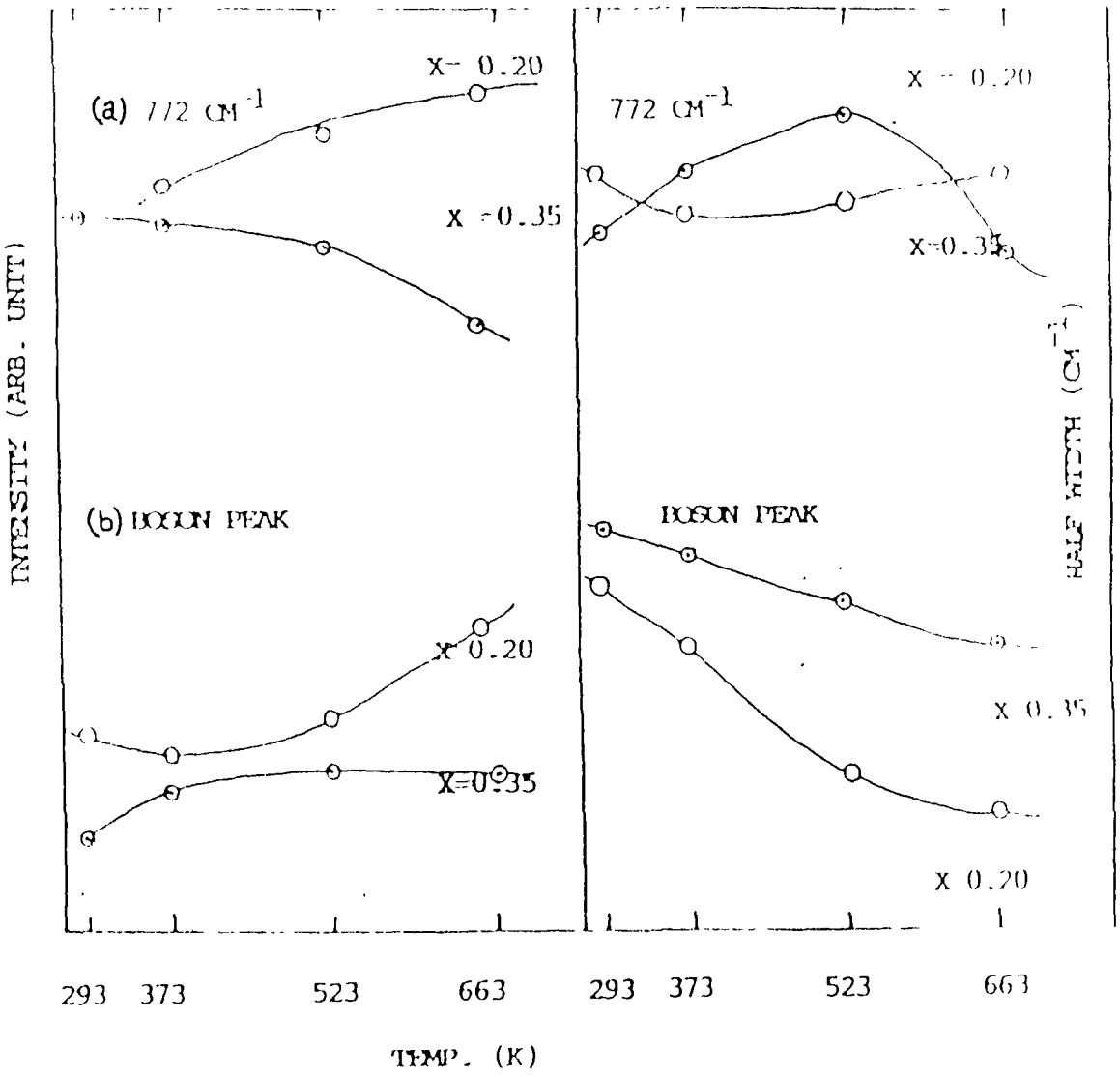

Fig. 4.10 Variation in peak intensity of (a) the 772 cm^{-1} band and (b) the boson peak with concentration x (=Ø.2Ø & Ø.35) as a function of temperature in the strontium borate binary glasses' spectra.

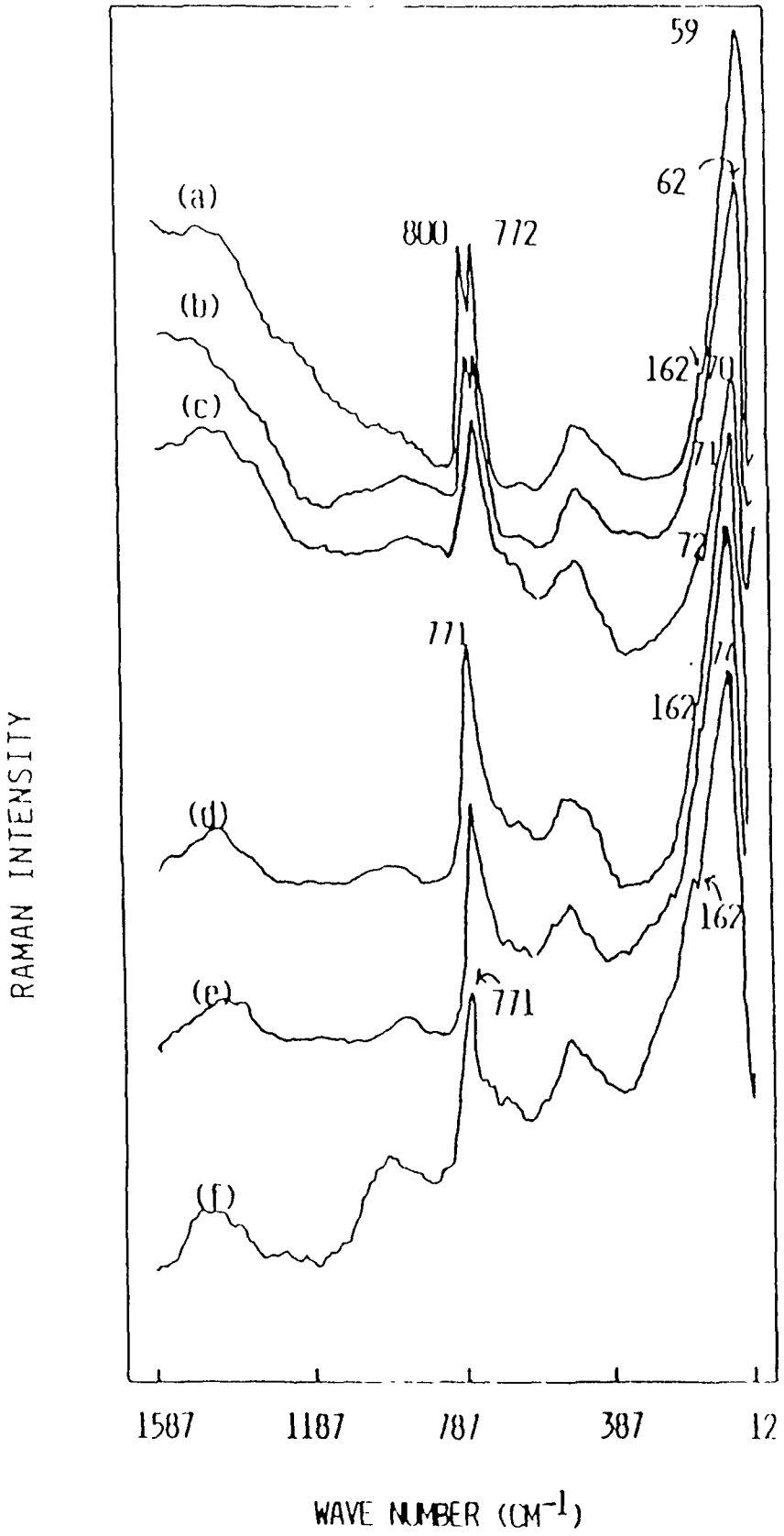

Fig. 4.11 Raman spectra of strontium borate glasses in the system $(SrCl_2)_y.[xSrO.(1-y-x)B_2O_3]_{1-y}$ for the values of x and y:

(a) x=0.20; y=0.10, (b) x=0.20; y=0.20,
(c) x=0.35; y=0.10, (d) x=0.35; y=0.20,
(e) x=0.35; y=0.30, (f) x=0.35; y=0.40

the binary glass structure in the region above 300 cm^{-1} (see for comparison Figures 4.5 and 4.11). We,however, observe noticeable modifications in the low frequency region of the spectra due to the addition of $SrCl_2$. The low frequency (less than 300 cm^{-1}) Raman results are the following:

(i) The overall intensity of the low frequency Raman scattering increases greatly by the addition of $SrCl_2$ into the binary glass (Fig.4.12a).

(ii) Boson peak shifts towards higher wave number (Fig.4.12b).

(iii) A small shoulder (on boson peak) around 162 cm^{-1} appears and tends to become clear with rise of concentration (y) of $SrCl_2$.

In the later sections we shall be discussing about this low frequency region of ternary glass spectra in greater detail.

(iii) Vibrational density of states and low frequency

The vibrational density of states $g_b(\omega)$ is expressed in terms of reduced Raman spectrum (equation 1.29,chapter 1) as,

$$g_b(\omega) = I(obs).\omega / C_b\{n(\omega,T) + 1\} = I_R, \qquad (4.1)$$

where as the frequency reduced Raman intensity I_R is given by

$$I_R^F (C_b=\omega^2) = I(obs)/\omega \{n(\omega,T)+1\} \qquad (4.2)$$

and

$$I_R^F (C_b=1) = I(obs).\omega / \{n(\omega,T)+1\} \qquad (4.3)$$

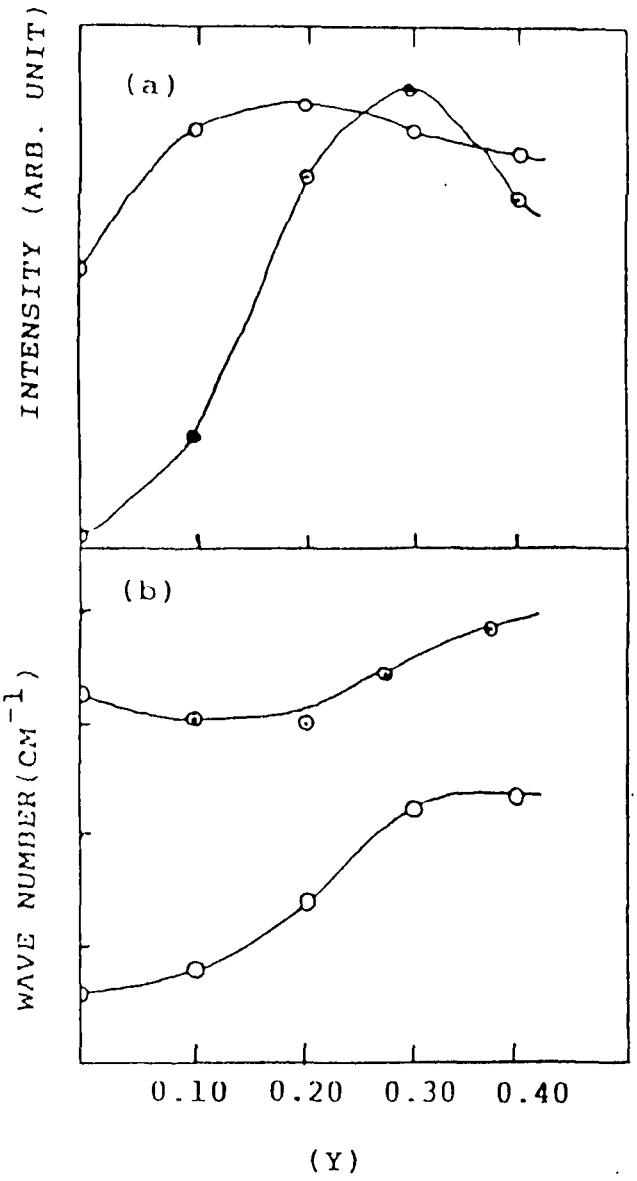

Fig. 4.12(a) Variation in peak intensity of boson peak with concentration (y) of $SrCl_2$.

(b) Shift in frequency of the boson peak with concentration (y) of strontium chloride.

The temperature reduced Raman spectra (I_R^T) is defined, when $C_b=\omega$, as

$$I_R^T = I(obs) / \{n(\omega,T)+1\} \qquad (4.4)$$

For strontium binary borate glasses, Figures 4.13a and 4.13c show the calculated reduced spectral density of states I_R^F ($C_b=\omega^2$) and $I_R^F(C_b=1)$ respectively for different values of concentrations (x).The temperature reduced Raman intensity $I_R^T(C_b=\omega)$ for different concentrations (x) is shown in the Fig.4.13b. We see that in the Fig.4.13a, the spectral shapes and boson peak positions are remarkably similar at all the concentrations (x) to those observed in the experimental (raw) Raman data in the low frequency region (<300 cm^{-1}) of Fig. 4.5. But in the calculated spectral density of states of Figures 4.13c and 4.13b for I_R^F ($C_b=1$) and I_R^T ($C_b=\omega$) respectively, the spectral shapes are not similar and some shoulder peaks around 95, 140, and 162 cm^{-1} along with the boson peak at 75 cm^{-1} are observed. The band near 140 cm^{-1} in the temperature reduced spectra is due to librational motion of boroxol rings in v-B_2O_3[32]. The peak at 75 cm^{-1} for $I_R^T(C_b=\omega)$ corresponds to the 50 cm^{-1} band in v-B_2O_3. These two bands at 75 and 140 cm^{-1} have been assigned to in-phase and out-of-phase motions[32] arising from a random distribution of mass and size of the boroxol ring structure in v-B_2O_3. Here in the present system, the bands may be asssociated with the librational motions of borate rings

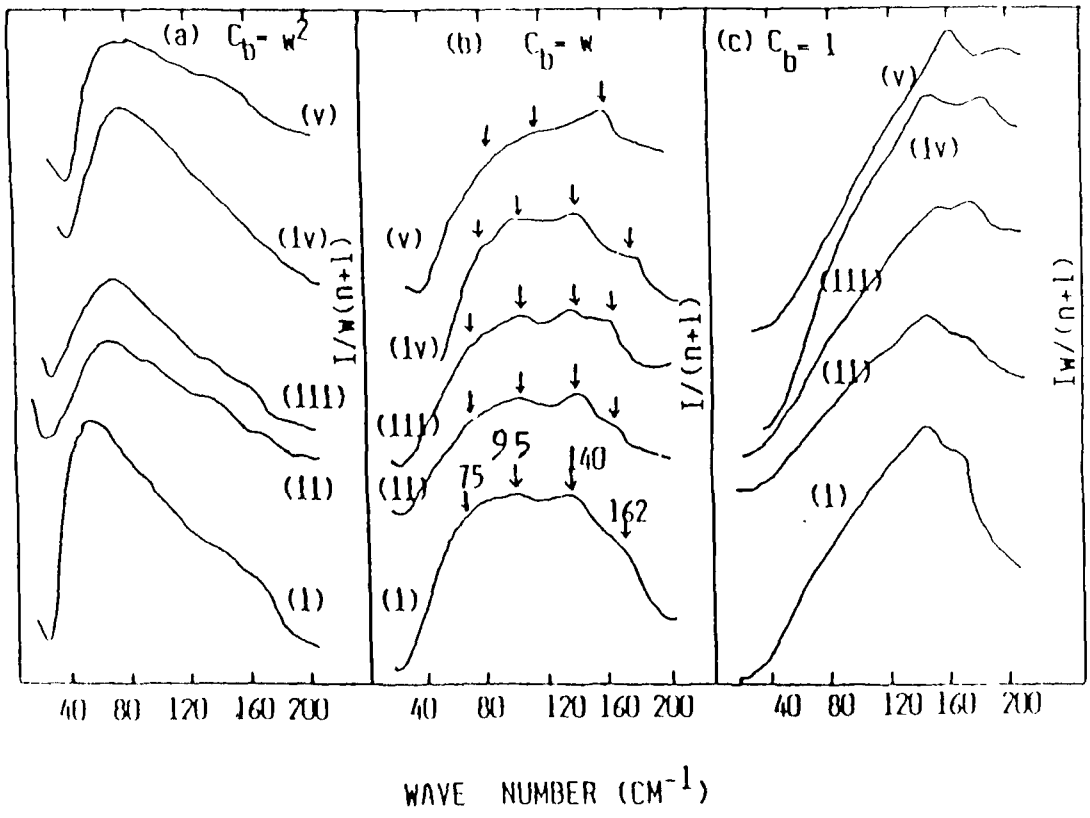

Fig. 4.13 Reduced Raman spectra for (a) I_R^F ($C_b=\omega^2$), (b) I_R^T ($C_b=\omega$) and (c) I_R^F ($C_b=1$) in strontium borate glasses in the system $xSrO.(1-x)B_2O_3$ for various x:
(i) Ø.2Ø, (ii) Ø.3Ø, (iii) Ø.35, (iv) Ø.4Ø and (v) Ø.5Ø

containing tetrahedral borons.

The addition of SrO to the v-B_2O_3 matrix plays an important role in the formation of tetrahedral BO_4 groups producing complex borate cyclic units and the introduction of $SrCl_2$ into the binary glass does not affect the vibrational dynamics in the high frequency region. But in the low frequency region, there is a large change in boson peak intensity along with the appearance of the band at 162 cm^{-1}. For this increase in intensity with increasing concentration of $SrCl_2$, two possibilities could be looked into: the addition of $SrCl_2$ helps either in the formation of BO_4 groups, or it takes part in the formation of tetrahedral units, such as BO_3Cl, which may cause the appearance of any band like the band at 162 cm^{-1}. Though the band around 162 cm^{-1} has not been observed in the experimental (raw) Raman spectra of strontium binary glass, it arises in the (raw) spectra of ternary and also in the reduced spectra of binary glasses. Comparing all the spectra, it can be concluded that since the band at 162 cm^{-1} arises in the vibrational density of states for binary, addition of $SrCl_2$ to the binary does not cause the creation of the band; it could only be suggested that the addition of $SrCl_2$ enhances the possibility of the appearance of this band and also, as a whole, the low frequency band contour intensity increases with rising concentration (y) of $SrCl_2$.

(iv) Martin-Brenig model and short range order calculation

In a disordered system of amorphous materials, the translational symmetry which characterizes a crystal structure is lost causing the correlation functions (see section 1.6, chapter I) to be localized. Here the normal modes have coherence lengths much less compared to optical wave lengths (1/10th of the optical wave lengths or less) and such modes will not be characterized by a single wave vector q and will not follow a momentum selection rule. The assumption of a short range R(r) in glass structure has the immediate consequence that its Fourier transform has a broad flat maximum around q=0 instead of being peaked at a particular wave vector q. This will be true for all j, so that all the modes of the material can give contributions to the light scattering spectrum and the normal vibrations are expected to fall into bands having similar microscopic motions e.g. stretching, bending bands etc. Hence the ordered micro-region or short correlation range (SCR) considered in the disordered system of glasses leads to a breakdown of the crystal momentum selection rule[33] and the continuous Raman spectra in glasses are ascribed to this disorder-induced scattering. The Martin-Brenig model is concerned with the low frequency light scattering from long wave length acoustic modes of disordered solids. Taking into the consideration the electrical as well as mechanical disorders,

Martin and Brenig derived expression for the Raman coupling coefficient C_b which is related to acoustic modes (ω <300 cm^{-1}) and short correlation range in the disordered system.

The theoretical investigation of Shuker and Gammon[33] shows that the stokes Raman intensity I_{obs} (given by equation 1.28, chapter I),

$$I_{obs}.\omega / \{n(\omega,T)+1\} = g_b(\omega).C_b, \qquad (4.5)$$

reflects the density of states $g_b(\omega)$ modulated by the Raman coupling coefficient C_b. Among the number of experimental procedures proposed[11,34,35] for the measurement of the size of ordered micro region or short correlation range (SCR) in glasses one due to Martin and Brenig[11] relates the position of boson peak to this coupling coefficient C_b which in turn is related to the structural correlation range.

The model of Martin and Brenig[11] attributes the low frequency peak to the structural disorder in glasses which affects the coupling coefficient C_b. The frequeny (ω) dependence of the Raman coupling coefficient C_b is expressed, according to the M-B model adapted to right angle scattering geometry (VH configuration) by Nemanich[12], as (see equation 1.25, chapter I),

$$C_b(\omega) = A\omega^2[3(v_l/v_t)^5\exp\{-(2\pi c\omega)^2\sigma^2/v_t^2\} + 2\exp\{-(2\pi c\omega)^2\sigma^2/v_l^2\}] \qquad (4.6)$$

where A is a constant, v_l and v_t are the longitudinal and the

transverse velocities of acoustic waves and 2σ is the structural correlation range (SCR) representing the extent of short range ordering with no damping for phonon propagation in the disordered system. The expression has been derived under the condition that only phonons of wave number ω, with

$$(2\pi c\omega / v_\mu)\sigma < 1, \text{ for } \mu = l \text{ or } t, \qquad (4.7)$$

play a significant role in the scattering. Neglecting the second term of the above expression for C_b and differentiating with respect to ω, one obtains a maximum for C_b at

$$\omega = \omega_{max} = v_t/2\pi c\sigma \qquad (4.8)$$

In Fig.4.14, typical calculated fits based on equation (4.6) are shown for the binary strontium borate glasses. The experimental points (smaller dots) deviate somewhat from the theoretical curves (bigger dots) because of the error involved in the estimation of the v_l and v_t values which have been taken from reference 36 for alkali borate glasses and the SCR (2σ) values are calculated for the binary strontium borate glasses (see Table-4.3). [The experimental points (C_b values) are obtained from (4.5) in the Debye density of states $g_b = \omega^2$, while the theoretical C_b values are calculated from equation (4.6)].

(B) IR results

Fig.4.15 shows the infrared spectra of strontium borate binary glasses $xSrO.(1-x)B_2O_3$ for $x = Ø.2Ø$, $Ø.3Ø$, $Ø.35$,

Table 4.3 The SCR values (2σ) for the system $xSrO.(1-x)B_2O_3$ with concentration (x)

Conc. (x)	v^*_l (cm/s)	v^*_t (cm/s)	2σ (A°) $v/\pi c\omega$	curve fitting
Ø.2Ø	4ØØØØØ	23ØØØØ	5.7654	5.1665
Ø.3Ø	4Ø5ØØØ	229ØØØ	5.Ø226	4.56Ø1
Ø.35	415ØØØ	236ØØØ	4.6667	4.5687
Ø.4Ø	42ØØØØ	242ØØØ	4.817Ø	4.1375
Ø.5Ø	43ØØØØ	25ØØØØ	4.5687	4.2451

* v_l and v_t values have been used from reference 36

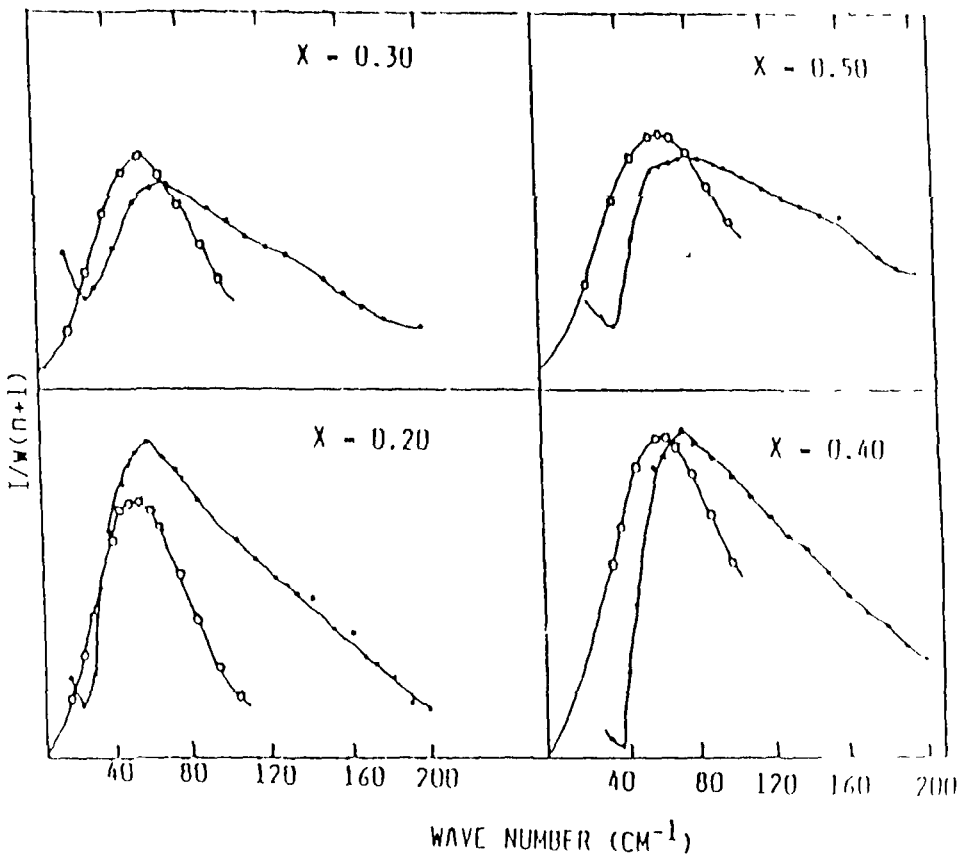

Fig. 4.14 Typical fit of theoretical C_b values with experimental reduced Raman spectra $I_R^F = I(obs)/\omega\ (n+1)$ in strontium borate binary glasses for different concentration (x) of SrO . Here, (•) experimental and (o) theoretical.

and Ø.5Ø in the range 6ØØ-16ØØ cm^{-1}. Fig.4.15a shows the spectrum for v-B_2O_3 (x=Ø) for comparison. We see that on increasing the concentration (x) of SrO, the band at 655 cm^{-1} is shifted to 7ØØ cm^{-1} and remains in the same position at 7ØØ cm^{-1} upto concentration x=Ø.5Ø. This band seems to belong to the B-O-B linkage in which both boron atoms are triangularly coordinated. The broad band centering around 8ØØ cm^{-1} in v-B_2O_3 has disappeared in the IR spectra of Figs.4.15(b-e) which shows that boroxol rings are absent in the strontium borate glass but Raman spectra shows the splitted bands at 8Ø1 and 772 cm^{-1} at concentration of x=Ø.2Ø. The strong band at 121Ø cm^{-1} observed in v-B_2O_3 is shifted to 126Ø cm^{-1} and decreases in intensity as a result of addition of SrO to v-B_2O_3 and then finally disappears at a concentration of x=Ø.5Ø. This band at 126Ø cm^{-1} is the characteristic of B-O stretch of mainly BO_3 triangles with bridging oxygens. The disappearance of the band at 126Ø cm^{-1} along with the broadening of the 7ØØ cm^{-1} band indicates the presence of pyro- and orthoborates, having non-bridging oxygens at higher concentrations of SrO. This is also supported by the appearance of the intense band at 14ØØ cm^{-1} (x=Ø.5Ø) which is attributed to the different types of boron oxygen stretching vibrations involving non-bridging oxygens[19,2Ø]. On the other hand, the appearance of the bands in the region 9ØØ-11ØØ cm^{-1} which arise from B-O stretch of tetrahedral (BO_4)

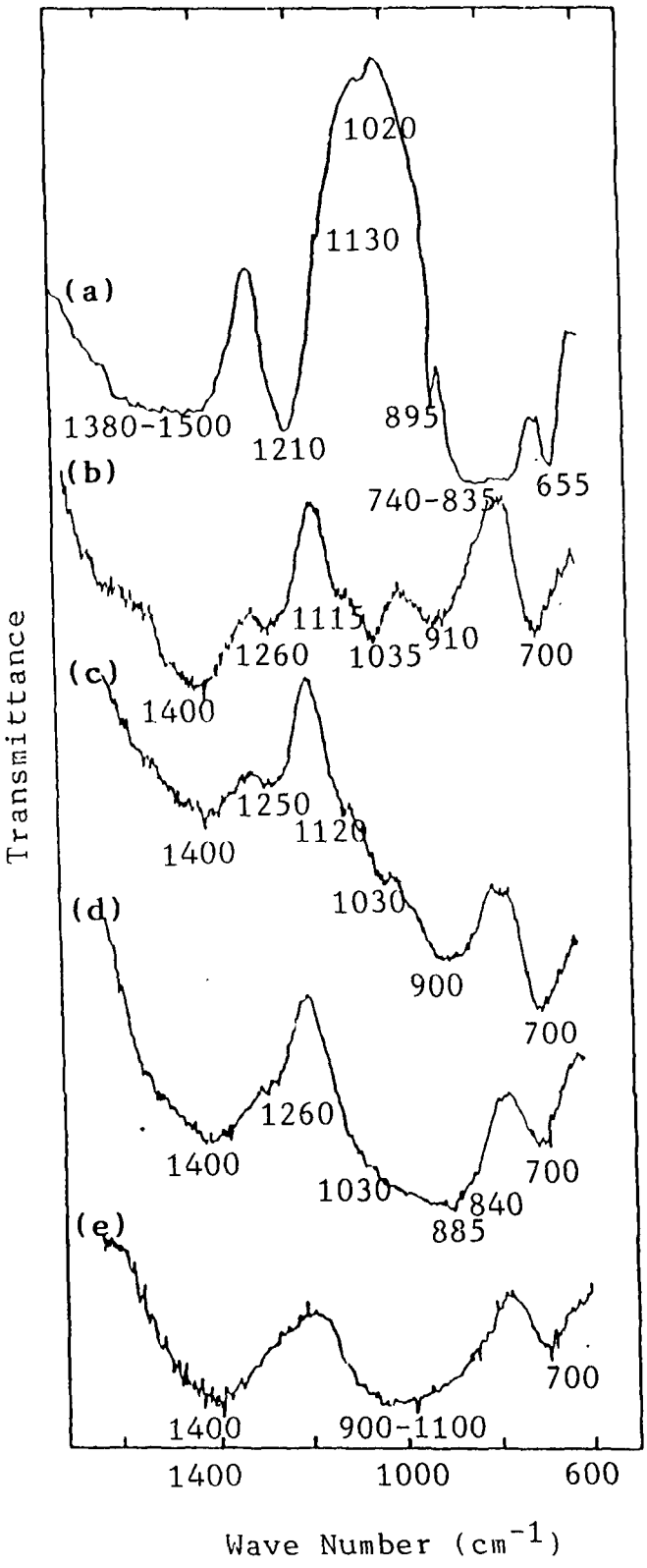

Fig. 4.15 Infrared spectra of strontium borate glasses in th system $xSrO.(1-x)B_2O_3$ for the concentrations (x): (a) Ø, (b) Ø.2Ø, (c) Ø.3Ø, (d) Ø.35 and (e) Ø.5Ø.

units, shows the formation of complex borate groups containing tetrahedral borons. More over, the bands in the region 122Ø-14ØØ cm^{-1} are also the characteristic of ≡B-O-B≡ group[37] containing tetrahedral boron. At concentration x=Ø.5Ø the IR bands in the region around 85Ø-11ØØ cm^{-1} form broad contour which shows the formation of different cyclic borate groups containing BO_4 and BO_3 units. Table 4.4 shows the comparison of the bands observed in Raman and IR spectra of binary stontium borate glasses.

4.6 Barium borate glasses' spectra

The Raman spectra of barium borate glasses in the system $xBaO.(1-x)B_2O_3$ for values of x=Ø.2Ø, Ø.25, Ø.3Ø, Ø.35, Ø.4Ø and Ø.5Ø in the range 12-16ØØ cm^{-1} are shown in Fig.4.16. The wave numbers of all the observed Raman bands are given in Table 4.1. The spectra are characterized mainly by a broad and intense band at 44-56 cm^{-1} in the low frequency region along with the bands at 474, 775 and 8Ø2 cm^{-1} in the high frequency region. With increasing BaO content, the 474 cm^{-1} band increases in intensity and shifts to 487 cm^{-1} at the concentration of x=Ø.5Ø, along with the appearance of another band at 424 cm^{-1}. The band at 487 cm^{-1} is similar to that observed in calcium borate glasses. The appearance of a shoulder at 424 cm^{-1} on this band at higher concentration of x may be due to the enhanced motion of barium ions (Ba^{++}) located at the oxygen sites (similar to magnesium

Table 4.4 The bands observed in the Raman and IR spectra of the glasses in the system $xSrO.(1-x)B_2O_3$ for concentrations x=Ø.2Ø, Ø.35 and Ø.5Ø.

Concentration (x)	Raman bands (cm^{-1})	IR bands (cm^{-1})
Ø.2Ø	1427 (w,b)	14ØØ (b)
	-*-	126Ø (w)
	-*-	1115 (vw)
	-*-	1Ø35 (w)
	942 (vw)	91Ø (b)
	8Ø1 (sh,i)	-*-
	772 (sh,i)	-*-
	662 (vw)	7ØØ (w,b)
Ø.35	1437 (w,b)	14ØØ (vb)
		126Ø (vw)
		1Ø3Ø (w)
	942 (vw)	885 (vb)
		84Ø (w)
	767 (sh,i)	-*-
	662 (vw)	-*-
		7ØØ (w,b)
Ø.5Ø	1452 (b,i)	14ØØ (vb)
	953 (w)	9ØØ-11ØØ (vb)
	762 (w,sh)	
	673 (w)	
		7ØØ (w,b)

w---> weak, b---> broad, vw---> very weak, sh---> sharp, i---> intense vb---> very broad, Assignments are given in the text (see Table 4.2).

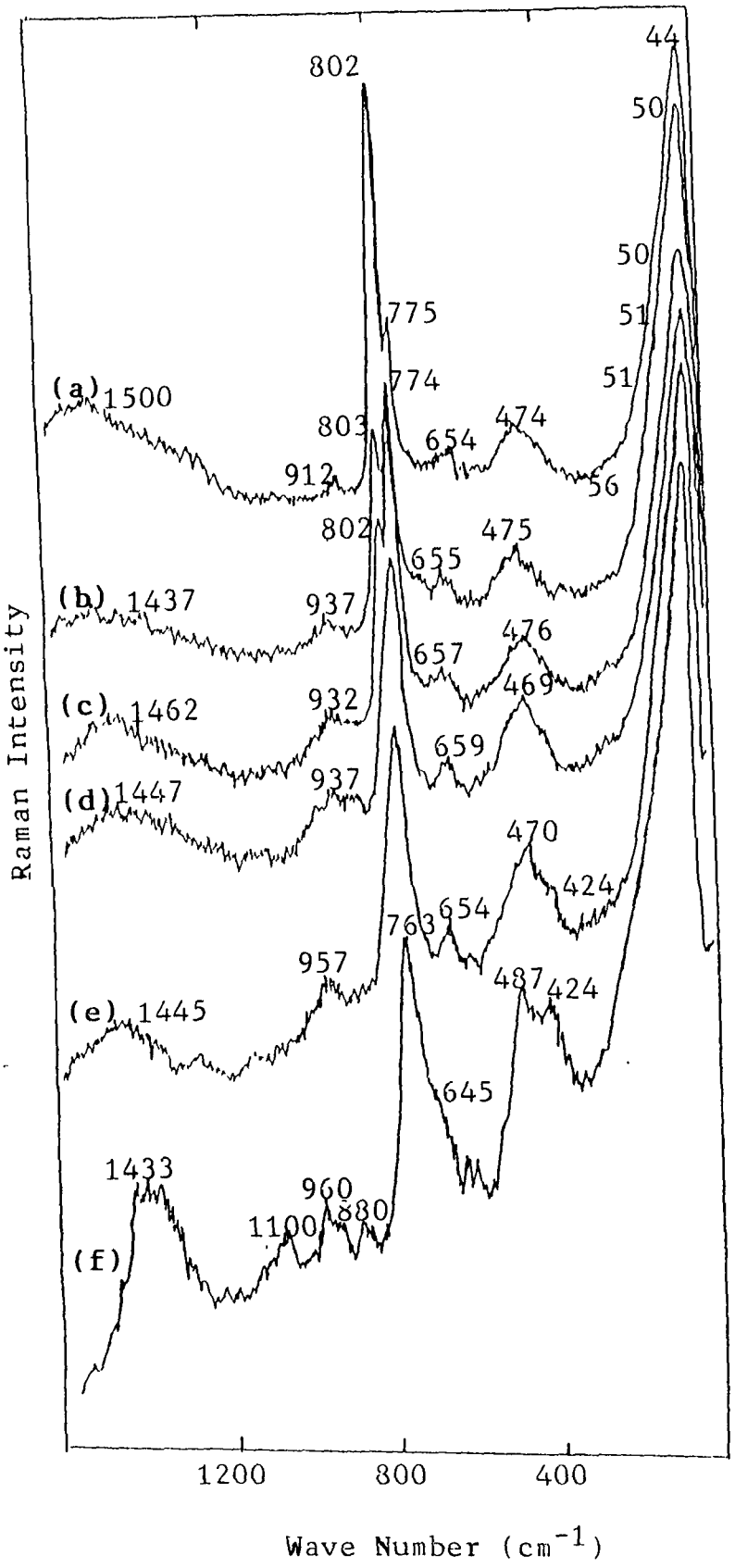

Fig. 4.16 Raman spectra of barium borate glasses in the system $xBaO.(1-x)B_2O_3$ for various x:

(a) Ø.2Ø, (b) Ø.25, (c) Ø.3Ø, (d) Ø.35, (e) Ø.4Ø and (f) Ø.5Ø.

ion motion at 35Ø cm^{-1} in magnesium borate glasses[38]) The band at 775 cm^{-1} (due to borate rings with one BO_4 unit) rises gradually in intensity with increasing concentrations (x), while the adjoining band at 8Ø2 cm^{-1}, characteristic of boroxol rings vibration, decreases with rise of concentration (x). This shows that the number of boroxol rings are decreasing while the corresponding increase in the borate rings containing BO_4 units is observed at higher concentrations of x. The shift of 775 cm^{-1} band towards lower wave number (Fig.4.17a) along with the rise of the band intensity (Fig.4.17b) with (x) indicates the modifying action of BaO similar to that observed in calcium borate glass. The disappearance of the band at 8Ø2 cm^{-1} for x=Ø.35 signifies that the formation of BO_4 units as a result of introduction of BaO to v-B_2O_3 reaches saturation in its network coherence at this concentration. Crystalline compound of $BaO.2B_2O_3$ contain[14] di-triborate and di-pentaborate groups. Block and Piermarini[39] have shown that vitreous and crystalline barium borates near the composition ($BaO.2B_2O_3$), have a nearest neighbor Ba-Ba distance which is equal in both the cases. Thus the same groups i.e., di-triborate and di-pentaborate groups are most probable in the glass of similar composition $Ø.35BaO.Ø.65B_2O_3$ in the present system. The appearance of the band at 11ØØ cm^{-1}, similar to that observed in Zinc diborate[5], shows that diborate groups are also probably present in the

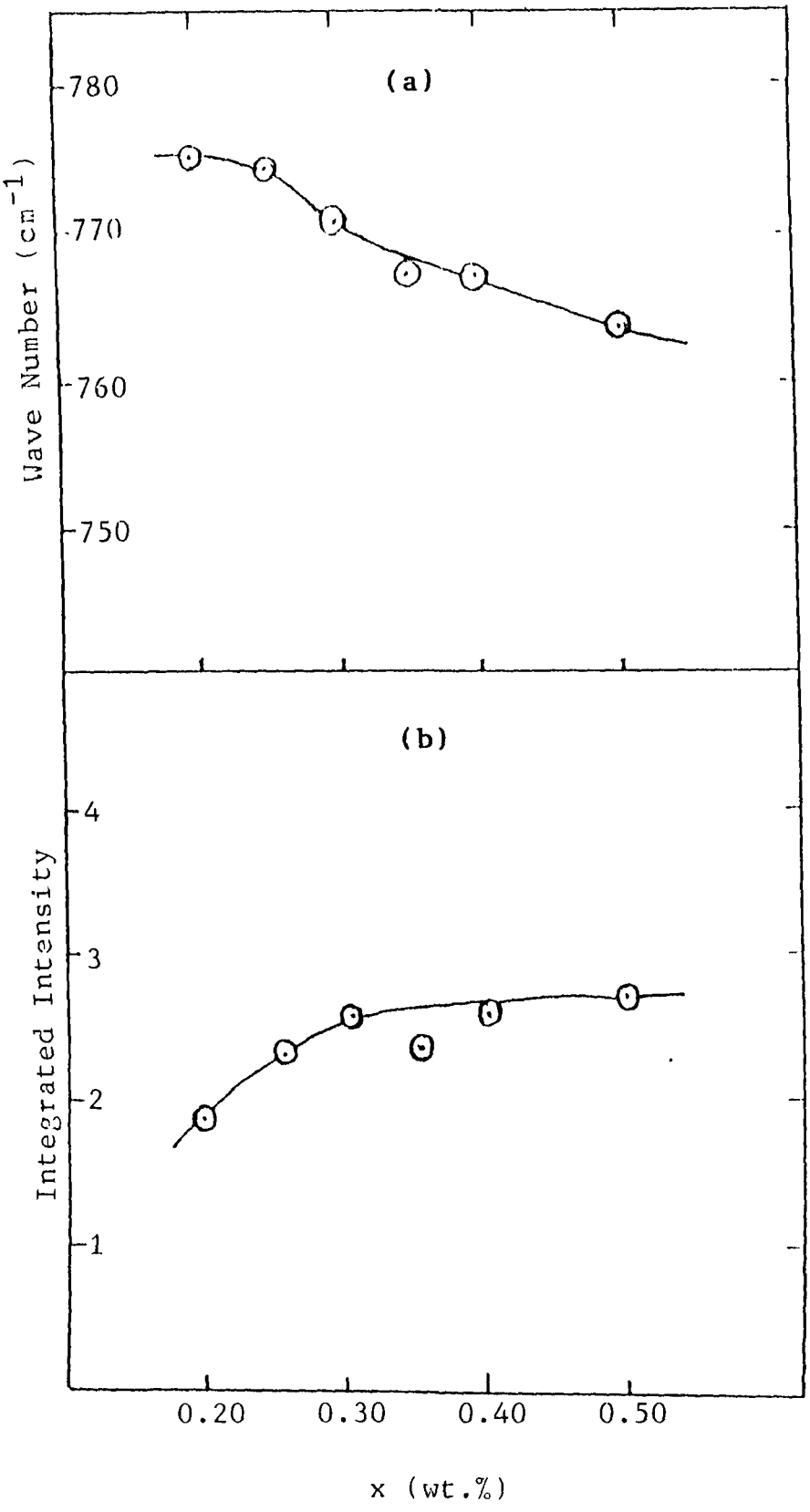

Fig. 4.17 Variations in (a) the position and (b) the integrated intensity of the 775 cm^{-1} band with concentration (x) in barium borate binary glasses' spectra.

glass of barium borate with x=Ø.5Ø. The hump type broad band at 1433 cm^{-1} for x=Ø.5Ø is sharper than that for lower concentrations. This feature at 1433 cm^{-1} shows the formation of greater number of $B_2O_5^{4-}$ and BO_3^{3-} groups involving $B\text{-}O^-$ units in the glass.

Thus from the Raman spectral results in the high frequency region, it may be argued that barium borate glasses with B_2O_3 contents (x <Ø.3Ø), possess primarily tetraborate and pentaborate groups with minor amounts of metaborate (664 cm^{-1}), orthoborate (932 cm^{-1}) and loose BO_4 units. Upon further introduction of BaO, the tetraborate groups change to the di-triborate, di-pentaborate and diborate groups with some fractions of ortho-, pyro- and metaborate groups and the glass structure becomes more randomized. This randomization is supported by the fact that the bands at 487 and 1433 cm^{-1} (at x=Ø.5Ø) have become comparable in intensity (see the spectrum of Fig.4.16f) to 763 cm^{-1} band relating to the six membered borate rings i.e., the increased number of free BO_4 and orthoborate units supports the above argument.

In the low frequency region of the spectra of Fig.4.16 (<3ØØ cm^{-1}), the intense band (boson peak) arises at 44 cm^{-1} (assigned earlier) Like other alkaline earth borate glasses, this band shifts towards higher wave number with change of concentration (x) (Fig.4.18) and also its intensity rises with (x)(Fig.4.22).

Fig.4.18

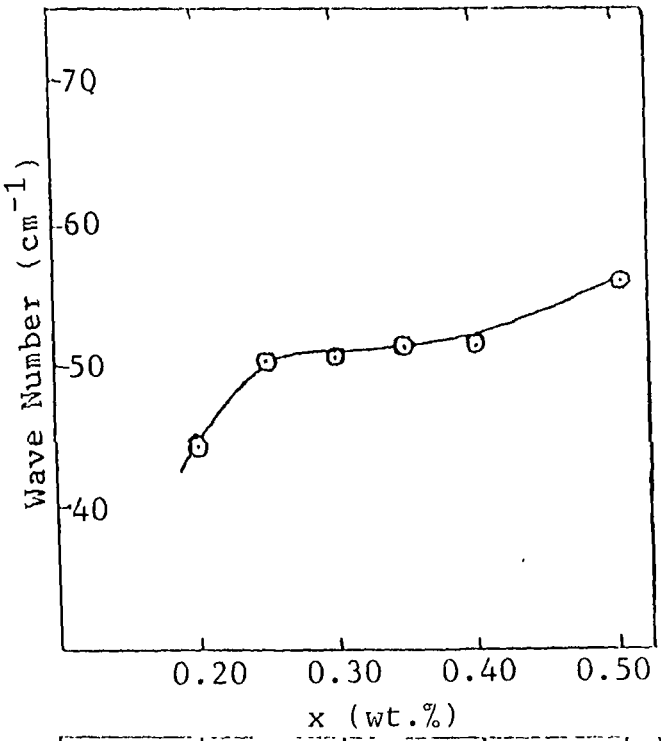

Fig.4.22

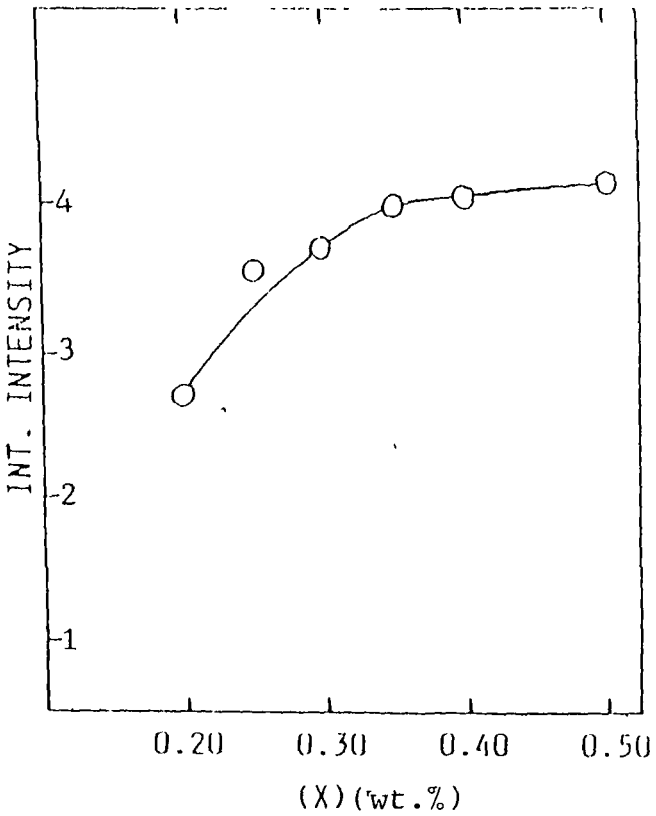

Fig.4.18 Variation in position of the boson peak with concentration (x) in barium borate binary glasses' spectra.

Fig.4.22 Integrated intensity of boson peak in binary barium borate glasses' spectra with concentration (x) of BaO.

(1) Effect of $BaCl_2$ on binary and boson peak

The effect of the introduction of $BaCl_2$ into the binary barium borate glass is similar to that observed when $SrCl_2$ is added to strontium borate binary glass. The main influence of $BaCl_2$ is in the low frequency region (<300 cm^{-1}) of the Raman spectra of barium borate binary and ternary glasses in the systems $xBaO.(1-x)B_2O_3$ and $(BaCl_2)_y.[(BaO)_x.(B_2O_3)_{1-y-x}]_{1-y}$ respectively for various x and y. The experimental (raw) Raman spectra of these glasses are shown in Figs. 4.19A and 4.20(A and B) respectively for binary and ternary systems, while the frequency and temperature reduced Raman spectra (defined from equation 1.30, chapter I) for the same systems have been shown in Figs.4.19B and 4.21(A &B) respectively. On comparing the spectra of these Figures with those of Fig.3.4 (for pure B_2O_3), we see that the addition of BaO to vitreous boron oxide glass leads to an increase in the over all Raman scattering intensity (see Table 4.5, Fig.4.22). Then the introduction of $BaCl_2$ into the binary glass of concentration x=0.35 and 0.20 of BaO shows that the over all intensity of boson peak again increases with increasing concentration (y) of $BaCl_2$ (Fig.4.23, Table 4.5).

A closer look of all the spectra reveals that when BaO is added to v-B_2O_3, the band at 25 cm^{-1} (observed in v-B_2O_3, Fig.3.4) is shifted to 67 cm^{-1} seen in the reduced spectra of

TABLE 4.5 Integrated intensity and position of boson peak in the binary and ternary barium borate glasses in the system $xBaO.(1-x)B_2O_3$ and $(BaCl_2)_y.[xBaO.(1-y-x)B_2O_3]_{1-y}$ for different x and y

concentration (x)	concentration (y)	Int.intensity* (arb. unit)	Wave number (cm^{-1})
Ø.2Ø		19	44
Ø.25		25	5Ø
Ø.3Ø		24	5Ø
Ø.35		25	51
Ø.4Ø		24	51
Ø.5Ø		26	56
Ø.2Ø	Ø.1Ø	16	44
Ø.2Ø	Ø.2Ø	17	49
Ø.2Ø	Ø.3Ø	21	52
Ø.2Ø	Ø.4Ø	2Ø	52
Ø.35	Ø.1Ø	23	5Ø
Ø.35	Ø.2Ø	15	52
Ø.35	Ø.3Ø	24	56
Ø.35	Ø.4Ø	28	58

*Integrated intensity = peak height x band width at half maximum

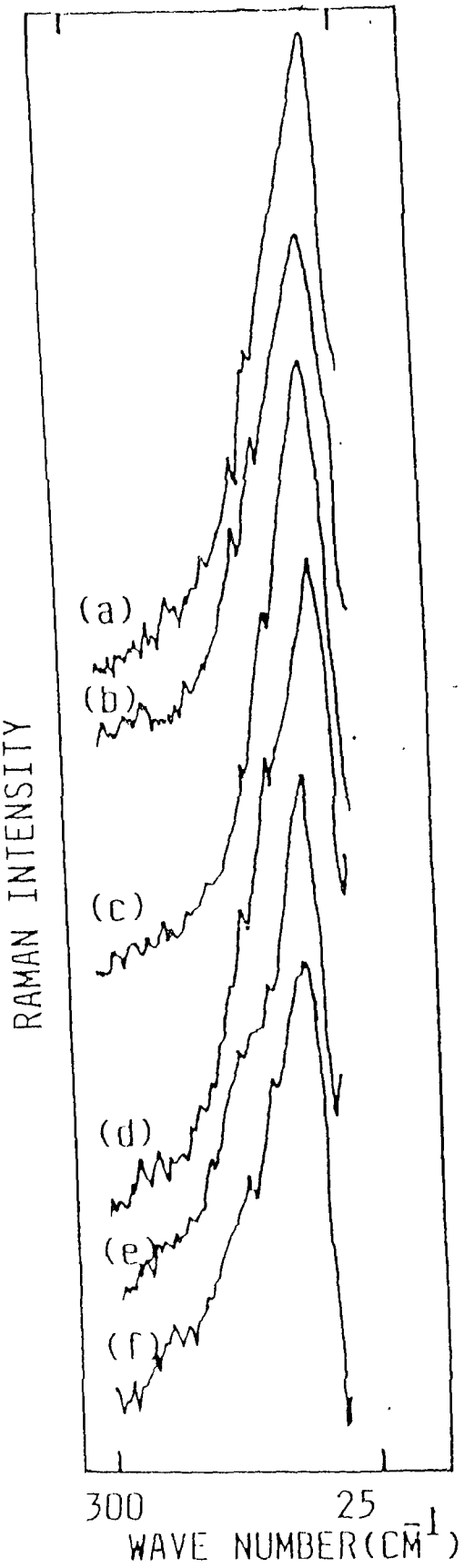

Fig.4.19(A) Low frequency Raman spectra of barium borate glasses in the system $xBaO.(1-x)B_2O_3$ for various x: (a) Ø.2Ø,(b) Ø.25, (c) Ø.3Ø, (d) Ø.35, (e) Ø.4Ø and (f) Ø.5Ø.

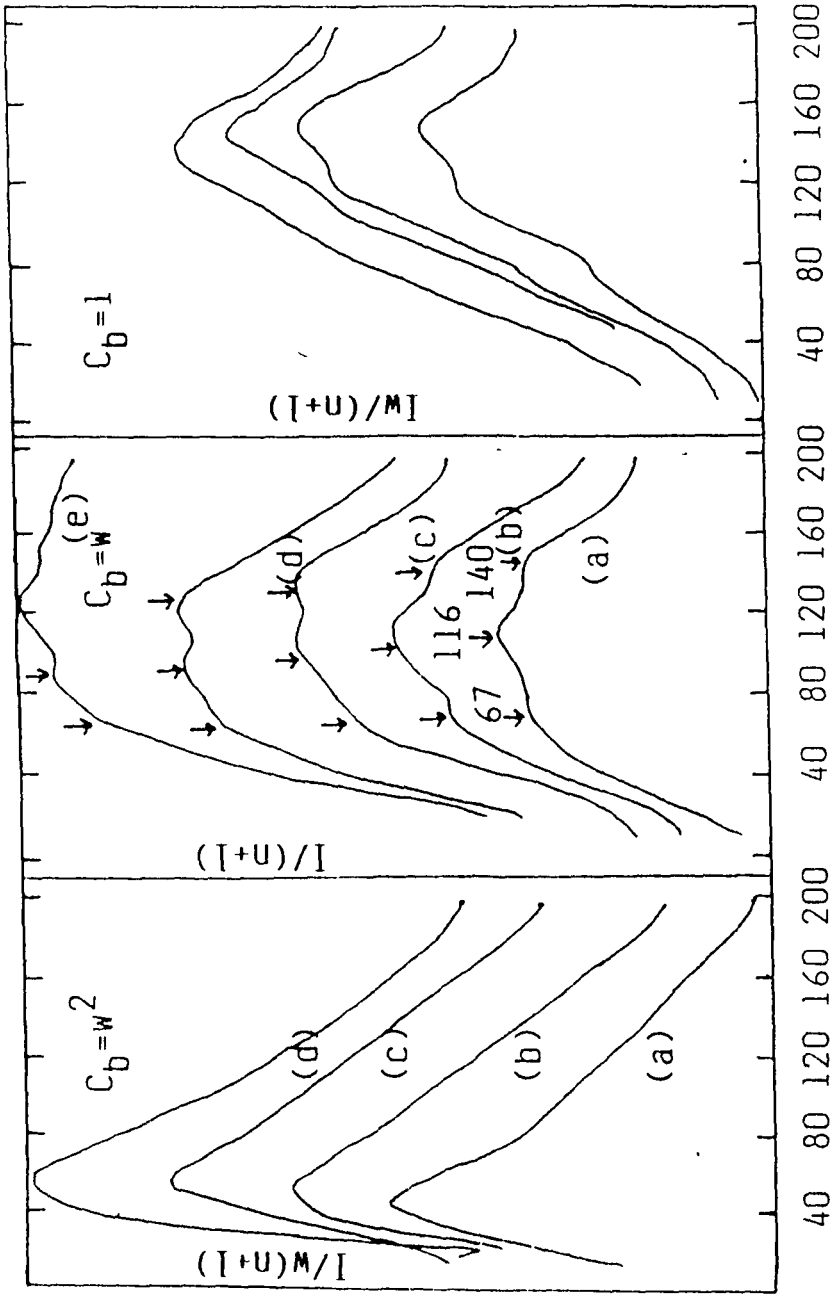

Fig. 4.19(B) Reduced Raman spectra of glasses in the system $xBaO.(1-x)B_2O_3$ for various x:
(a) Ø.2Ø, (b) Ø.3Ø, (c) Ø.35, (d) Ø.4Ø and (e) Ø.5Ø

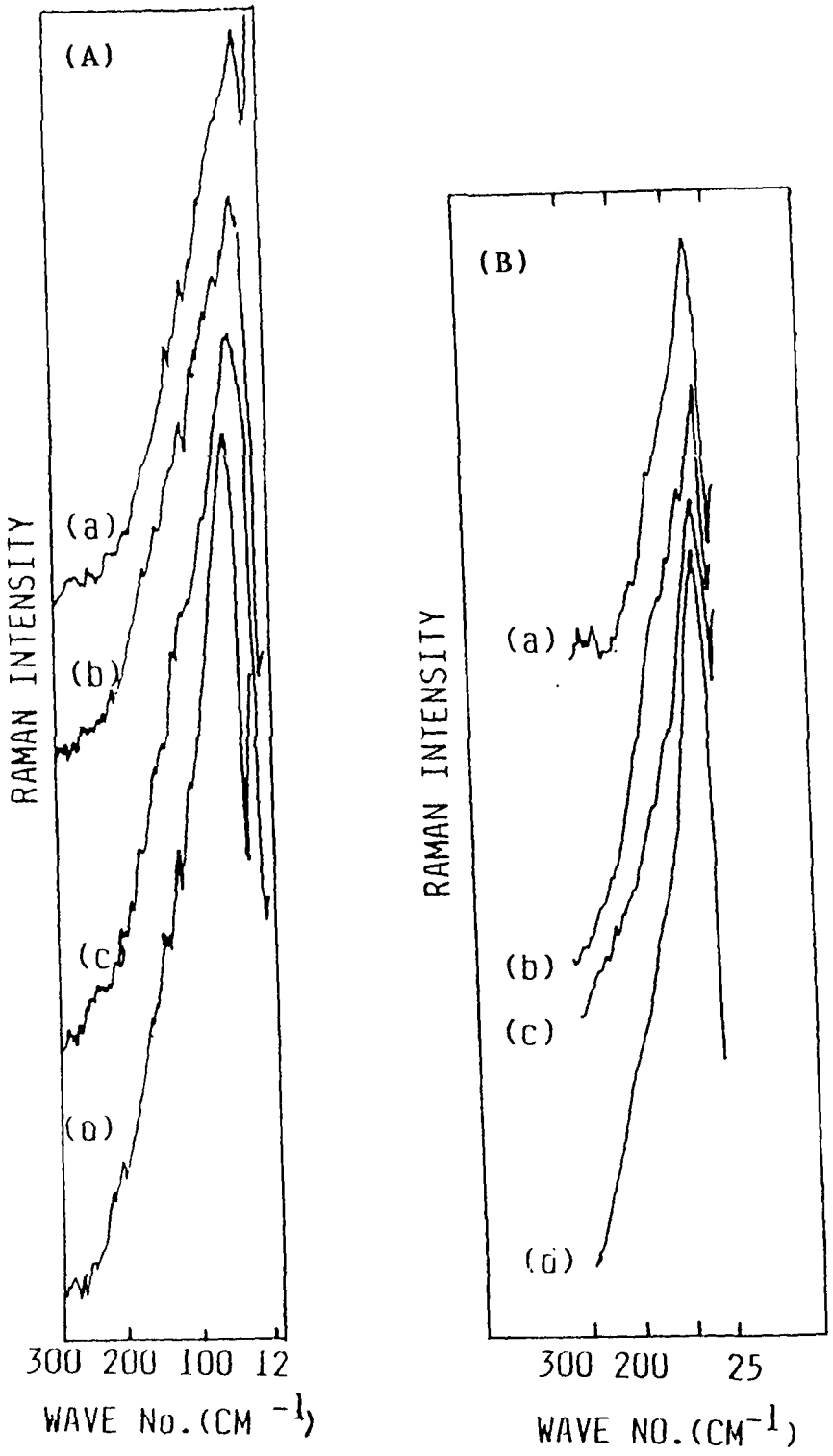

Fig. 4.20 Low frequency Raman spectra of barium borate glasses in the system $(BaCl_2)_y.[xBaO.(1-y-x)B_2O_3]_{1-y}$, for
(A) x=Ø.2Ø & y: (a) Ø.1Ø, (b) Ø.2Ø, (c) Ø.3Ø and (d) Ø.4Ø
(B) x=Ø.35 & y: (a) Ø.1Ø, (b) Ø.2Ø, (c) Ø.3Ø and (d) Ø.4Ø

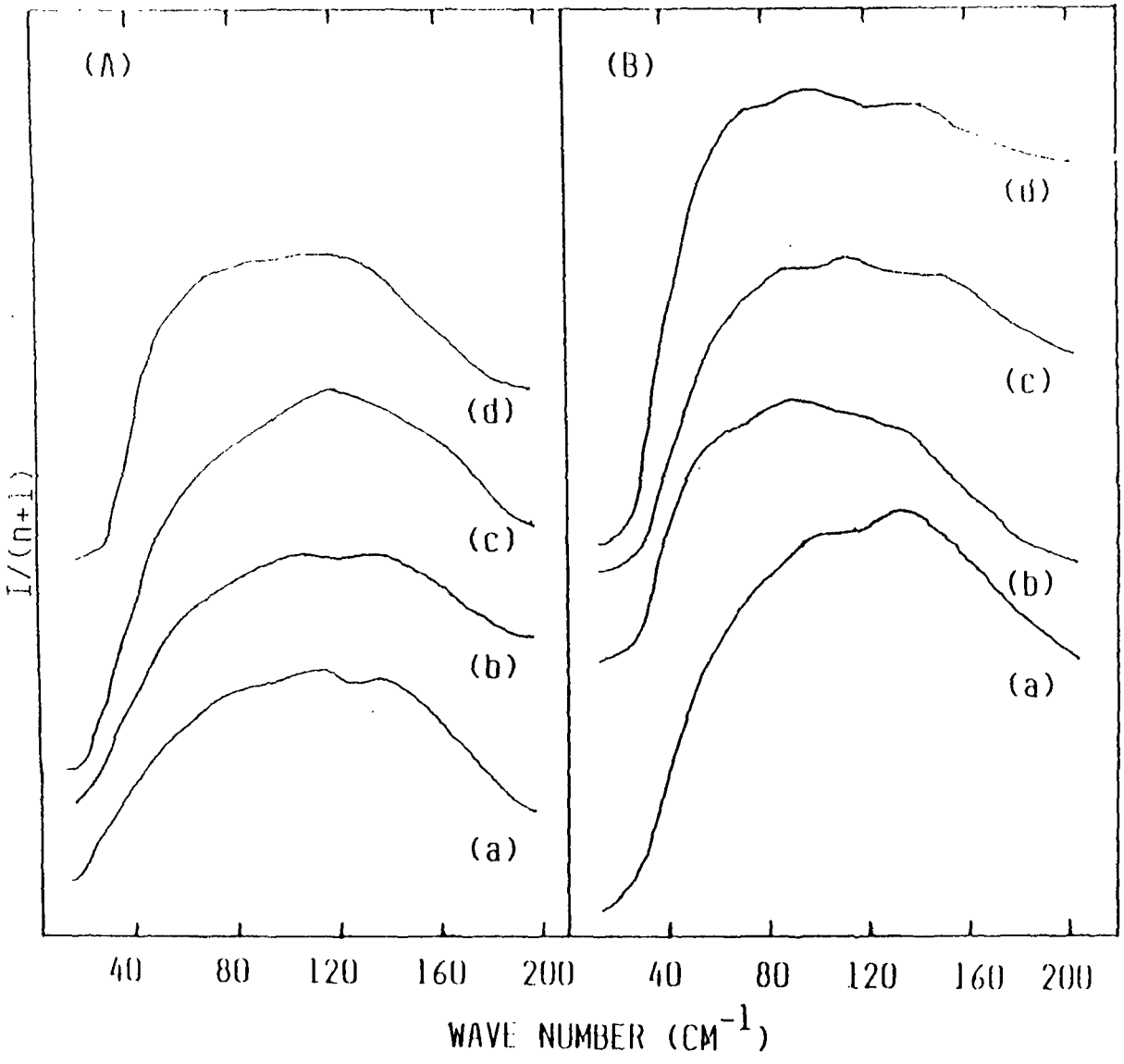

Fig. 4.21 Temperature reduced Raman spectra of barium borate glasses in the system $(BaCl_2)_y.[xBaO.(1-y-x)B_2O_3]_{1-y}$, for,
(A) x=Ø.2Ø & y: (a) Ø.1Ø, (b) Ø.2Ø, (c) Ø.3Ø and (d) Ø.4Ø
(B) x=Ø.35 & y: (a) Ø.1Ø, (b) Ø.2Ø, (c) Ø.3Ø and (d) Ø.4Ø

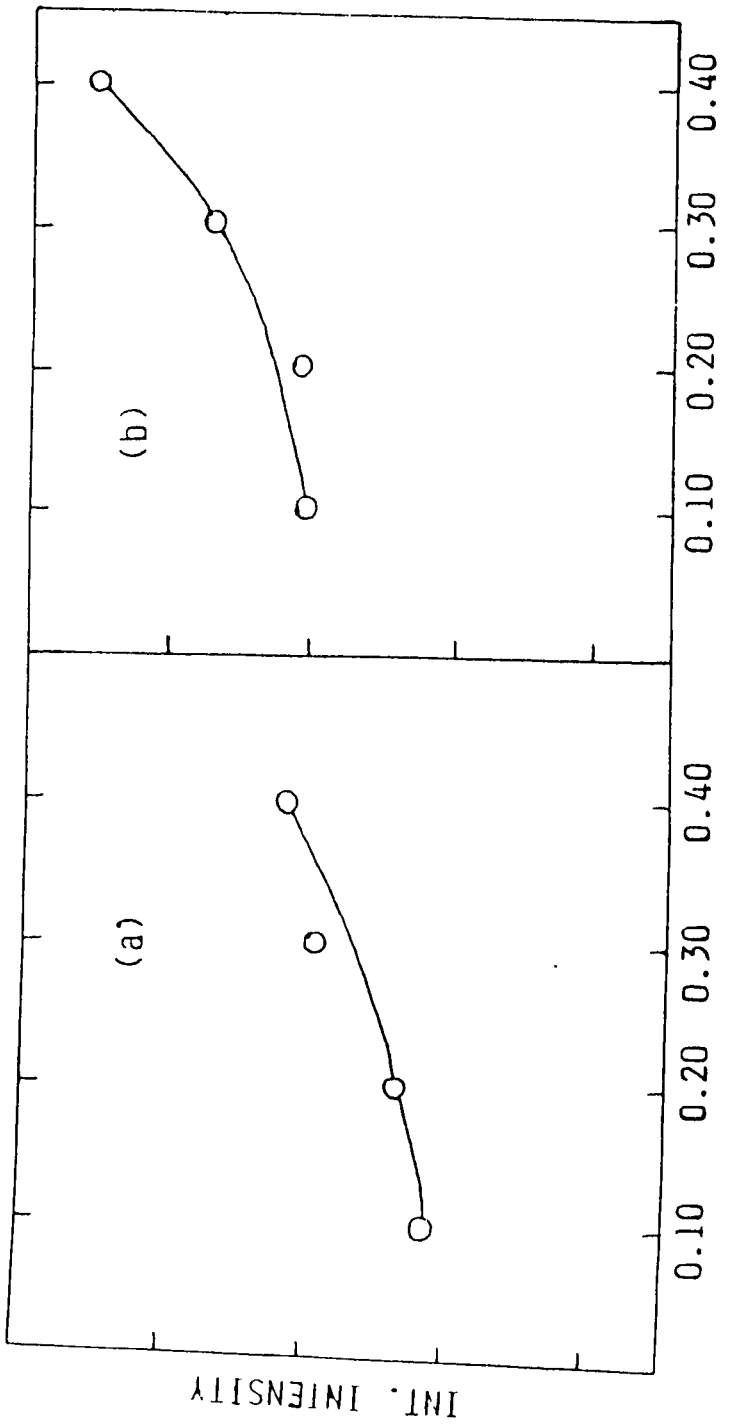

Fig.4.23 Integrated intensity of boson peak in ternary barium borate glasses' spectra with concentration (y) of $BaCl_2$ for x: (a) Ø.2Ø and (b) Ø.35.

binary barium borate glasses (Fig. 4.19B). The 137 cm^{-1} band (for v-B_2O_3) is shifted to 14Ø cm^{-1}, where as an additional band at 116 cm^{-1} is also seen in all the reduced spectra. This band at 116 cm^{-1} is probably associated with the librational motion of BO_3 triangles. The 14Ø cm^{-1} band is attributed (as in strontium borate glasses) to the librational motion of cyclic borate groups containing tetrahedral borons. The peak around 67 cm^{-1} which is the contour maximum (boson peak) appears to be a common feature of all borate glasses and arises due to the limited structural correlation range of glass structure which causes a maximum in the frequency dependent Raman coupling coefficient C_b (equation 1.25, chapter I)

Addition of BaO to v-B_2O_3 provides oxygens to form BO_4 units, where as large barium ions (Ba^{++}) also enhance the number of non-bridging oxygens. The formation of BO_4 units influences the preferential ordering (preference or tendency of BO_3 triangles to be connected to each other or joined with BO_4 units) of the BO_3 triangles causing structural range of these units BO_3 or BO_4 to reduce[4Ø]. As a result, the low frequency $BaCl_2$ into the binary borate glasses does not produce any band in this frequency range, though there may be the possibility of formation of BO_3Cl groups. An increase in intensity , however, may be interpreted in terms of the enhancement of the formation rate of BO_4 units in the sense that

it also relates to the preferential ordering of BO_3 triangles so that structural range reduces. The barium and chlorine ions are incorporated in the interstitial vacancies of the glass network, which leads to an expansion of the network structure.

(ii) Vibrational density of states

The vibrational density of states $g_b(\omega)$ is expressed in terms of reduced Raman spectrum of binary barium borate glasses. The three different forms of spectral density of states,, assuming $C_b=1,\omega$ and ω^2, are shown in Fig.4.19B. The temperature reduced Raman spectra with $C_b=\omega$ show all the peaks that have been observed in the experimental Raman spectra (Fig.4.19A). It may be concluded that the temperature reduced spectra ($C_b=\omega$) represents the true vibrational density of states in barium borate glasses in the region $30 < \omega < 300$.

(iii) IR results

The infrared spectra of the barium borate glasses in the system $xBaO.(1-x)B_2O_3$ for x=0, 0.20, 0.35 and 0.50 are displayed in the Fig.4.24 in the range of wave numbers (600-1600 cm^{-1}). The spectrum for the glass of composition $0.20BaO.0.80B_2O_3$ is characterized by absorption bands at 660,900,990,1045,1210 and 1330 cm^{-1}. On comparison between this spectrum (4.24b) and that for x=0 (4.24a), important changes are

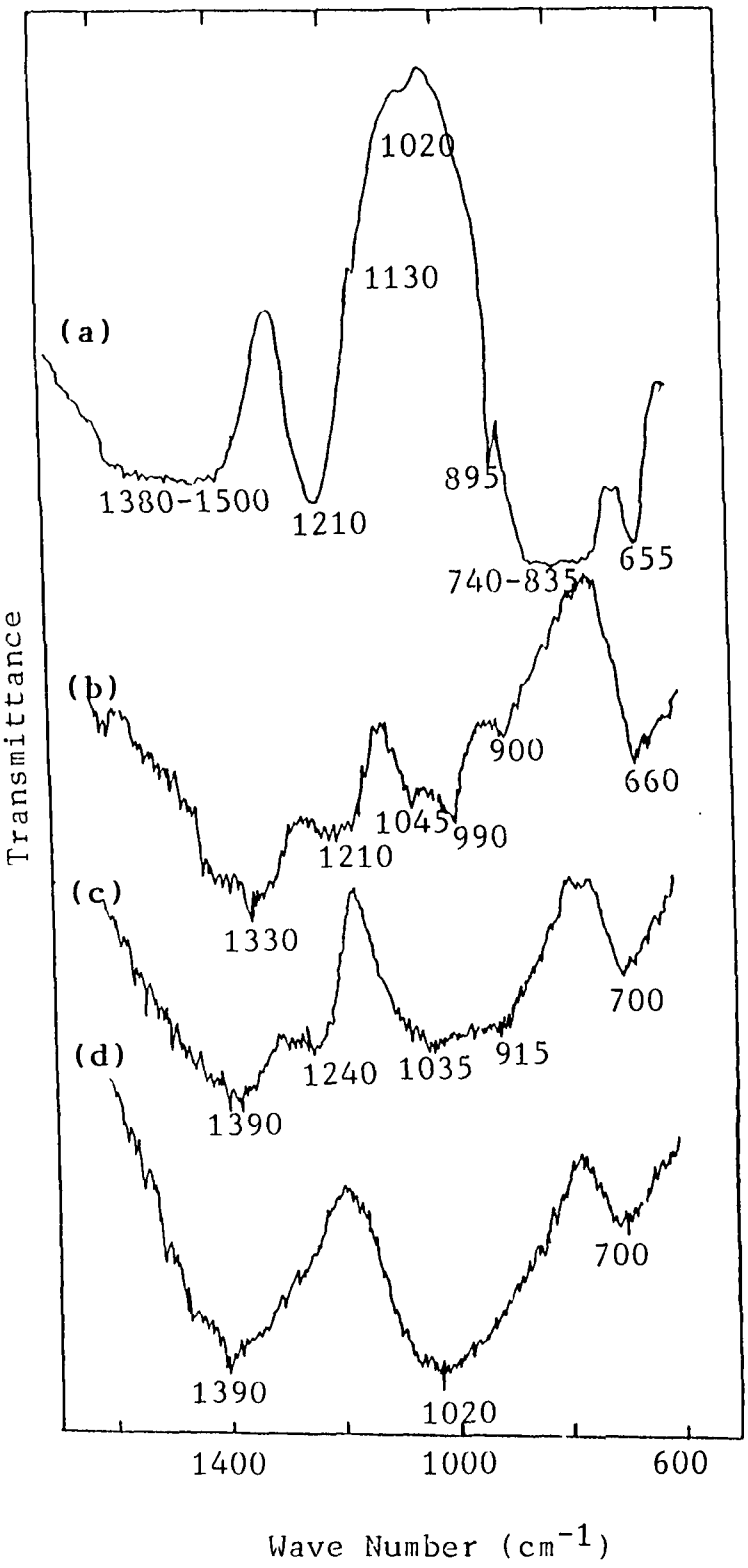

Fig. 4.24 Infrared spectra of barium borate glasses in the system $xBaO.(1-x)B_2O_3$ for various x:
(a) Ø, (b) Ø.2Ø, (c) Ø.35 and (d) Ø.5Ø.

noticeable as a result of addition of BaO to v-B_2O_3. The band at 1210 cm^{-1} is much reduced in intensity and with increase of concentration (x) first shifts to 1240 cm^{-1} and then disappears. The band at 1330 cm^{-1} for x=0.20 is shifted to 1390 cm^{-1} at x=0.50. This shift of 1330 cm^{-1} band and the disappearance of the band of 1210 cm^{-1} may be attributed to the linking up of BO_3 units with non-bridging oxygens[17,19,26] i.e., indicates the formation of orthoborate and pyroborate units at higher concentrations of BaO in v-B_2O_3 network (since the bands at 1225-1270 cm^{-1} corresponds to pyro- and orthoborate units[16]). The bands in the region 850-1100 cm^{-1} originates from B-O bond stretching of BO_4 units. Here the bands in this region 900,990 and 1045 cm^{-1} altogether merge to form a very broad band contour centering around 1020 cm^{-1} when the concentration (x) of BaO is 0.50. This shows the formation of tetra- and diborate groups[16]. The 660 cm^{-1} band is shifted to 700 cm^{-1} for high BaO content and is associated with oxygen bridges between two trigonal boron atoms. Table 4.6 shows the comparison of the bands observed in Raman and IR spectra for the binary system of barium borate glasses.

4.7 Cadmium borate spectra and comparison

The Raman spectrum of binary cadmium borate glass of composition 0.35 CdO.0.65 B_2O_3 is shown in Fig.4.25. The

Table 4.6 The bands observed in Raman and IR spectra of the glasses in the system $xBaO.(1-x)B_2O_3$ for x=Ø.2Ø, Ø.35 and Ø.5Ø.

conc. (x)	Raman bands (cm^{-1})	IR bands (cm^{-1})
	15ØØ (w,b)	133Ø (vb)
		121Ø (w)
		1Ø45 (vw)
		99Ø (w)
Ø.2Ø	912 (vw)	9ØØ (w)
	8Ø2, 775 (splitted sh,s)	
	654 (vw)	66Ø (w,sh)
	1447 (b)	139Ø (vb)
		124Ø (w)
		1Ø35, 915 (vb)
Ø.35	937 (w,b)	
	767 (sh,s)	
	659 (w)	7ØØ (w,sh)
	1433 (b,i)	139Ø (vb,i)
	11ØØ (vw)	
		1Ø2Ø (vb,i)
Ø.5Ø	96Ø (w)	
	88Ø (vw)	
	763 (sh,s)	
	645 (vw)	7ØØ (w,b)

w--->weak, b---> broad, vw---> very weak, sh---> sharp, i-->intense, vb-->very broad. Assignments are similar to those in Table 4.2

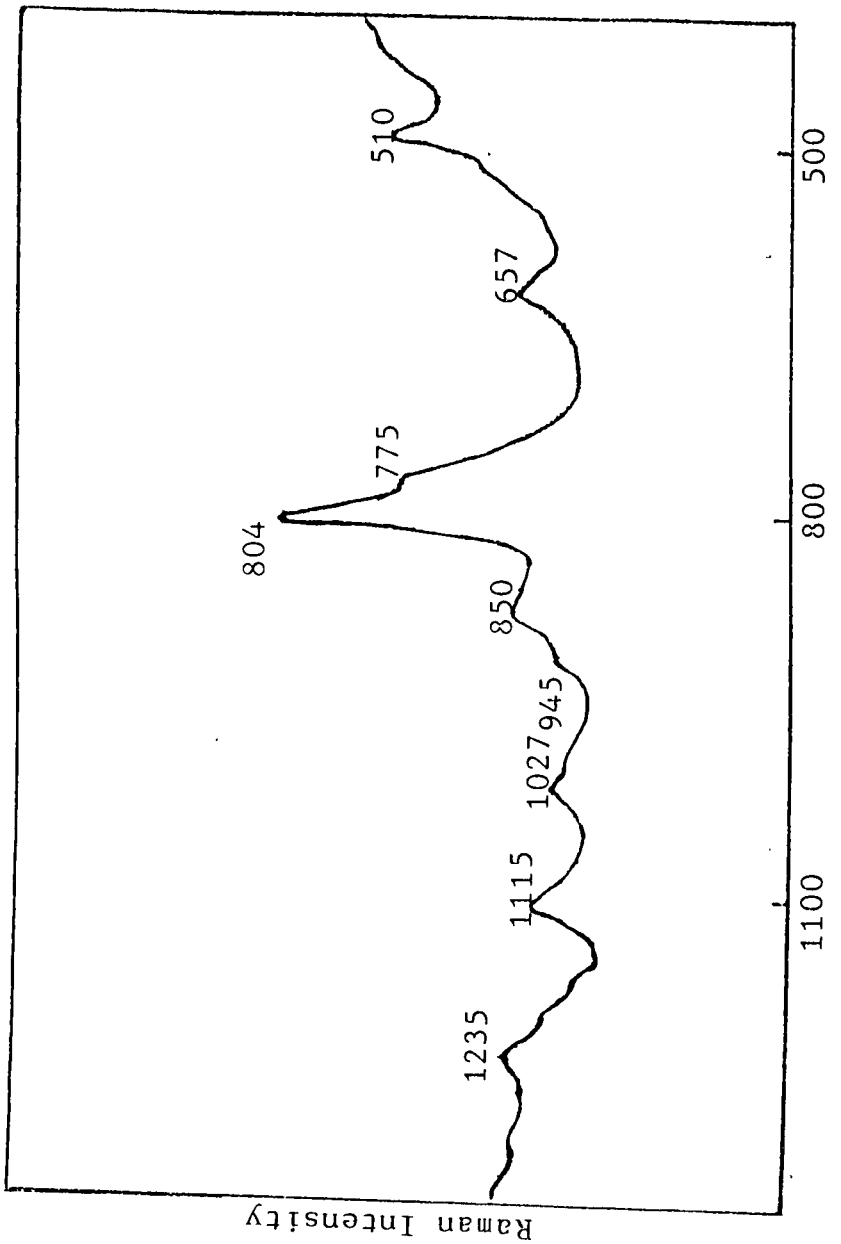

Fig. 4.25 Raman spectrum of cadmium borate binary glass of composition $Ø.35CdO.Ø.65B_2O_3$.

spectrum is characterized by Raman bands at 510, 657, 775, 804, 850, 945, 1027, 1115 and 1235 cm^{-1}. The main feature is a very broad band contour between 755-810 cm^{-1} which is separated into two components; one is relatively sharp at 804 cm^{-1} and the other is the shoulder of it at 775 cm^{-1}. The developement of this shoulder as a result of the addition of 0.35 CdO to $0.65B_2O_3$ is of main interest since it discriminates cadmium borate glass from its alkaline earth as well as alkali borate analogs. At the composition of ($0.35CdO.0.65B_2O_3$) of cadmium borate glass, the 775 cm^{-1} band just begins to appear where as, the situation is unlike in alkaline earth borate glasses in the system $xMO.(1-x)B_2O_3$ for M=Ca,Sr & Ba with x=0.35. In these borate glasses[5], the splitting of 806 cm^{-1} band starts at a concentration less than x=0.20. The lower concentration of cadmium borate glass $xCdO.(1-x)B_2O_3$ with x<0.20 does not form transparent glass.

Assignments of all the Raman bands in the spectra of $0.35CdO.0.65B_2O_3$ glass are, however, similar to those in calcium-,strontium- and barium borate glasses. The spectrum shows , on the basis of the relative intensity, that a greater number of boroxol rings (804 cm^{-1}), some fractions of triborate (775 cm^{-1}), small fractions of diborate (1027-1115 cm^{-1}), meta- (657 cm^{-1}), pyro- (1235,850 cm^{-1}) and orthoborate (945 cm^{-1}) units are present in the cadmium borate glass of

$Ø.35CdO.Ø.65B_2O_3$ composition.

Fig.4.26(a-d) shows the comparison of the Raman spectrum of the $Ø.35CdO.Ø.65B_2O_3$ glass with those of the glasses of composition $xMO.(1-x)B_2O_3$ with x=Ø.25 and M=Ca,Sr & Ba. NMR data have shown[41] that for given values of x in the range $Ø < x < Ø.5Ø$, the proportion of BO_4 groups is the same in all alkali borate glasses in the system B_2O_3-xM_2O (here M is alkali metal) and this should also be similar with alkaline earth borate glasses. But marked differences are seen on their Raman spectra (see Figs.4.26(a-c). The spectrum of strontium borate (Fig.4.26b) shows that the 8Ø6 cm^{-1} Raman line due to boroxol rings has completely disappeared and only one band at 772 cm^{-1} appears, while the spectra of calcium- and barium borate of same composition (Figs.4.26a&c) indicates clear splitting of the band at 8Ø6 cm^{-1} having about equal intensities. Thus it can be inferred from this comparison that the network modifying nature of calcium and barium borate glasses are similar but strontium borate has some deviating characteristics. And the spectrum of Fig.4.26d shows that the addition of Ø.35CdO to $Ø.65B_2O_3$ just begins to split the band at 8Ø6 cm^{-1} (for v-B_2O_3) which shows that the structure of cadmium borate glasses is different from that of alkaline earth borates.

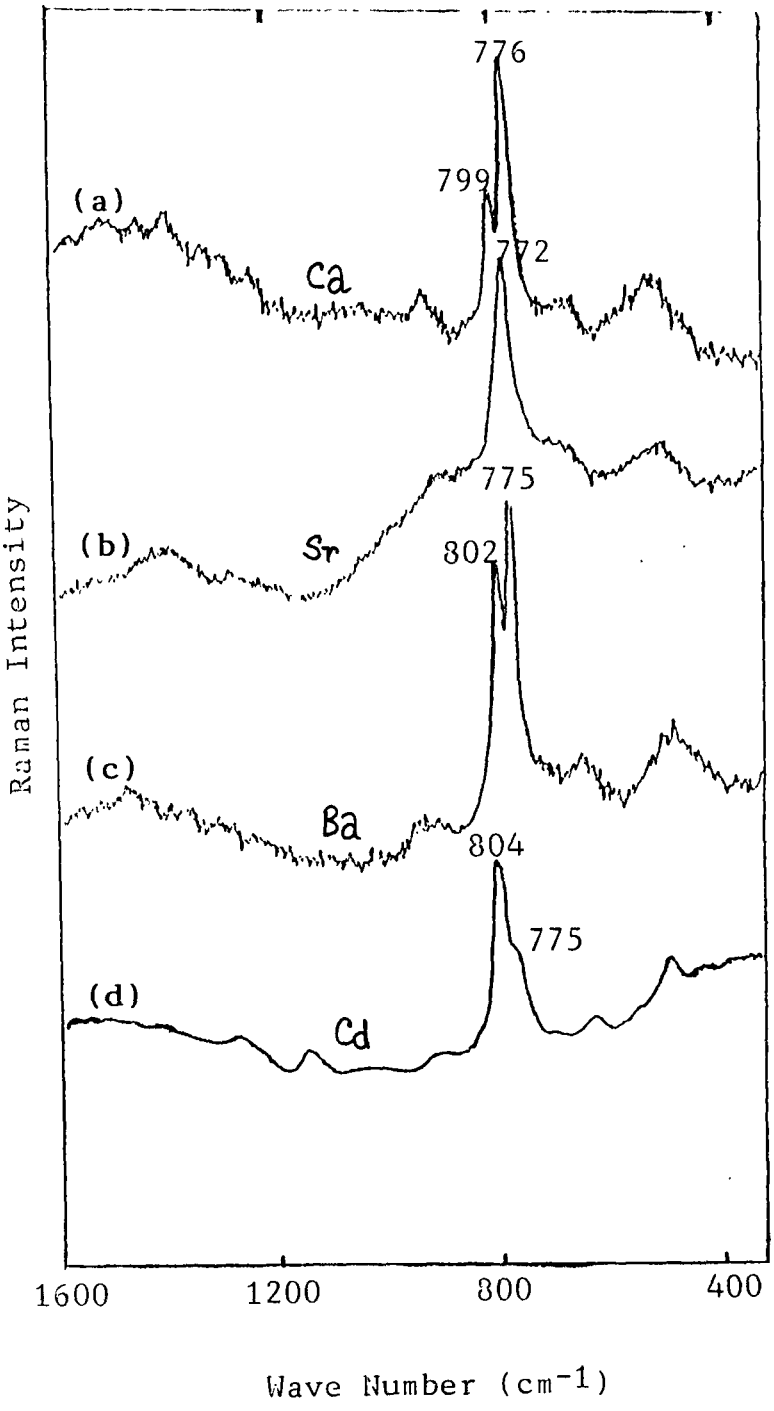

Fig. 4.26 Comparison of Raman spectra of alkaline earth borate glasses of composition $\emptyset.25MO.\emptyset.75B_2O_3$ with that of cadmium borate glass of composition $\emptyset.35CdO.\emptyset.65B_2O_3$.

4.8 conclusions

Raman and IR spectra of alkaline earth borate glasses in the system $xMO.(1-x)B_2O_3$ with M= Ca,Sr and Ba for Ø.2Ø ≤ x ≤ Ø.5Ø show experimental evidence of glass network modifying nature of MO (M=Ca,Sr&Ba) in borate matrix. MO causes a change of boron atom coordination number from 3 to 4 resulting in the complex structural groupings comprising of BO_4 and BO_3 units. Thus it is established that boron has two stable coordination (triangular and tetrahedral) in alkaline earth borate systems. Systematic variation of MO in $v\text{-}B_2O_3$ shows the formation of larger structural groupings containing BO_4 and BO_3 units. For lower concentration of MO, x <Ø.35, triborate, pentaborate and tetraborate cyclic rings are predominantly formed due to the destruction of boroxol rings; where as, at the higher concentration x >Ø.35, diborate, di-triborate groups are predominant along with some fractions of meta-, pyro-, orthoborates and loose BO_4 units, mostly having associated with nonbridging oxygens (NBO). At x=Ø.35 (for Ca and Ba), Raman spectra shows that the glass network becomes saturated in the conversion of boron coordination from triangular to tetrahedral. Cations liberated take their places in the interstitial vacancies of the network near NBO's or BO_3 triangles. At higher concentrations, the decrease of the band centered around 76Ø cm^{-1}, with corresponding increase of other bands in intensity

clearly indicates that the complex cyclic groups, di-triborate or diborates, undergo destruction to form linear groups e.g., pyro-, ortho-, metaborates etc. with NBO's and the larger size of cations tend to break up the network in accomodating themselves in the interstices of the glass structure. The glass structure becomes more randomized. The developement of the bands in the region 275-425 cm^{-1} related to the cation motions in the oxygen sites (mainly the non-bridged oxygens get influenced by the cations interstitially accomodated, giving rise to cation motion), confirms the above argument at higher MO content in these borate glasses. In calcium borate glasses at higher concentrations, chain type metaborates are found to be formed at the destruction of ditriborates at x=Ø.5Ø. In the IR spectra of these glasses, the band at 71Ø cm^{-1} are due to chain type metaborates and in Raman spectra, the shifting of the 652 cm^{-1} band towards higher wave number at 687 cm^{-1}, shows the conversion of ring type metaborate to chain type. In barium borate glasses, the broad feature around 1447 cm^{-1} becomes sharper (atx=Ø.5Ø) and shifted to 1433 cm^{-1} (also observed in IR spectra) shows the formation of greater number of $B_2O_5^{4-}$ and BO_3^{3-} groups involving $B\text{-}O^-$ units in the glass. The large cation size of Ba^{++} ions enhances the number of NBO's. This is supported by the developement of the band at 424 cm^{-1} which is associated with the motions of Ba^{++} ions in their oxygen sites.

In strontium borate glasses, the network modification becomes saturated in its coherence degree at the concentration of x=Ø.25; which is different in nature from other alkaline earth modifiers. Also the constant band position of 772 cm^{-1} band (which appears at concentration lower than Ø.2Ø) and still its intensity decrease with increasing concentration upto x=Ø.3Ø, shows some characteristics deviated from other alkaline-earth borate glasses. Again, the bands at 8Ø6 and 772 cm^{-1} due to boroxol rings and borate cyclic rings respectively, are not observed in the IR spectra of strontium borate binary glasses However, from the general appearance of the spectra of alkaline earth borate glasses, the similar characteristic features are obvious.

The low frequency wing of Raman spectra is characterized by an unpolarized band (known as boson peak) whose position varies in the range 25-1ØØ cm^{-1} in these borate glasses. This band, according to Martin-Brenig model, is attributed to structural disorder and is caused due to the limited structural correlation range of glass structure (SCR). This limitation in SCR (2σ) causes a maximum in the frequency (ω) dependent Raman coupling coefficient C_b which decreases to zero when $\omega > v_t/2\pi c\sigma$. In strontium borate glasses, the SCR values are calculated tentatively using Martin-Brenig model. The introduction of MCl_2 (M=Sr & Ba) into the binary borate matrix does not modify

substantially the vibrational dynamics of the binary glass structure in the region above 300 cm^{-1}. However, the addition of $SrCl_2$ to the binary glass causes a noticeable modification in the low frequency region of Raman spectra. The low frequency Raman scattering intensity increases considerably with rise of concentration of MCl_2 and the boson peak shifts towards higher wave number; of course, no new bands arise in the region 12-1600 cm^{-1}. The MCl_2 helps either in the formation of BO_4 groups or it takes part in the formation of tetrahedral units, like BO_3Cl. However, the above changes correspond to the more randomization of the glass network and barium (Ba^{++}) and chlorine (Cl^-) ions in the ternary glass are incorporated in the oxygen sites which leads to an expansion of the network structure.

REFERENCES

1. D. White, D.E.Mann, P.N.Walsh and A.Sommer, J.Chem.Phys. 32 (196Ø) 481
2. J.Krogh-Moe, Ark Kemi, 12 (1958) 475
3. J.Krogh-Moe, Phys. Chem. Glasses, 3 (1962) 1
4. J.Krogh-Moe, J. Non-Crystalline Solids, 1 (1969) 269
5. W.L. Konijnendijk, Philips Res.Rep.Suppl. 1 (1975)
6. H.Doweidar, Journal of Mater. Sc. 25 (199Ø) 253
7. M.Irion, M. Couzi, A.Levasseur, J.M.Reau and J.C. Brethous, J. Solid State Chem. 31 (198Ø) 285
8. A.Levasseur, J.C.brethous,J.M.reau, P.Hagen-Muller and M. Couzi, Solid st. Ionics, 1 (198Ø) 177
9. A.Levasseur, M.Kbala, J.C.Brethous, J.M.Reau, P.Hagen-Muller and M.Couzi, J. Solid State Commn. 32 (1979) 839
10. A.Levasseur, R.Olazcuaga, M.Kbala, M.Zahir, P.Hagen-Muller and M.Couzi, Solid state Ionics, 2 (1981) 2Ø5
11. A.J.Martin and W.Brenig, Phys.Status Solidi B, 64 (1974) 163
12. R.J.Nemanich, Phys.Rev., 16 (1977) 1655
13. T.W.Brill, Philips Res.Rep.Suppl., 2 (1976) 1
14. W.L.Konijnendijk and J.M.stevels, J. Non-Crystalline Solids, 18 (1975) 3Ø7
15. G.Carini, M.Cutroni, A.Fontana, G.Mariotto and F.Rocca, Phys.Rev. B, 29 (1984) 3567
16. E.I.Kamitsos, M.A.Karakassides and G.D.Chryssikos, J.

Phys.Chem., 91 (1987) 1Ø73

17. Y.T.Quan and C.E.Adams, J. Phys.Chem. 70 (1966) 331

18. N.F.Borrelli, B.D.Mc Swain and G.Su, Phys. Chem. Glasses, 4 (1963) 11

19. E.I.Kamitsos, M.A..Karakassides and G.D.Chryssikos, J. Phys.Chem., 90 (1986) 4528

2Ø. W.B.White, S.A.Brawer, J.Furukawa and G.J.Mc Carthy, *in* ''Borate Glass Structures, Properties, Applications'', Ed. by L.D.Pye, V.D.Frechette and N.J.Kreidl (Plenum,New York,1978)

21. Ulagaraj Selvaraj and Kalya J.Rao, Spectrochim.Acta, 40 A (11/12) (1984) 1Ø81

22. J.Krogh-Moe, Phys. Chem. Glasses, 6 (1965) 46

23. W.L.Konijnendijk and J.M.Stevels, *in* ''Borate Glasses'', Mat. Sc. Res. 12 (1977) 259

24. I.N.Chakraborty and R.A. Condrate, *in* ''Advances in Materials Characterization'', Ed. by D.R.Rossington, R.A. Condrate and R.L.Synder (Plenum, New York,1983)

25. T.W.Brill, Thesis; Technical University of Eindhoven, The Netherlands (1975)

26. T.Minami, Y.Ikeda and M.Tanaka, J. Non-Crystalline Solids, 52 (1982) 159

27. W.L.Konijnendijk, Phys. Chem. Glasses, 17 (1976) 2Ø5

28. H.Hosono, H.Kawazoe and T.Kanazawa, J. Non-Crystalline Solids, 34 (1979) 339

29. T.Nishida and Y.Takashima, J. Non-Crystalline Solids, 37 (1980) 37

30. Y.Ohta, M.Shimada and M.Koizumi, J.Non-Crystalline Solids, 51 (1982) 161

31. R.M.Almeida, J. Non-Crystalline Solids, 106 (1988) 347

32. S.Guha and G.E.Walrafen, J. Chem.Phys. 80 (1984) 3807

33. R.Shuker and R.W.Gammon, Phys. Rev. Letters, 25 (1970) 222

34. G.J.Morgan and D.Smith, J. Phys. C , 7 (1974) 694

35. B.Huttner and W.Pompe, Phys. Status Solidi (b), 114 (1982) 503

36. J.Lorosch, M.Couzi, J.Pelous, R.Vacher and A.Levasseur,J. Non-Crystalline Solids, 69 (1984) 1

37. C.A.Hogarth and M.M.Ahmed, J. Materials Sc. Letters, 2 (1983) 649

38. E.I.Kamitsos, M.A.Karakassides and G.D.Chryssikos, Solid State Commn, 60 (1986) 885

39. S.Block and G.J.Piermarini, Phys. Chem. Glasses, 5 (1964) 138

40. W.Soppe, W.Ebens and H.W.Hartog, J. Non-Crystalline Solids, 105 (1988) 251

41. P.J.Bray, in ''Magnetic Resonance'' (Plenum, New York, 1970) p-11

CHAPTER V

RAMAN AND IR STUDIES OF CERIUM DIOXIDE DOPED CALCIUM BORATE GLASSES

5.1 Introduction

The characteristic properties of glasses containing rare earth ions are of considerable interest in optical data transmission, signal detection and laser technologies. Among other applications, CeO_2 is of particular interest in the production of photosensitive glasses[1] and glass ceramics[2] both as a constitueent and as a decolorizer of amorphous materials. The addition of CeO_2 lowers the melting temperature of silicate glasses while increasing their stability[3]. Interest has grown to evaluate the influence of CeO_2 on borate glasses. In binary alkali or alkaline earth borate glasses, Krogh-Moe[4] had proposed a model in which borate glasses were described as a random network consisting of boroxol tri-, tetra- and diborate structural groups etc. according to the specific concentration of alkali or alkaline earth oxides into the B_2O_3 glass. This model describes borate glasses as a random network former comprising of "B" atoms which are partly tri-coordinated and partly tetra-coordinated with "O" atoms. In general, the units BO_3 and BO_4 are included in larger structural groups whose type and distribution change with changing composition.

We have studied, in this chapter, the laser Raman and infrared spectra of cerium di-oxide doped calcium borate glasses in the system $(CeO_2)_y.[xCaO.(1-y-x)B_2O_3]_{1-y}$ for different values of x and y. The spectral results have been discussed and interpreted in terms of the various structural groups that are formed in the glass system.

5.2 Experimental

Glasses with composition $(CeO_2)_y.[xCaO.(1-y-x)B_2O_3]_{1-y}$ for x=Ø.2Ø& Ø.35 and y= Ø.Ø5 & Ø.1Ø were prepared from analar grades of CeO_2, $CaCO_3$ and boric acid by heating the appropriate amounts of these chemicals in a china clay crucible at 14ØØ K for two hours. A home made furnace was used for this purpose.The clear melts were poured on a stainless steel plate to obtain transparent, homogeneous and redish colored glass pellets of about 1.5 mm thickness.

The Raman spectra were recorded from the experimental set up consisting of argon ion laser as the exciting source, double monochromator with holographic gratings (Jobin Yvon Ramanor HG2S model) equipped with photoelectric detection to record the Raman signals. The emission line of the argon ion laser at 5145 A^o was used with the output laser power of 86Ø mW. The scattered light of Raman signals were collected in the conventional $9Ø^o$ scattering geometry.

The infrared spectra of the glass samples were recorded

using KBr pellet technique. The glass samples were grinded into powder form and then the pellets with KBr were prepared for I.R scanning. The I.R spectral measurements were made using a Perkin Elmer model-681 spectrophotometer.

5.3 Raman spectral results

Pure v-B_2O_3 Raman spectrum shows that an intense and sharp band at 806 cm^{-1} is the characteristic feature representing planar hexagonal boroxol ring structure[5] of the amorphous glass. This band is attributed to the totally symmetric breathing vibration of the boroxol ring with very little boron motion involved. At room temperature, the structure of v-B_2O_3 comprises mainly of boroxol rings with some fractions of BO_3 triangles[6]. The introduction of calcium oxide into the matrix of boric acid glass causes a breakdown of some of the boroxol rings, resulting in a change of boron atom coordination number from three to four, which leads to the formation of BO_4 units. Calcium cations are liberated to increase the ionic conductivity of the glass. The appearance of the band at 778 cm^{-1} (Fig.5.1a) at concentration x = 0.20 & y = 0, due to the splitting of the band at 806 cm^{-1} for v-B_2O_3, shows the modifying nature of CaO in the B_2O_3 matrix and exhibits the experimental evidence of BO_4 formation. In Fig.5.2a for x = 0.35 & y = 0, the band at 806 cm^{-1} is absent, but the split component at 778 cm^{-1} for x = 0.20 (Fig.5.1a) is displaced to 766 cm^{-1}. These facts show that the

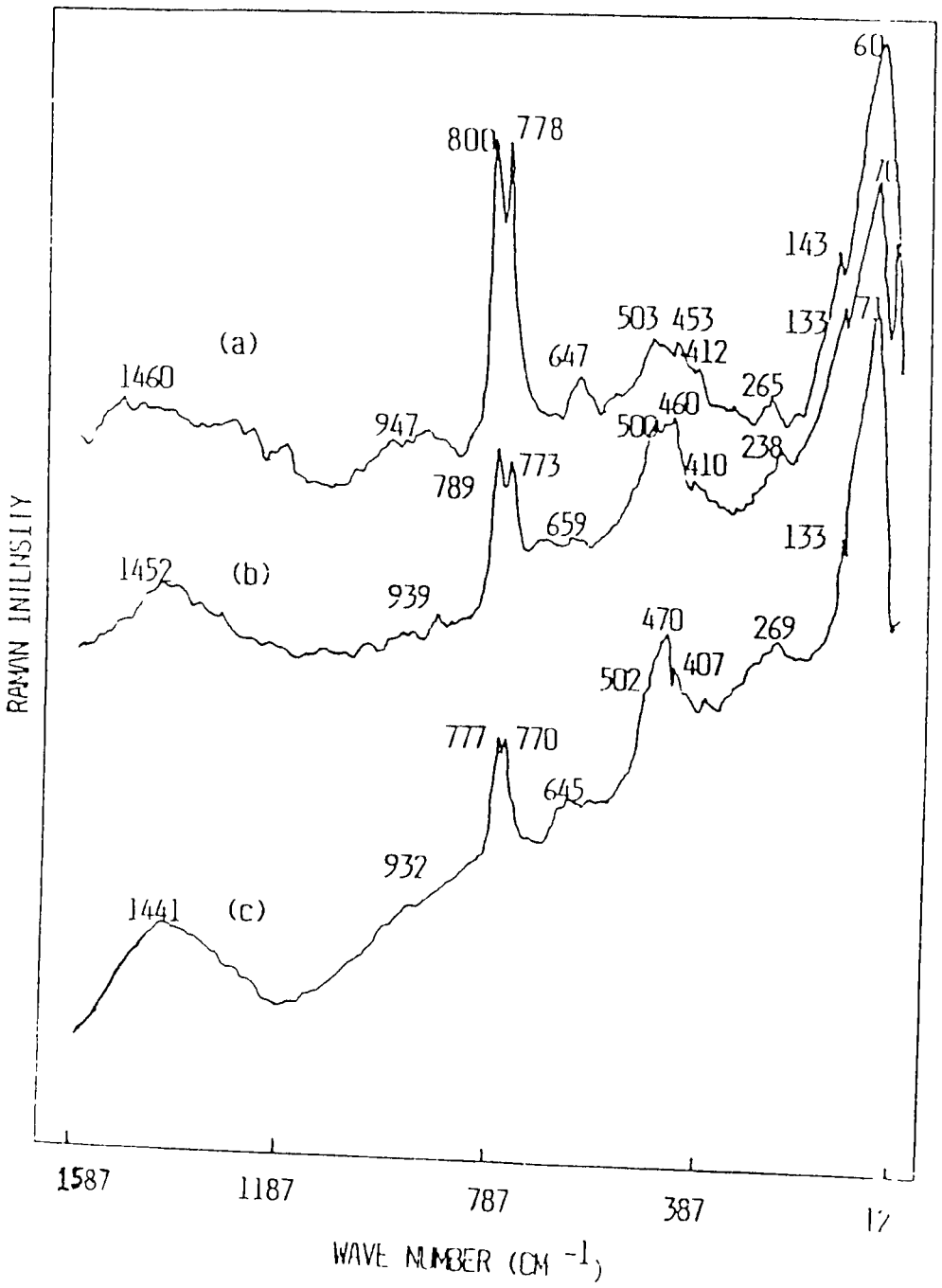

Fig. 5.1 Raman spectra of glasses in the system $(CeO_2)_y.[xCaO.(1-y-x)B_2O_3]_{1-y}$ for the values of x=Ø.2Ø and y: (a) Ø, (b) Ø.Ø5 and (c) Ø.1Ø.

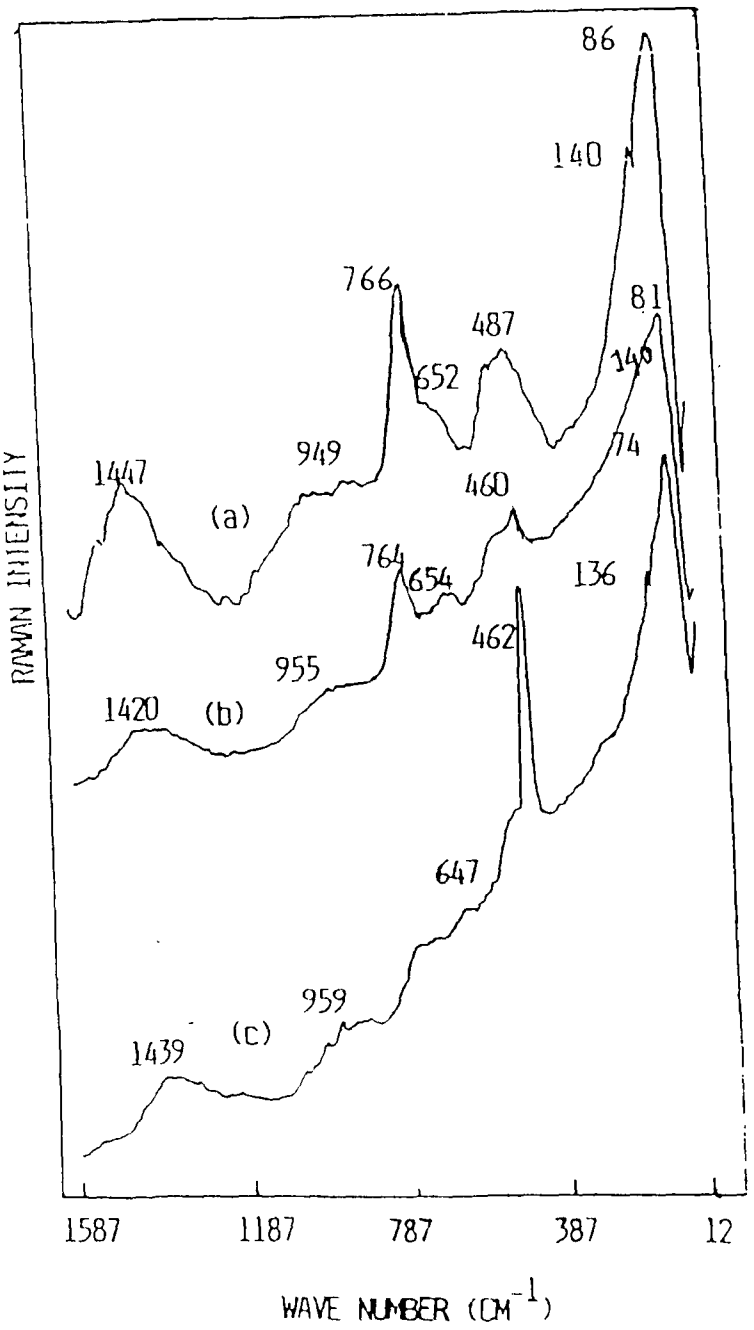

Fig.5.2 Raman spectra of glasses in the system $(CeO_2)_y.[xCaO.(1-y-x)B_2O_3]_{1-y}$ for the values of x=Ø.35 and y: (a) Ø, (b) Ø.Ø5 and (c) Ø.1Ø.

boroxol ring (B_3O_6) are changed into different cyclic borate rings which contain one or two tetrhedrally coordinated borons. The band at 778 cm^{-1} is assigned to the symmetric stretching mode of such cyclic rings. As a result of the gradual addition of CaO to the v-B_2O_3 matrix, the intensity of the band at 778 cm^{-1} increases along with the decrease in intensity of the 8Ø6 cm^{-1} band which completely disappears at x=Ø.35.

The introduction of CeO_2 causes a decrease in integrated intensity (peak height x full width at half maximum) of the splitted bands (Fig.5.1 b & c). The peak intensities and half widths of the 778 cm^{-1} band for specified values of x and y in system are tabulated in Table 5.1. The positions of the two splitted bands are also shifted towards lower wave number (Table 5.2). Fig.5.2 shows that the band at 766 cm^{-1} for x = Ø.35 & y = Ø gradually decreases in intensity with increasing concentration (y) of CeO_2 and finally disappears. These facts indicate that the cyclic rings containing BO_4 & BO_3 groups which caused the appearance of the 778 cm^{-1} band in $xCaO.(1-x)B_2O_3$ glasses have broken down. On the other hand, a sudden sharp increase in intensity of the band at 462 cm^{-1} is observed with the simultaneous disappearance of the band at 778 cm^{-1} for y = Ø.1Ø (Fig.5.2c). Such a perceptible change is, however not observed in Fig.5.1c. The band at 462 cm^{-1} is attributed to the motion of free BO_4 units. The sharp increase in intensity of the band at 462 cm^{-1} is associated with the

Table 5.1 Intensity and half width (FWHM) for 778 cm^{-1} band in the system $(CeO_2)_y[xCaO.(1-y-x)B_2O_3]_{1-y}$ for the values of x and y:

(x)	(y)	Intensity (peak height)	Half width (cm^{-1})
Ø.2Ø	Ø.ØØ	12.Ø	35
	Ø.Ø5	7.Ø	32
	Ø.1Ø	6.Ø	25
Ø.35	Ø.ØØ	9.Ø	5Ø
	Ø.Ø5	4.Ø	38
	Ø.1Ø	Ø.Ø	ØØ

Table 5.2 Observed Raman bands in the system of glasses $(CeO_2)_y[xCaO.(1-y-x)B_2O_3]_{1-y}$ for the values of x & y

(x)	(y)	Wave Numbers (cm^{-1})										
Ø.2Ø	Ø.ØØ	6Ø	143	265	412	453	5Ø3	647	778	8ØØ	947	146Ø
	Ø.Ø5	7Ø	133	238	41Ø	46Ø	5ØØ	659	773	789	939	145Ø
	Ø.1Ø	71	133	269	4Ø7	47Ø	5Ø2	645	77Ø	777	932	1441
Ø.35	Ø.ØØ	86	14Ø	-	41Ø	-	487	652	766	-	949	144
	Ø.Ø5	81	14Ø	-	-	-	46Ø	654	764	-	955	142
	Ø.1Ø	74	136	-	-	-	462	647	-	-	959	143

increase in the number of free BO_4 units. The large rare earth cations tend to break up the glass network to accomodate themselves in the interstitial vacancies of the structure, causing an increased number of non-bridging oxygens.

The observed Raman bands for various values of x and y in the system $(CeO_2)_y.[xCaO.(1-y-x)B_2O_3]_{1-y}$ are tabulated in Table-5.2, while their assignments are given in Table 5.3 . The broad band (hump type) seen in the region 142Ø-146Ø cm^{-1} is similar to that observed in the spectra of large number of modified borate glasses with relatively high modifier contents. According to Konijnendijk[7], we attribute this band to a triangular boron-oxygen stretch which involves non-bridging oxygens[8]. The increase in intensity of the band around 1452 cm^{-1} for x = Ø.2Ø (see Fig.5.1b) and shifting of it towards lower wave number with increase of cerium di oxide concentration involves greater number of orthoborate and pyroborate units at the expense of cyclic borate groups. The appearance of this band is a common feature of crystalline borates which contain large borate groups with dangling $>B-O^-$ bonds[7]. The band around 144Ø cm^{-1} in the present glass system may be associated with the orthoborate groups .The weak band in the region 932-959 cm^{-1} corresponds to the stretch of tetrahedrally coordinated borons associated with the group $\equiv B-O-B\equiv$ at lower concentration while at higher modified content, it is related to orthoborate groups. A band at 93Ø cm^{-1} is also observed in crystalline

Table 5.3 Assignments of bands observed in CeO_2-doped calcium borate glasses in the system $(CeO_2)_y.[xCaO.(1-y-x)B_2O_3]_{1-y}$

Wave number (cm^{-1})	Assignments
1420-1460	Stretch of $B-O^-$ bonds attached to large borate groups
932-959	Vibration associated with orthoborate units
800	Symmetric stretch in boroxol hexagonal rings
763-778	Stretching in cyclic borate rings containing one or two BO_4 units
645-659	Vibrational motion in metaborate rings
460-503	Motion in loose BO_4 units attached to borate complexes
238-269	Motion associated with cations in non-bridged oxygen sites
133-143	Librational motion in borate groups
60-86	(Boson peak) due to thermal population increase and limited structural correlation range in glass

Table 5.4 Observed IR. bands in the system of glasses $(CeO_2)_y[xCaO.(1-y-x)B_2O_3]_{1-y}$ for the values of x & y.

x	y	Wave Numbers (cm^{-1})						
	0.00	665	790-820	900	945	1045	1120	1210	1465
0.20	0.05	710	-*-	900-1100		-*-	-*-	-*-	1390
	0.10	710	-*-	-*-		1000-1100		1260	1430
	0.00	710		900-1100				1360-1500	
0.35	0.05	700		900-1100				1390	1465
	0.10	700		980	1040			1260	1390

orthoborates[9]. A weak Raman band in the region 645-659 cm^{-1} is observed in the spectra of Figs.5.1 & 5.2. This band is assigned to the bond bending vibration of the B-O-B linkage associated with metaborate groups which are also found to occur in the crystalline compound of calcium borate of composition $CaO.B_2O_3$[10].

An important feature in the low frequency region of the Raman spectra is characterized by an unpolarized or very weakly polarized band known as boson peak whose position varies from 60 cm^{-1} to 86 cm^{-1} in these borate glasses. It is believed that this boson peak results from the competition between the decreasing density of vibrational states and the increasing thermal population that occurs as the vibrational frequency decreases towards zero[11]. The low frequency wing in Raman spectra have been explained on the basis of the model proposed by Martin and Brenig[12]. This model gives expressions for the frequency dependent Raman coupling coefficient C_b (which appears in the Stokes Raman intensity expression 1.21, chapter I) relating to low lying acoustic vibrational modes and structural correlation range 2σ (SCR) in the glass. The theoretical values of C_b corresponding to these acoustic modes have been fitted to the experimentally obtained reduced Raman spectra (see equation 1.28, chapter I) and structural correlation ranges (2σ) have been calculated sucessfully. Thus according to the M-B model the boson peak is interpreted as arising from limited structural

correlation range in the glass structure.

5.4 IR spectral results

The I.R spectra of the system $(CeO_2)_y[xCaO.(1-y-x)B_2O_3]_{1-y}$ at various values of x and y are shown in the Figs.5.3 & 5.4 in the region 600-1600 cm^{-1}. In rare earth oxide doped sodium borate glasses in the system $Na_2O.B_2O_3.Ln_2O_3$, where Ln = Sm, Pr, the I.R bands in the region 900-1100 cm^{-1} have been assigned to the B-O stretching of BO_4 tetrahedral units[13]. The bands lying between 1100-1500 cm^{-1} and 650-700 cm^{-1} are assigned to the B-O stretching and out-of-plane bending vibration of BO_3 units respectively. The I.R spectra of the present system of glasses with x = 0.20 and y = 0 in the Fig.5.3a consist of a number of bands which are tabulated in Table 5.4. The splitted band at 790-820 cm^{-1} corresponds to the symmetric stretch of borate cyclic rings containing BO_3 and BO_4 groups. The band 665 cm^{-1} is assigned to the metaborate groups. Bands in the region 900-1120 cm^{-1} are due to boron oxygen stretch in BO_4 tetrahedral units. The band at 1210 cm^{-1} is assigned to the B-O stretch of the triangular units and the broad band centered at 1465 cm^{-1} is mainly due to different types of B-O stretching vibrations associated with $>B-O^-$ groups similar to those observed in alkali borate glasses[14]. In the spectra of Fig.5.3(b & c), at CeO_2 concentration of y = 0.05 & 0.10, the IR bands appear to form broad envelopes and it is noteworthy that the

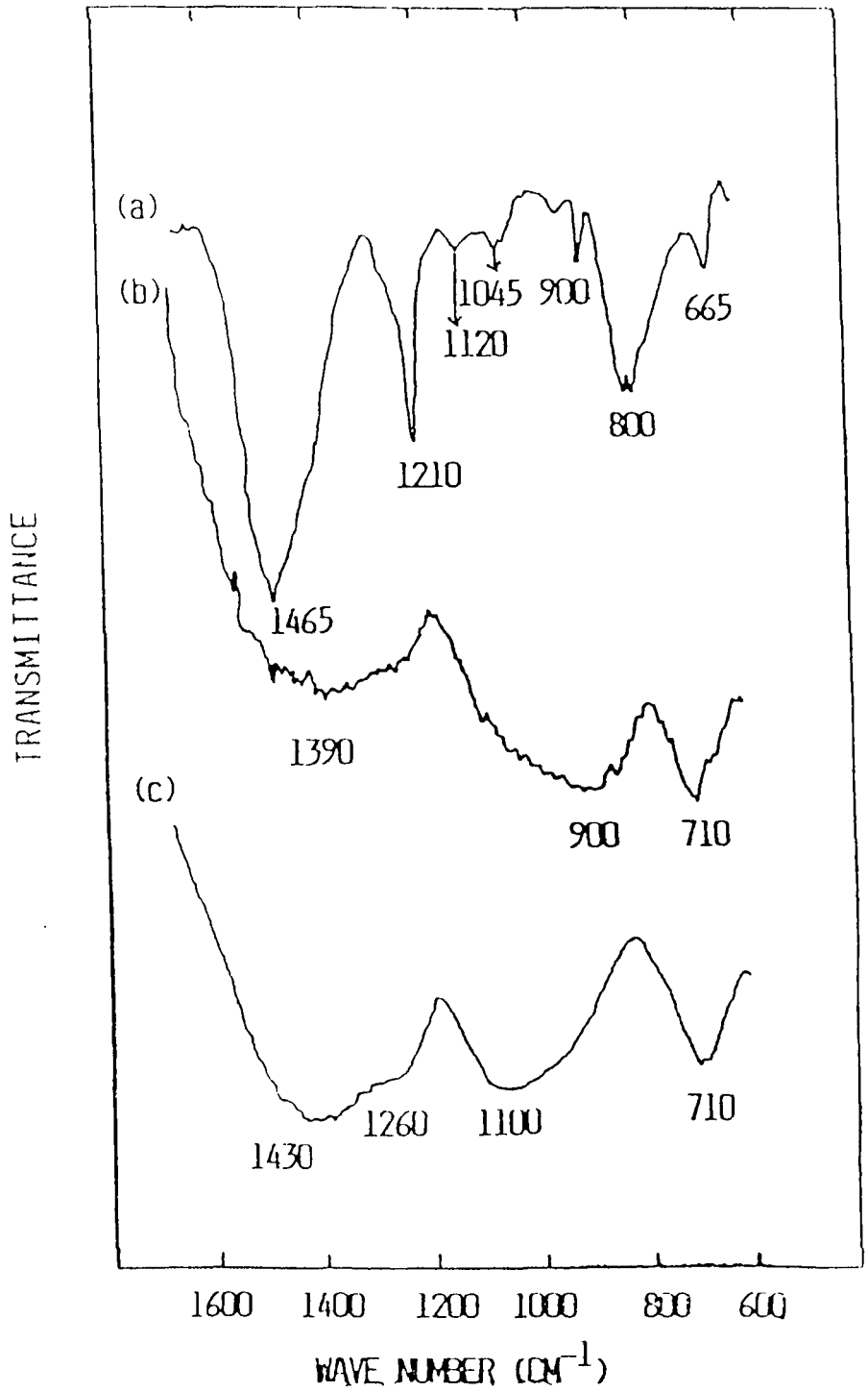

Fig.5.3 IR spectra of glasses in the system $(CeO_2)_y.[xCaO.(1-y-x)B_2O_3]_{1-y}$ for the values of x=Ø.2Ø and y: (a) Ø, (b) Ø.Ø5 and (C) Ø.1Ø.

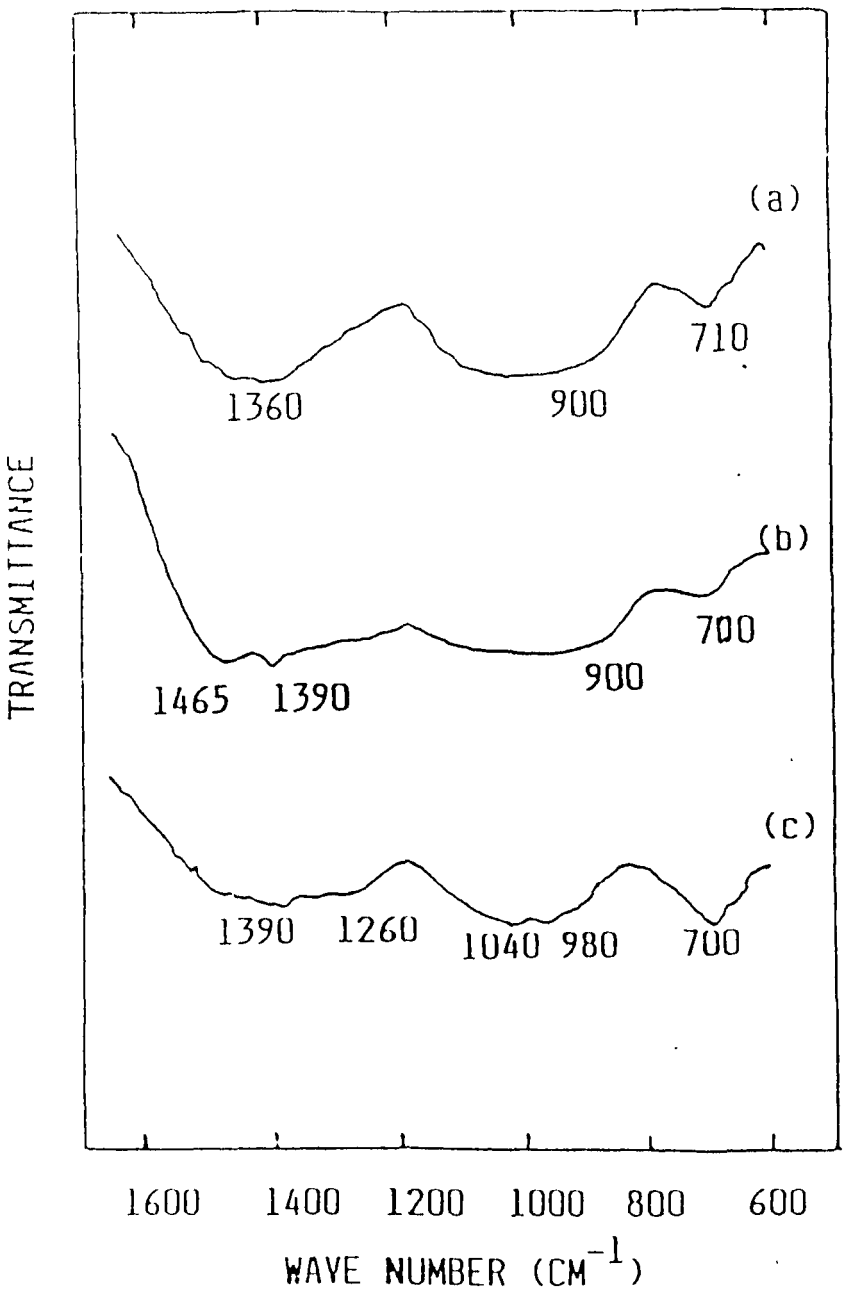

Fig.5.4 IR spectra of glasses in the system $(CeO_2)_y.[xCaO.(1-y-x)B_2O_3]_{1-y}$ for the values of x=Ø.35 and y: (a) Ø, (b) Ø.Ø5 and (c) Ø.1Ø.

splitted band between 790-820 cm^{-1} has disappeared. Only three main broad band contours are present in the spectra. The region 650-720 cm^{-1} corresponds to BO_3 bending motion, 900-1100 cm^{-1} represents the stretch of BO_4 units and the broad envelope around 1430 cm^{-1} indicates non-bridged groups of BO_3 units. The disappearance of the band at 790-820 cm^{-1} clearly indicates the absence of cyclic borate rings containing BO_3 and BO_4 units. The IR spectra in the Fig.5.4a for y =0 and x=0.35 shows two envelopes between 900-1100 cm^{-1} and 1360-1500 cm^{-1} along with the band at 710 cm^{-1}. But for y = 0.05 & 0.10, some other bands at 980, 1040, 1260 & 1390 cm^{-1} appear. The band at 1260 cm^{-1} may be assigned to the stretching vibration of boron sub lattice against oxygen sub lattice, while 1390 cm^{-1} band is due to B-O bond stretching vibration in BO_3 units. All the observed IR bands are tabulated in Table 5.4.

5.5 Discussions and Conclusions

Comparing IR and Raman spectra, we observe that in Raman spectra, the band near 659 cm^{-1} for y = 0.05 has been assigned to the motion of metaborate and a similar band in the region 665-710 cm^{-1} also appears in IR spectra with greater intensity (Fig.5.3). The disappearance of the splitted bands around 800 cm^{-1} with the addition of CeO_2 is a common feature in both IR and Raman spectra of these glasses and indicates the breakdown of cyclic borate rings. Abdullaev et al.[15] concluded from their

single crystal X-ray analysis of rare earth metaborates that all rare earth metaborates (crystalline compounds) contain (B_3O_6) chains in which the tetrahedra and triangles are linked to each other to form a chain (Fig.5.5). In the present system, the absence of cyclic borate rings containing BO_3 and BO_4 units along with the intensity rise and shift of 665 cm^{-1} band towards higher wave numbers[16,17] at 710 cm^{-1} with concentration y in IR spectra indicates that the metaborate chain is most probable in CeO_2 doped calcium borate glasses of composition x = 0.20 & 0.35 & y = 0.05 & 0.10. The band between 932-959 cm^{-1} in the Raman spectra is weak, while in the IR spectra, the broad intense feature observed at 900-1100 cm^{-1} for concentration of x=0.20 & y=0.05 & 0.10 has become more broad with less intensity for concentration of x=0.35 & y=0.05 & 0.10. So this region is mainly due to calcium borate glass and the role of CeO_2 seems to decrease the intensity of this band contour at 900-1100 cm^{-1}. The 1210 cm^{-1} band (for x=0.20 & y=0) in the IR spectra (shifted to 1260 cm^{-1}) is, however, not observed in Raman and corresponds to B-O stretch involving different groups[4]. Another broad feature at 1420-1460 cm^{-1} observed in Raman spectra is also found to appear in IR spectra at 1360-1465 cm^{-1} and involves stretching of non-bridged ($B-O^-$) bonds. Thus it is concluded that cerium di-oxide doped calcium borate glasses in the composition range $0.20 \leq x \leq 0.35$ and $0 \leq y \leq 0.15$, mainly contain

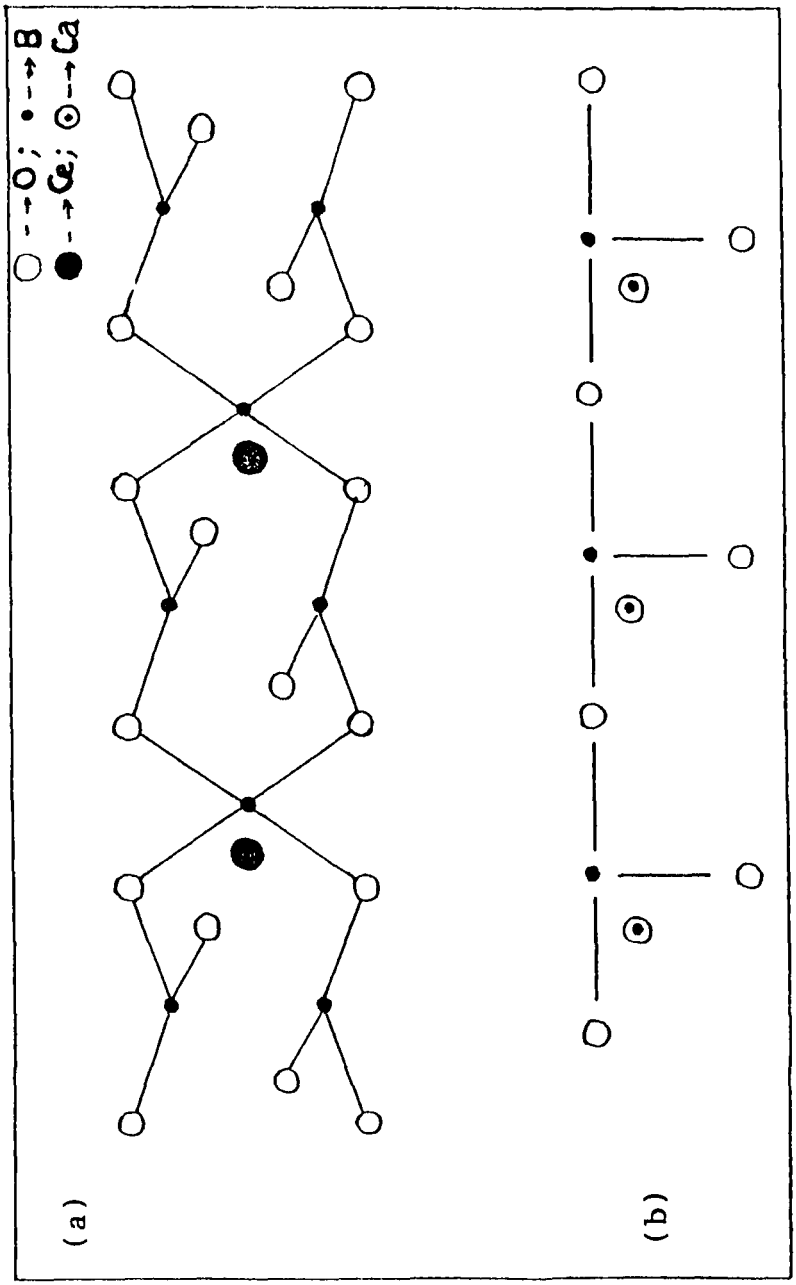

Fig.5.5 Structural representation of metaborate chain observed in
(a) Cerium di oxide doped calcium borate glasses.
(b) Calcium borate glasses of composition $CaO.B_2O_3$.

metaborate chains. It is also obvious that CeO_2 acts as a good modifier in these glass matrices.

REFERENCES

1. P.W.Mc Millan, *in* "Glass ceramics", (Academic press, London, (1964)
2. O.H.Bayoumi and K.N.Subramanian, J. Am. Ceramic Soc., 60 (3,4) (1977) 161
3. W.J.Zdaniewski, J. Am. Ceramic Soc., 58(5,6) (1975) 163
4. (i) Krogh-Moe, Phys. Chem. Glasses, 6 (1965) 46
   (ii) Krogh-Moe, Phys. Chem. Glasses, 3 (1962) 101
5. F.L.Galeener, Solid State Commn., 44 (1982) 1037
6. S.Guha and G.E.Walrafen, J. Chem. Phys., 80(8) (1984) 3807
7. W.L.Konijnendijk, Philips Res. Rept. Suppl. No.1, (1975)
8. E.I.Kamitsos, M.A.Karassidesand G.D.Chryssikos, J. Phys. Chem., 90 (1986) 4528
9. W.L.Konijnendijk and J.M.Stevels, *in* "Borate Glasses", Mat. Sc. Res.(Plenum Press, New York) 12 (1977) 259
10. W.L.Konijnendijk and J.M.Stevels, J. Non-Crystalline Solids, 18 (1975) 307
11. R.M.Almeida, J. Non-Crystalline Solids, 106 (1988) 347
12. A.J.Martin and W.Brenig, Phys. Status Solidi B 64 (1974) 163
13. V.I.Tananaev, B.F.Dzhurinskii and I.M.Belykov, *in* "Rare Earth Borates", Neorg. Mater., 2(10) (1966) 1543
14. (i) Y.T.Quan and C.E.Adams, J. Phys. Chem., 70 (1966) 331
   (ii) N.F.Borelli, Phys. Chem. Glasses, 4 (1963) 11
15. G.K.Abdullaev, K.S.Mamedov and G.G.Dzhafarov, *in* "Crystal

Structure of Metaborates", Sov. Phys-Crystallogr. (Eng. Transl.) 20(2) (1975) 161

16. I.N.Chakraborty and R.A.Condrate, in "Advances in Materials Characterization", Ed. by D. R. Rossington, R.A.Condrate and R.L.Synder (Plenum,New York,1983)

17. E.I.Kamitsos, M.A.Karakassides and G.D. Chryssikos, J. Phys. Chem. 91 (1987) 1073

CHAPTER VI

SPECTRAL STUDIES OF V_2O_5 DOPED CALCIUM BORATE GLASSES

6.1 Introduction

The investigations on oxide glasses containing two or more different glass network formers have been performed in the past in order to obtain an understanding of their structural and transport properties[1-3]. Vanadate glasses are of importance because of their switching and semiconducting properties[4,5]. These glasses have been studied in the past with glass formers, such as, P_2O_5, TeO_2 etc. Studies relating to the electrical conduction[6,7], dielectric relaxation[8,9] and structural investigation by spectroscopic methods[10], have been performed on these glasses.

In this chapter, Raman and IR spectral measurements of the calcium borate glasses doped with vanadium oxide (V_2O_5) have been undertaken.

6.2 Experimental

Analar grade chemicals, H_3BO_3, $CaCO_3$ and V_2O_5 (BDH, Bombay, India) were well mixed and melted in a china clay crucible at a temperature of 1150 °C and maintained at this temperature for two hours before quenching. The clear melt was quenched at room

temperature and pressed between two stainless steel plates to obtain about 1.5 mm thick glass sample for Raman study. These glasses so prepared in the system $(V_2O_5)_y.[xCaO.(1-y-x)B_2O_3]_{1-y}$ for x= Ø.2Ø & Ø.35 and y=Ø.Ø5, Ø.1Ø and Ø.15, were homogeneous and blackish-brown in colour. Raman spectra of these glasses were recorded on a Jobin-Yvon Ramanor HG2S spectrometer equipped with Spectra Physics 171 argon ion laser (5145 A° line) in the $9Ø^{\circ}$ scattering geometry.

The infrared tranmission spectra were recorded on a Perkin-Elmer spectrophotometer model 681. The glass samples were grinded thoroughly to fine powder and KBr pellets were prepared using the procedure described in chapter II.

6.3 Raman results

Figure 6.1 shows the Raman spectra of the glasses in the system $(V_2O_5)_y.[xCaO.(1-y-x)B_2O_3]_{1-y}$ for x=Ø.2Ø and y=Ø, Ø.Ø5, Ø.1Ø and Ø.15, while Fig.6.2 shows the same for x=Ø.35 and y=Ø, Ø.Ø5, Ø.1Ø and Ø.15 in the range of wave numbers 12-16ØØ cm^{-1}. The Raman spectrum of pure v-B_2O_3 is characterized mainly by a sharp band at 8Ø6 cm^{-1} which is assigned to the totally symmetric stretching mode of planar hexagonal B_3O_6 boroxol rings. The Raman spectra of calcium borate binary glasses have been discussed in the chapter IV. When CaO is added to v-B_2O_3, the boron atom coordination number is changed from 3 to 4 so

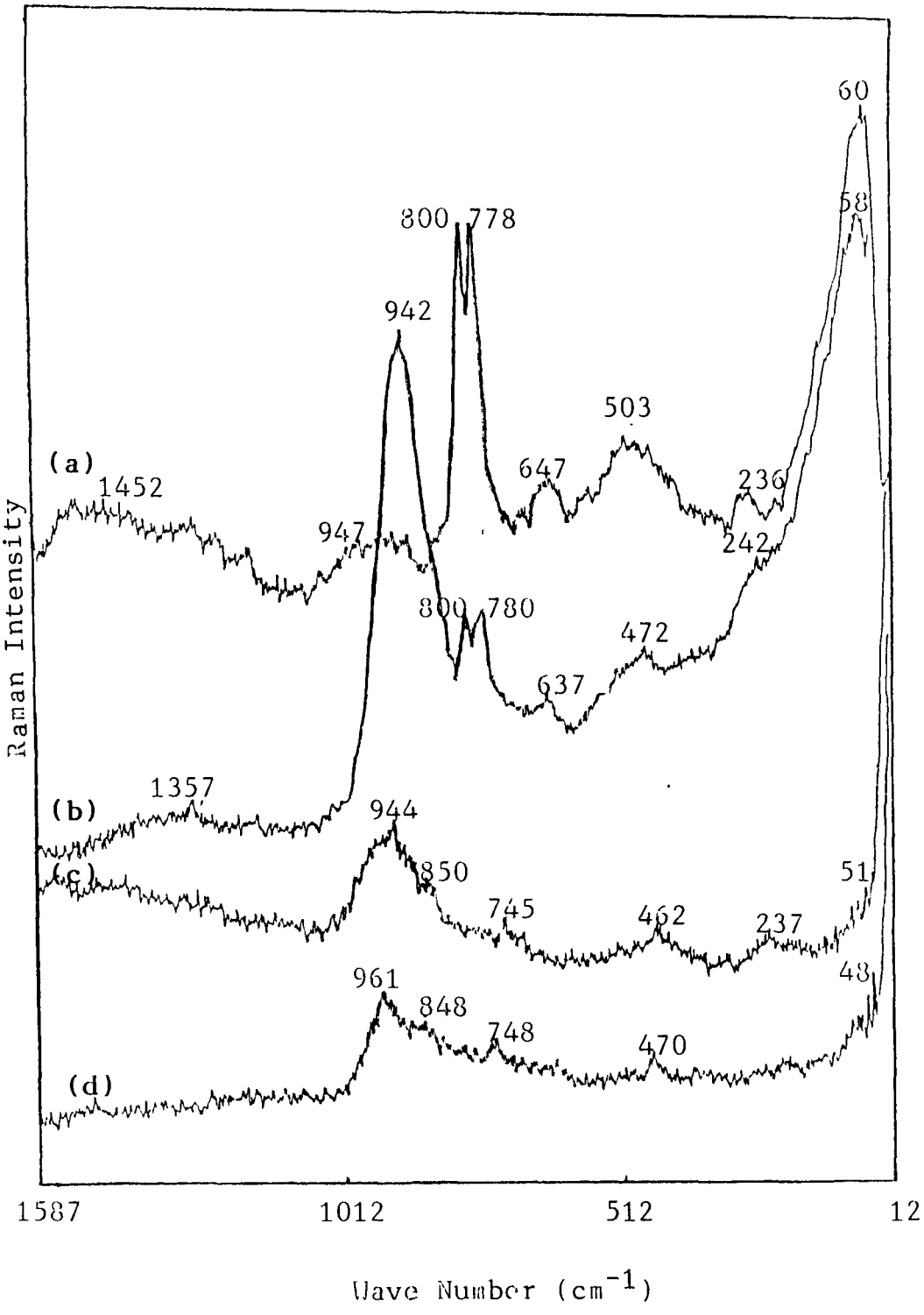

Fig. 6.1 Raman spectra of glasses in the system $(V_2O_5)_y.[xCaO.(1-y-x)B_2O_3]_{1-y}$ for the values of x=Ø.2Ø and y: (a) Ø, (b) Ø.Ø5, (c) Ø.1Ø and (d) Ø.15.

that boroxol rings are destroyed to form complex cyclic rings containing one or two BO_4 and BO_3 units. As a consequence, the band at 806 cm^{-1} splits, giving rise to a new band at 778 cm^{-1} for x=0.20 (Fig.6.1a) together with the 806 cm^{-1}band displaced to 800 cm^{-1}. All the observed Raman bands are shown in Table 6.1. In Fig.6.1b, the split components (800 and 778 cm^{-1}) are much diminished in intensity as a result of addition of V_2O_5 (y=0.05) to the binary 0.20 CaO.0.80B_2O_3, while the weak band at 947 cm^{-1} (of the binary) shows an abrupt rise in its intensity with its peak position shifted to 942 cm^{-1}. However, for y=0.10 and x=0.20 (Fig.6.1c), the bands at 800 and 778 cm^{-1} completely disappear with the appearance of new bands at 745 and 850 cm^{-1} while the 942 cm^{-1} band diminishes in intensity. With further addition of V_2O_5 (y=0.15, Fig.6.1d), the intensity of the 961 cm^{-1} band further decreases.

The disappearance of the bands at 800 and 778 cm^{-1} at higher concentrations of V_2O_5 indicates the absence of the cyclic borate rings which are formed due to the addition of CaO in v-B_2O_3. On the other hand, the appearance of an additional intense band centered at 942 cm^{-1} indicates the formation of vanadium polyhedral groups. Of course, the interpretation is complicated because of the presence of two network forming oxides B_2O_3 and V_2O_5 and the fact that boron is known to have two stable coordinations (triangular and tetrahedral) while V_2O_5

have VO_4, VO_5 and VO_6 coordinations. We see that the band at 942 cm^{-1} (Fig.6.1b) spans the range of wave numbers from 815 to 1035 cm^{-1} and its full width at half maximum is 115 cm^{-1} for the spectra of Fig.6.1(b). The Raman feature of crystalline [11] V_2O_5 at 997 cm^{-1} is attributed to the symmetrical stretching mode of V = O bond having five fold coordination structure (VO_5). Now if we think of calcium vanadate glass structure in which CaO goes as a network modifier of V_2O_5 matrix, then Ca^{++} ions can be thought to go interstitially into vanadate chains by interacting directly with V = O bonds, which results in a shift of frequency of the vibrational spectra towards lower wave numbers due to the formation of longer bonds. The presence of CaO would also cause a series of complexes consisting of chains of tetrahedra (VO_4) due to the destruction of vanadate groups (VO_5). Because of these above causes, the symmetrical stretching frequency of V = O bonds at 997 cm^{-1} (for crystalline V_2O_5) shifts to lower wave number when V_2O_5 is added to calcium borate binary glass and overlaps with the vibrations due to orthoborates (at 945 cm^{-1}) [12] and pyroborates (at 850 cm^{-1}) to appear as a broad and intense band contour between (815-1035 cm^{-1}) centering at 942 cm^{-1}.

However, with further increase of V_2O_5 concentration (y=0.10 and 0.15; Fig.6.1c & d), this band decreases in intensity along with the other bands in the spectra also showing

a decreasing trend in their intensities. Having fixed amount of modifier concentration of calcium oxide (x), the glass formers B_2O_3 and V_2O_5 form a quasi-complex in this concentration range ($Ø.Ø5 \leq y \leq Ø.15$). Thus the appearance of the new band at 745 cm^{-1} is possibly due to vanadate ion of some form or possibly to B-O-V-O-B units and the band at 85Ø cm^{-1} is due to pyroborate units. The band at 647 cm^{-1} which is associated with metaborate groups (for y=Ø,Fig.6.1a) is shifted towards lower wave number and then disappears at the concentration, y=Ø.1Ø. The 5Ø3 cm^{-1} band also shifts towards lower wave number and diminishes in intensity with rise of concentration (y). This band has been attributed to either free BO_4 units or to those BO_4 units attached loosely to ring type borate groups. The very broad and weak band centering around 1452 cm^{-1} can be attributed to $B\text{-}O^-$ stretch involved in large borate groups and this band disappears with rise of concentration (y) of V_2O_5.

In the **low frequency region**, the band at 6Ø cm^{-1} (known as boson peak) for the glass of concentration, x=Ø.2Ø and y=Ø, starts to disappear with increase of concentration (y). This boson peak is a common feature in borate glasses and arises from thermal population increase and limited structural correlation range of glass structure. But this feature is very weak here in the present system of ternary glasses when y=Ø.1Ø and Ø.15. The bands at 242 and 237 cm^{-1} at y=Ø.1Ø & Ø.15 concentration

respectively may be related to cation motions in non-bridging oxygen sites.

Fig.6.2a shows the Raman spectrum of the system (for x=Ø.35 & y=Ø) in which the v-B_2O_3 matrix is modified by the addition of CaO to the extent that the formation scheme of BO_4 tetrahedral groups from BO_3 triangles is saturated in its network coherence at the specified composition . The band at 773 cm^{-1} has been attributed to tetraborate groups. This band completely disappears as a result of addition of V_2O_5 to the binary calcium borate glasses (Fig.6.2b-d) along with the appearance of a very weak band ~ 75Ø cm^{-1} due to the formation of the complex B-O-V-O-B linkage. However, an appreciable rise in intensity of the broad band at 949 cm^{-1} along with its shift towards lower frequencies with increasing concentration (y) of V_2O_5 is noticeable. For this glass at higher concentration of CaO (x=Ø.35), Ca^{++} ions are expected to go into either interstitial or substitutional sites in vanadate chains. Both the situations would exert an influence on the isolated V = O bonds and affect their vibrations, depending on the position of the Ca^{++} ions. If these ions occupy substitutional sites, then the V-O-V bonds would break up and form V-O-Ca-O-V linkages, which could restrict the influence of the ions on V = O bonds and thus will tend to preserve the position of the 997 cm^{-1} band (for crystalline V_2O_5). And if the ions (Ca^{++}) enter the vanadate

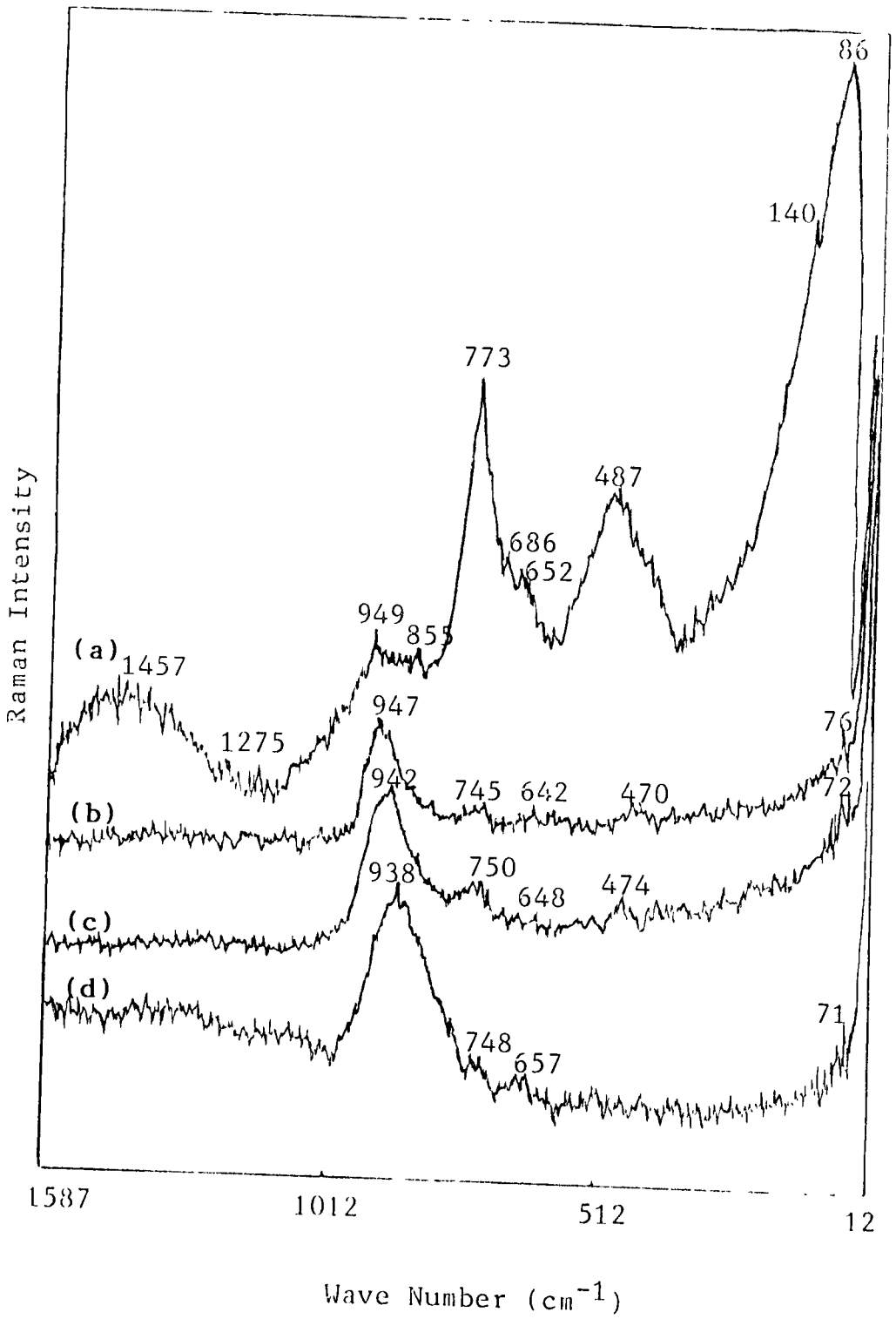

Fig.6.2 Raman spectra of glasses in the system $(V_2O_5)_y.[xCaO.(1-y-x)B_2O_3]_{1-y}$ for the values of x=Ø.35 and y: (a) Ø, (b) Ø.Ø5, (c) Ø.1Ø and (d) Ø.15.

chains interstitially, they will interact directly with isolated V = O bonds, making them longer and thus shifting the vibrational frequency towards lower wave numbers. Both the situations may have the possiblity to co-exist in the present system of glasses for x=Ø.35 and y=Ø.Ø5, Ø.1Ø and Ø.15 (Fig.6.2b-d).

The band at 947 cm^{-1} for y=Ø.Ø5 and x=Ø.35 shifts to 938 cm^{-1} at concentration y=Ø.15. Broadness of the band may be interpreted as follows: the influence of Ca^{++} ions on V = O bonds may be expected to differ at different sites so that vibrational frequencies associated with these V = O bonds are differing, though close to each other[13]. Since these overlapping bands can not be resolved, a broad maximum is observed which shifts towards lower frequencies due to the elongation of the bonds, forming VO_4 tetrahedra. This band around 942 cm^{-1} may be attributed to the stretching vibrations of VO_2 sub groups in VO_4 polyhedra. The absence of the band at 773 cm^{-1} observed for (x=Ø.35 and y=Ø) in the spectra of glasses with x=Ø.35 and y≥Ø.Ø5 shows that no six membered borate cyclic rings are present in these glasses.

It is also noticeable that other Raman bands are observed very weakly in the spectra of these glasses. The observed Raman bands are tabulated in Table 6.1.

6.4 IR results

Figs.6.3 & 6.4 show the infrared spectra of the glasses in the system $(V_2O_5)_y.[xCaO.(1-y-x)B_2O_3]_{1-y}$ for x=Ø.2Ø & Ø.35 and y=Ø, Ø.Ø5, Ø.1Ø and Ø.15. The spectrum of Fig.6.3a for x=Ø.2Ø and y=Ø shows a splitted band at 79Ø-82Ø cm^{-1} which corresponds to six membered borate cyclic rings containing BO_4 and BO_3 units. In borate glasses, the broad absorption region 12ØØ-145Ø cm^{-1} is attributed to B-O bond stretching of trigonal BO_3 units and the region 85Ø-11ØØ cm^{-1} originates from B-O bond stretching of BO_4 tetrahedral units and the band at 665 cm^{-1} is due to B-O-B bending motion.

The infrared spectra[15] of amorphous and crystalline V_2O_5 shows an intense absorption band at 1Ø25 cm^{-1} which corresponds to an isolated V = O bond having a five fold coordination and a band between 82Ø-78Ø cm^{-1} is associated to the asymmetric stretching vibrations due to V-O-V bonds.

When V_2O_5 concentration is y=Ø.Ø5 in the borate glass for x=Ø.2Ø, the spectrum shows (Fig.6.3b) the broadening of the bands to appear in three regions, 9ØØ-11ØØ, 12ØØ-15ØØ and 65Ø-75Ø cm^{-1}. This broadening is attributed to the random network and lack of long range order[16]. With increasing concentration (y) of V_2O_5 (y=Ø.1Ø & Ø.15; Fig.6.3c&d), the noticeable change is in the region of 9ØØ-11ØØ cm^{-1}. This broad region becomes sharper and centered at 94Ø cm^{-1} for y=Ø.15

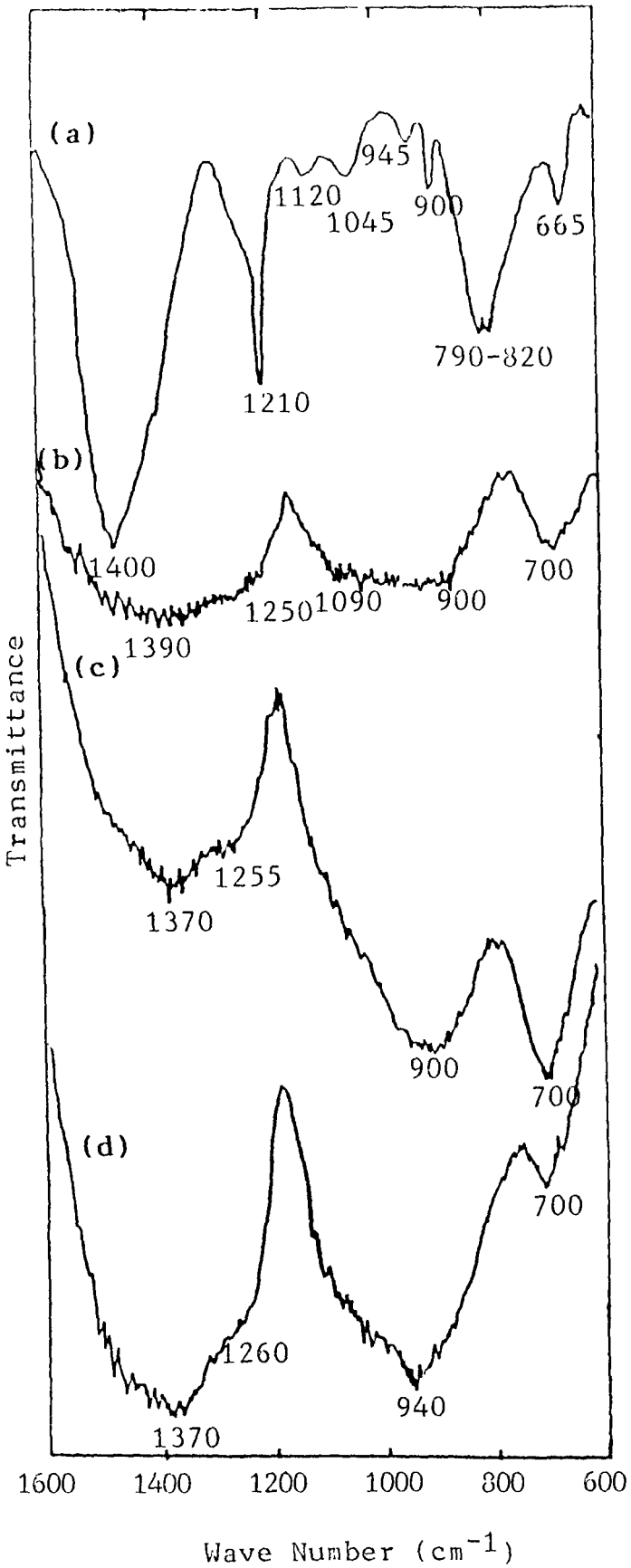

Fig.6.3 IR spectra of glasses in the system $(V_2O_5)_y.[xCaO.(1-y-x)B_2O_3]_{1-y}$ for the values of x=Ø.2Ø and y: (a) Ø, (b) Ø.ØŠ, (c) Ø.1Ø and)d) Ø.15.

(Fig.6.3d). The band at 940 cm^{-1} is attributed to orthoborate groups in binary borate glasses; but the increase in its intensity as a result of the addition of V_2O_5 shows that the band is also associated with the stretching vibrations of VO_2 groups in VO_4 polyhedra.

In other regions of these spectra, though some change is observed as a result of addition of V_2O_5, the characteristic features of the calcium borate binary are retained in these vanadium oxide doped glasses. No new peaks are observed. The band at 700 cm^{-1} is associated with the metaborate groups and is reduced in intensity with rise of concentration of V_2O_5 at y=0.15.

For the glass of concentration x=0.35, the spectra (Fig.6.4b-d) show that the characteristics of calcium borate binary glass is retained in these glasses with rise of concentration (y) of V_2O_5. Only noticeable change in the region (850-950 cm^{-1}) centering at 920 cm^{-1} (for y= 0.15; Fig.6.4d) is observed as a result of addition of V_2O_5. All the IR bands observed are tabulated in Table 6.2.

6.5 Discussions and conclusions

Raman spectra of vanadium oxide doped calcium borate glass for x=0.20 (Fig.6.1a & b) show that the bands at 800 and 778 cm^{-1} due to boroxol rings containing BO_3 and BO_4 units,

Table 6.1 Raman bands observed in the system of glasses $(V_2O_5)_y.[xCaO.(1-y-x)B_2O_3]_{1-y}$ for various x and y.

Concentration		Position of Raman bands (cm^{-1})									
(x)	(y)										
	Ø.ØØ	6Ø	236	5Ø3	647	-*-	778	8ØØ	-*-	947	1452
	Ø.Ø5	58	242	472	637	-*-	78Ø	8ØØ	-*-	942	1357
Ø.2Ø	Ø.1Ø	51	237	462	-*-	745	-*-	-*-	85Ø	944	-*-
	Ø.15	48	-*-	47Ø	-*-	748	-*-	-*-	848	961	-*-
	Ø.ØØ	86	14Ø	487	652	686	773	855	949	1275	1457
	Ø.Ø5	76	-*-	47Ø	642	-*-	745	-*-	947	-*-	-*-
Ø.35	Ø.1Ø	72	-*-	474	648	-*-	75Ø	-*-	942	-*-	-*-
	Ø.15	71	-*-	-*-	657	-*-	748	-*-	938	-*-	-*-

Table 6.2 Infrared bands observed in the system of glasses $(V_2O_5)_y.[xCaO.(1-y-x)B_2O_3]_{1-y}$ for various x and y

Concentration		Position of Infrared bands (cm^{-1})						
(x)	(y)							
	Ø.ØØ	665	79Ø-82Ø	9ØØ-945	1Ø45	112Ø	121Ø	14ØØ
	Ø.Ø5	7ØØ	-*-	9ØØ	-*-	1Ø9Ø	125Ø	139Ø
Ø.2Ø	Ø.1Ø	7ØØ	-*-	9ØØ	-*-	-*-	1255	137Ø
	Ø.15	7ØØ	-*-	94Ø	-*-	-*-	126Ø	137Ø
	Ø.ØØ	71Ø		9ØØ-11ØØ			1245	146Ø
	Ø.Ø5	7ØØ		9ØØ			126Ø	1365
Ø.35	Ø.1Ø	7ØØ		93Ø			126Ø	1365
	Ø.15	7ØØ		92Ø			-*-	136Ø

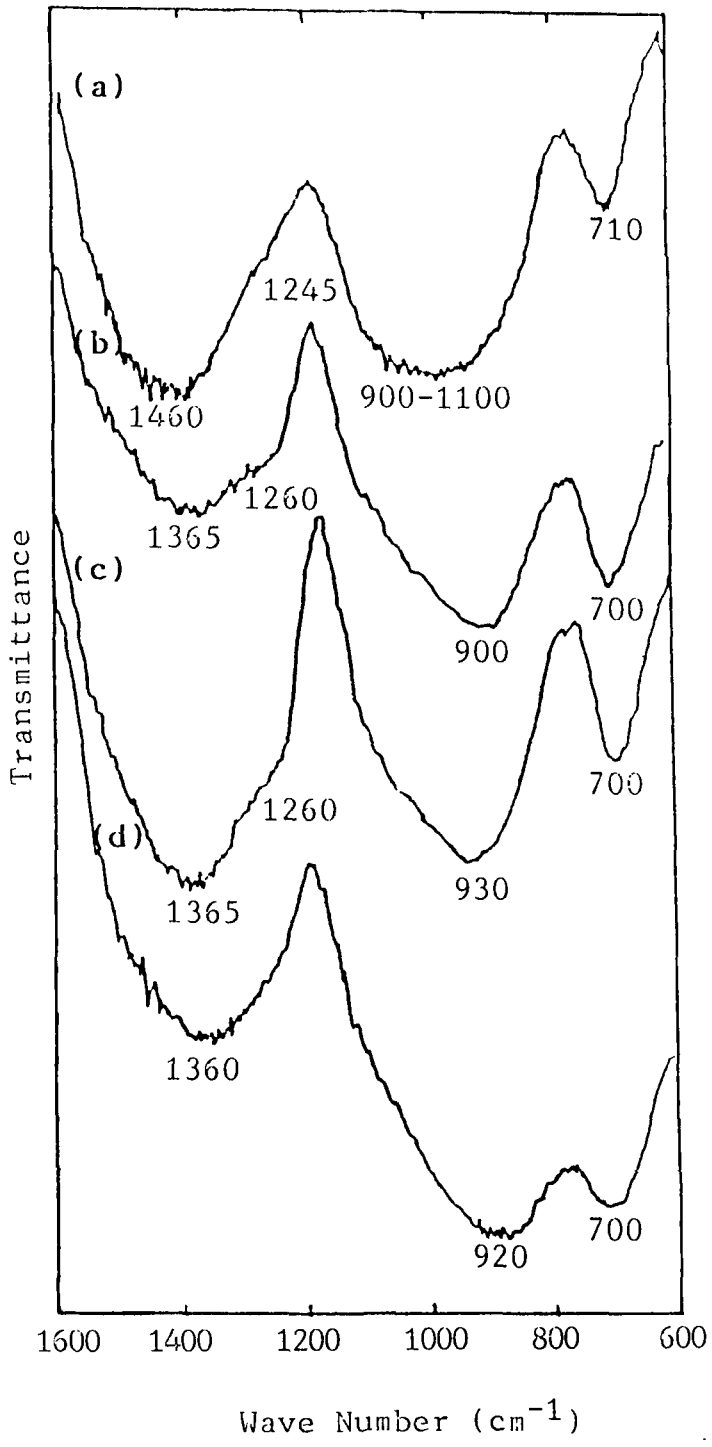

Fig.6.4 IR spectra of glasses in the system $(V_2O_5)_y.[xCaO.(1-y-x)B_2O_3]_{1-y}$ for the values of x= Ø.35 and y: (a) Ø, (b) Ø.Ø5, (c) Ø.1Ø and (d) Ø.15.

respectively, appear with much reduced intensity as a result of addition of V_2O_5 (y=Ø.Ø5), along with the corresponding abrupt growth of a broad and intense band around 942 cm^{-1}. It is clear that the formation of calcium vanadate glass is characterized by the appearance of this strong band at this composition with the simultaneous disappearance of the bands associated with cyclic borate groups. Calcium ions (Ca^{++}) enter interstitially into the vanadate chains by interacting directly with V = O bonds, which results in a shift of frequency towards lower wave number due to elongation of the bonds. The CaO causes the appearance of series of complexes consisting of VO_4 tetrahedra. However, with rising concentration (y) of V_2O_5, the band around 942 cm^{-1} decreases in intensity along with the appearance of the new bands around 75Ø (due to the formation of the complex B-O-V-O-B)[15] and 85Ø cm^{-1} (associated with pyroborate groups) in the spectra of Fig.6.1 and all other Raman bands tend to disappear. These observstions indicate that the two glass formers, B_2O_3 and V_2O_5 form a quasi-complex in the concentration range Ø.Ø5 < y ≤ Ø.15 and V_2O_5 acts as modifier upto the concentration of y=Ø.Ø5 in the calcium borate glass of composition Ø.2ØCaO.Ø.8ØB_2O_3.

On the other hand, IR spectra of the glasses show that the characteristic features at 7ØØ, 9ØØ-11ØØ, 12ØØ-15ØØ cm^{-1} bands due to calcium borate glasses are retained in these vanadium

oxide doped glasses. Although the band around 900 cm^{-1} at the concentration y=0.05 in the IR spectra does not appear with appreaciable intensity contrary to that observed in the Raman spectra for the same composition y=0.05, it becomes noticeably sharp and intense with rising V_2O_5 concentration.

On comparing the Raman with IR spectra of the glasses in the system $(V_2O_5)_y.[xCaO.(1-y-x)B_2O_3]_{1-y}$ and also with the spectra of each corresponding separate systems, it appears obviously that the Raman spectra of these glasses containing two glass forming oxides are not simple addition of the spectra of each system. Again, because of the interaction between the glass forming oxides and changes in the short range order in the glass structure, the variations of the frequency shifts, intensities and band widths of Raman lines take place.

Since the characteristic band at 942 cm^{-1}, due to the addition of V_2O_5, appears with much intensity and retains its relative intensities compared to other bands through out this concentration range, it appears from the general appearance of the spectra of these glasses that the characteristic of calcium vanadate is predominant in these glasses in the composition range $0.20 \leq x \leq 0.35$ and $0 \leq y \leq 0.15$.

REFERENCES

1. A.K.Bandyopadhaya and J.O.Isard, J. Phys.D, **10** (1977) L99
2. T.Nishida, T.Hirai and Y.Takashima, Phys. Chem. Glasses, **24**(5) (1983) 113
3. L.D.Bogomolova, M.P.Glassova, O.E.Dubatorko, S.I.Reiman and S.N.Spasikina, J. Non-Crystalline Solids, **58** (1983) 71
4. A.D.Pearson, J.F.Dewald, W.R.Northover and W.F.Peck, *in* ''Advances in Glass Technology'', Vol.**1** (Plenum, New York, 1962) p-357; ibid,vol.**2** p-145
5. Y.Kawamoto, M.Fukuzuka, Y.Ohta and M.Imai, Phys. Chem. Glasses, **20**(3) (1979) 54
6. G.S.Linsey, A.E.Owen and F.M.Hayatee, J. Non-Crystalline Solids, **4** (197Ø) 2Ø8
7. V.K.Dhawan, A.Mansingh and M.Sayer, J. Non-Crystalline Solids, **51** (1982) 87
8. K.W.Hansen and M.T.Splann, J. Electrochem. Soc. **113** (1966) 895
9. M.Sayer and A.Mansingh, J. Non-Crystalline Solids, **31** (1979) 385
10. G.W.Anderson and W.D.Compton, J. Chem. Phys. **52** (197Ø) 6166
11. S.S.Chan, I.F.Wachs, L.L.Murrel, L.Wang and W.Keith Hall, J. Phys. Chem. **88** (1984) 5831
12. E.I.Kamitsos, M.A.Karakassides and G.D.Chryssikos, J. Phys. Chem. **91** (1987) 1Ø73

13. Y.Dimitriev, V.Dimitrov, M.Arnaudov and D.Topalov, J. Non-Crystalline Solids, 57 (1983) 147

14. L.Rivoalen, A.Reveolevschi, J.Livage and R.Collongues, J. Non-Crystalline Solids, 21 (1976) 171

15. D.K.Kanchan, R.K.Puri and R.G.Mendiratta, Phys. Chem. Glasses, 26 (1985) 217

16. Y.Dimitriev, V.Dimitrov and M.Arnaudov, J. Mater. Sc. 14 (1979) 723